

Induction of Apoptosis in Neuroblastoma

Analysis of apoptotic pathways and
putative apoptosis-mediating receptors



University of Hamburg



**Cancer Research Center
of Hawaii**

A Dissertation in the Partial Fulfillment of the Requirements
for the Degree of Doctor of Natural Science

by

Sven Heiligtag

Hamburg 2001

The present work was done between June 1998 and December 2000 in the Department of Biochemistry and Molecular Biology, University of Hamburg, Hamburg, Germany (June 1998 - February 1999) and the Cancer Research Center of Hawaii, Honolulu, Hawaii, USA (June 1999 - December 2000) in the laboratory of Prof. Dr. Dr. Carl-Wilhelm Vogel.

This work is dedicated to my parents for their
indefatigable support over 29 years

Abstract

The treatment of Neuroblastoma (NB) is still very difficult and the search for new modalities of therapy is of great significance. The fungal antibiotic cerulenin and human anti-NB IgM antibodies have recently been identified in our group as potent mediators of cytotoxicity in NB cells, apparently by induction of apoptosis (David 1996; Heiligtag 1998).

The initial characterization of the involved apoptotic pathway and the identification of potential receptors/targets, respectively, were performed in this study.

Cerulenin was identified as a potent inducer of apoptosis in a variety of tumor cells by both the externalisation of phosphatidylserine residues and the cleavage of PARP with NB cell lines showing a particular high sensitivity. The induction of apoptosis by cerulenin is apparently independent of its function as noncompetitive inhibitor of fatty acid synthase (FAS). The amount and the endogenous activity of FAS did not show any relationship to the sensitivity of the respective cell lines against cerulenin. Furthermore the dose-dependent effects of cerulenin regarding inhibition of FAS activity and induction of apoptosis were contrary.

The DNA-damaging potential of cerulenin was then demonstrated by overexpression of the tumor suppressor protein p53 as well as of the growth arrest & DNA-damage-inducible protein 153 (GADD153). However, induction of apoptosis and regulation of the p53 responsible gene products p21/WAF and Bax are independent of p53. The apparent loss of p53 function is probably due to differences in post-translational modifications since cytoplasmatic sequestering could be excluded as reason for p53 nonfunctionality and comparison with the effects of the known DNA damaging drugs doxorubicin and etoposide showed similar increases in p53 levels. The induction of apoptosis involved the early mitochondrial release of cytochrome C independent of overexpression of

Abstract

Bax at this time and the subsequent activation of caspases 9 and 3, but not of caspase 8. A strong overexpression of Bax was observed in the most susceptible cell lines including all NB cell lines at later time points. The NB cell lines showed furthermore the development of an additional band of 18 kDa, apparently a recently described more cytotoxic cleavage product of Bax. This cleavage product appears to be necessary for the mitochondrial breakdown in the cerulenin system. Since induction of apoptosis is independent of the p53 status as well as of caspase 8 cerulenin is a very promising new agent in the treatment of cancer, in particular NB.

In the IgM mediated apoptosis two potential receptors had been identified by immunoblot analysis, namely hsp 90 and a so far unknown protein termed NB-p260 and were now more thoroughly characterized. It was verified that hsp 90 might function as apoptosis-mediating cell surface receptor, but since preadsorption experiments had shown that its ability to inhibit IgM mediated apoptosis was small compared to that of NB-p260, the latter appears to be the predominant apoptosis-mediating receptor.

For the molecular characterization of NB-p260, the protein was purified to homogeneity by sequential anion, cation exchange and hydroxyapatite chromatography as well as preparative gelelectrophoresis. NB-p260 was then unambiguously identified by both MALDI-MS and N-terminal sequence analysis to be comprised of two different actin-binding proteins, ABP-278 and ABP-280. However, only the recently identified ABP-278 but not ABP-280 was presented on the surface of LAN-1 NB cells as measured by biotinylation analysis. The apoptosis-mediating capability of NB-p260 was confirmed by preadsorption experiments of anti-NB IgM antibodies with the purified protein that resulted in the complete abolishment of induction of apoptosis by anti-NB IgM. The involved apoptotic pathway induced by binding of IgM is not mediated by caspase 8, but probably by the stress-activated protein kinase pathway.

Zusammenfassung

Die Behandlung des Neuroblastoms (NB) ist nach wie vor außerordentlich schwierig, weswegen die Suche nach neuen Therapieformen von größter Bedeutung ist. Das Pilzantibiotikum Cerulenin sowie humane anti-NB IgM Antikörper wurden kürzlich in unserer Gruppe als potente Vermittler von Zytotoxizität in NB-Zellen identifiziert, wahrscheinlich durch Induktion der Apoptose (David 1996; Heiligtag 1998).

Die initiale Charakterisierung der dabei involvierten apoptischen Signalwege und die Identifizierung möglicher Rezeptoren bzw. Zielstrukturen wurden im Rahmen dieser Arbeit durchgeführt.

Cerulenin konnte mittels der Externalisierung von Phosphatidylserin-Resten und der Spaltung von PARP als potentes Apoptose-auslösendes Agens in verschiedensten Tumorzelllinien identifiziert werden, wobei sich humane NB Zelllinien durch eine besondere Anfälligkeit auszeichneten. Die Auslösung der Apoptose scheint unabhängig von der Funktion Cerulenins als nichtkompetitiver Inhibitor der humanen Fettsäuresynthase (FAS) zu sein. Weder die Expression noch die endogene Aktivität der FAS korrelierten mit der Sensitivität gegenüber Cerulenin. Darüber hinaus waren die dosis-abhängigen Effekte von Cerulenin auf die Inhibierung der FAS-Aktivität und der Induktion der Apoptose gegenläufig.

Das DNA-schädigende Potential von Cerulenin konnte dann mittels der Überexpression des Tumorsuppressor-Proteins p53 und des „growth arrest & DNA-damage-inducible“ Proteins 153 (GADD153) gezeigt werden. Allerdings waren die Induktion der Apoptose und die Regulierung der p53 induziblen Genprodukte p21/WAF und Bax p53-unabhängig. Dieser offensichtliche Verlust der p53-Funktion ist wahrscheinlich durch post-translationale Modifikationen verursacht, denn sowohl cytoplasmatische Sequestrierung als auch die Akkumulation zu geringer Mengen an p53 konnten durch Vergleich mit den bekannt DNA-schädigenden Substanzen Doxorubicin und Etoposid als Gründe für die Nichtfunktionalität von p53 ausgeschlossen werden.

Zusammenfassung

Die Induktion der Apoptose ging einher mit der frühen mitochondrialen Freisetzung von Cytochrom C und der nachfolgenden Aktivierung der Caspase 9 und 3, während Caspase 8 nicht beteiligt war. Eine Überexpression von Bax konnte allerdings erst später und nur in den anfälligsten Zelllinien, u.a. allen NB Zelllinien, beobachtet werden. Des Weiteren trat exklusiv in allen NB Zelllinien zusätzlich eine weitere Bande von 18 kDa auf, bei der es sich wahrscheinlich um ein kürzlich beschriebenes cytotoxischeres Spaltprodukt von Bax handelt. Dieses Spaltprodukt scheint im Falle des Cerulenins für den Zusammenbruch der Mitochondrien verantwortlich zu sein. Da die Induktion der Apoptose sowohl vom p53 Status als auch von Caspase 8 unabhängig ist, stellt Cerulenin ein vielversprechendes neues Agens in der Krebsbehandlung und dabei insbesondere beim NB dar.

Bei der IgM-vermittelten Apoptose waren zwei potentielle Rezeptoren mittels Immunoblotanalyse identifiziert worden, hsp 90 und ein bisher unbekanntes als NB-p260 bezeichnetes Protein, die im Rahmen dieser Untersuchungen genauer charakterisiert werden sollten. Es konnte bestätigt werden, daß hsp 90 als Apoptose-vermittelnder Zelloberflächenrezeptor agieren könnte. Allerdings haben Preadsorptionsexperimente gezeigt, daß die Fähigkeit von hsp 90 die IgM-vermittelte Apoptose zu inhibieren im Verhältnis zu der des NB-p260 klein ist, weswegen das NB-p260 als der dominante Apoptose-vermittelnde Rezeptor angesehen wird. Zur Charakterisierung des NB-p260 wurde das Protein mittels Anionenaustausch-, Kationenaustausch- und Hydroxylapatit-Chromatographie sowie preparativer Gelelektrophorese vollständig gereinigt und anschließend mittels MALDI-MS und N-terminaler Sequenzierung als Mischung aus ABP-278 und ABP-280 identifiziert. Allerdings konnte nur das kürzlich identifizierte ABP-278, nicht aber ABP-280 mittels Biotinylierungsanalyse auf der Oberfläche von LAN-1 NB Zellen nachgewiesen werden. Die Apoptose-vermittelnde Wirkung des NB-p260 konnte über Preadsorptionsversuche mit dem gereinigten Protein nachgewiesen werden, die zum vollständigen Verlust der Induktion der Apoptose durch anti-NB IgM führten. Der beteiligte apoptotische Signalweg ist unabhängig von Caspase 8 und scheint über den Stress-aktivierten Protein-Kinase (SAPK) Weg zu laufen.

| | |
|---|----|
| Table of Contents | 1 |
| I. Abbreviations | 6 |
| II. List of Figures | 9 |
| III. List of Tables | 12 |
| | |
| 1. Introduction | 13 |
| | |
| 2. Materials | 22 |
| 2.1. Cell lines | 22 |
| 2.2. Materials for cell culture | 22 |
| 2.3. Sera | 23 |
| 2.4. Antibodies | 23 |
| 2.4.1. Monoclonal Antibodies | 23 |
| 2.4.2. Polyclonal Antibodies | 24 |
| 2.4.3. Secondary antibodies | 24 |
| 2.5. Chemicals | 25 |
| 2.6. Buffer and Solutions | 26 |
| | |
| 3. Methods | 28 |
| 3.1. Tissue Culture | 28 |
| 3.1.1. Cultivation of cells | 28 |
| 3.1.2. Determination of the cell number | 29 |
| 3.1.3. Longterm storage of cells | 29 |
| 3.2. Protein Biochemistry | 30 |
| 3.2.1. Preparation of cell extracts | 30 |
| 3.2.2. Purification of proteins | 31 |
| 3.2.2.1. Purification of fatty acid synthase (FAS) | 32 |
| 3.2.2.2. Purification of NB-p260 | 32 |
| 3.2.2.3. Purification of heat shock protein 27 (hsp 27) | 33 |
| 3.2.2.4. Purification of heat shock protein 60 (hsp 60) | 33 |
| 3.2.2.5. Purification of heat shock protein 70 (hsp 70) | 33 |
| 3.2.2.6. Purification of heat shock protein 90 (hsp 90) | 34 |
| 3.2.3. SDS-polyacrylamid-gelelectrophoresis (SDS-PAGE) | 35 |

| | | |
|----------|---|----|
| 3.2.4. | Storage of gels | 35 |
| 3.2.5. | Staining of proteins with Coomassie Brilliant Blue R-250 .. | 36 |
| 3.2.6. | Staining of proteins with silvernitrate | 36 |
| 3.2.7. | Determination of protein concentrations | 37 |
| 3.2.8. | Electrophoretic transfer of proteins | 37 |
| 3.2.9. | Expression of FAS in different cell lines | 38 |
| 3.2.10. | Expression of hsp 60, hsp 70 and hsp 90 in different cell lines | 38 |
| 3.2.11 | Screening of patient sera for immunoreactivity against heat shock proteins hsp 60, hsp 70 and hsp 90 | 39 |
| 3.2.12. | Labeling of cell surface proteins with Sulfo-NHS-LC- Biotin | 39 |
| 3.2.13. | Isolation of biotin-labeled proteins by monomeric avidin ... | 39 |
| 3.2.14. | Generation of internal fragments of NB-p260 by endoproteinase Lys-C digestion | 40 |
| 3.2.15. | Amino acid sequencing | 41 |
| 3.2.16. | Protein identification by Toplab | 42 |
| 3.3. | Immunology | 43 |
| 3.3.1. | Immunoblotting | 43 |
| 3.3.2. | Purification of human IgM antibodies | 44 |
| 3.3.3. | Inhibition of anti-NB IgM-induced apoptosis by NB-p260 .. | 45 |
| 3.3.4. | Serological screening of recombinant cDNA expression libraries (SEREX)..... | 46 |
| 3.3.5. | Preadsorption of IgM antibodies at E. coli phage lysate (ECPL) | 47 |
| 3.3.6. | Cytofluorometric Binding assays | 49 |
| 3.4. | Apoptosis | 50 |
| 3.4.1. | Induction of apoptosis with human anti-NB IgM | 50 |
| 3.4.2. | Induction of apoptosis with cerulenin | 50 |
| 3.4.3. | Cytofluorometric determination of apoptotic cells | 50 |
| 3.4.4. | Assessment of the mitochondrial potential ($\Delta\Psi_m$) | 51 |
| 3.4.5. | Detection of cytochrome C release | 51 |
| 3.5. | Molecular Biology | 52 |
| 3.5.1. | RNase decontamination of equipment and buffers | 52 |
| 3.5.2. | Construction of a cDNA library..... | 52 |
| 3.5.2.1. | Isolation of poly(A)+ RNA | 52 |

| | | |
|-----------|---|-----------|
| 3.5.2.2. | cDNA synthesis | 53 |
| 3.5.2.3. | Construction of the cDNA library in the λ ZAP Express vector | 56 |
| 3.5.2.4. | Assessment of the cDNA library | 57 |
| 3.5.3. | In vivo excision | 58 |
| 3.5.4. | Plasmid DNA isolation | 59 |
| 3.5.5. | Ethidium bromide plate assay | 60 |
| 3.5.6. | Blue white screening | 60 |
| 3.5.7. | Agarose gel electrophoresis | 61 |
| 3.5.8. | Cultivation and storage of bacterial cell cultures | 61 |
| 3.5.9. | DNA sequencing | 62 |
| 3.6. | Radioactive Methods | 64 |
| 3.6.1. | Determination of endogenous FAS activity | 64 |
| 3.6.2. | Inhibition of endogenous FAS activity by cerulenin | 64 |
| 4. | Results | 65 |
| 4.1. | Cerulenin-mediated apoptosis | 65 |
| 4.1.1. | Induction of apoptosis by cerulenin | 65 |
| 4.1.1.1. | Annexin V assay | 66 |
| 4.1.1.2. | Cleavage of PARP | 67 |
| 4.1.2. | Investigation of FAS as a potential target of cerulenin | 69 |
| 4.1.2.1. | Purification of FAS | 69 |
| 4.1.2.2. | Expression of FAS in different human tumor and normal cell lines | 71 |
| 4.1.2.3. | Endogenous FAS activity in different human tumor and normal cell lines | 72 |
| 4.1.2.4. | Inhibition of endogenous FAS activity by cerulenin | 75 |
| 4.1.2.5. | Investigation of the ability of palmitate to rescue cells from cerulenin-induced apoptosis | 78 |
| 4.1.3. | Induction of DNA damage by cerulenin | 79 |
| 4.1.3.1. | Expression of the tumor suppressor protein p53 | 79 |
| 4.1.3.2. | Expression of GADD 153 | 82 |
| 4.1.3.3. | Expression of p21/WAF | 83 |
| 4.1.3.4. | Expression of Bax | 85 |
| 4.1.4. | Induction of apoptosis and DNA damage by doxorubicin and etoposide | 87 |

| | | |
|-----------|---|------------|
| 4.1.5. | Cerulein-mediated signal transduction pathway | 90 |
| 4.1.5.1. | Time dependence of PARP cleavage | 90 |
| 4.1.5.2. | Involvement of mitochondria | 93 |
| 4.1.5.3. | Activation/Involvement of caspases | 97 |
| 4.2. | IgM-mediated apoptosis and putative receptors | 100 |
| 4.2.1. | Identification and characterization of NB-p260 | 101 |
| 4.2.1.1. | Purification of NB-p260 | 101 |
| 4.2.1.2. | Molecular characterization of the NB-p260 | 104 |
| 4.2.1.3. | Function of NB-260 as apoptosis inducing receptor | 113 |
| 4.2.1.4. | Cell surface expression of ABP-278 and ABP-280 | 115 |
| 4.2.2. | Possible role of heat shock proteins | 117 |
| 4.2.2.1. | Cell surface expression of heat shock proteins on NB cells | 117 |
| 4.2.2.2. | Reactivity of patient sera against heat shock proteins | 119 |
| 4.2.3. | SEREX | 123 |
| 4.2.3.1. | Construction of a cDNA library from LAN-1 cells | 123 |
| 4.2.3.2. | Assessment of the constructed cDNA library and establishment of the SEREX approach | 125 |
| 4.2.3.3. | Screening of the cDNA expression library with human anti-NB IgM antibodies | 126 |
| 5. | Discussion | 128 |
| 5.1. | Cerulein-mediated apoptosis | 128 |
| 5.2. | Anti-NB IgM mediated apoptosis | 140 |
| 6. | Appendix | 154 |
| I. | Amino acid sequence of ABP-280 | 154 |
| II. | Amino acid sequence of ABP-278 | 155 |
| III. | Lambda ZAP system | 156 |
| 7. | Abstracts | 157 |

| | |
|-------------------------------|------------|
| 8. Publications | 158 |
| 9. References | 159 |
| Curriculum Vitae | 184 |
| Acknowledgements | 185 |
| Affidavit | 186 |

I. Abbreviations

| | |
|--------------------|---|
| ABP | actin binding protein |
| ABPAF | ABP associated factor |
| ADCC | antibody-dependent cellular cytotoxicity |
| ADP | adenosine-5'-diphosphate |
| anti-NB IgM | IgM antibodies with cytotoxicity greater 80 % against NB cell lines |
| AP | alkaline phosphatase |
| Apaf1 | apoptotic-protease-activating factor 1 |
| APS | ammonium persulfate |
| ASK1 | apoptosis-signaling kinase 1 |
| ATP | adenosine-5'-triphosphate |
| BCA | bicinchonin acid |
| BCIP | 5-bromo-4-chloro-indoylphosphate |
| BSA | bovine serum albumine |
| CAPS | cyclohexylamino-propylsulfonic acid |
| CDK | cyclin dependent kinase |
| cDNA | complementary DNA |
| cerulenin | 2,3-epoxy-4-oxo-7, 10-dodecadienamid |
| CTL | cytotoxic T lymphocyte |
| DD | death domain |
| dH ₂ O | distilled water |
| ddH ₂ O | double distilled water |
| DED | death effector domain |
| DEPC | diethyl pyrocarbonate |
| DMSO | dimethylsulfoxid |
| DNA | desoxyribonucleotide acid |
| DTAF | dichlorotriacetyl-aminofluorescein |
| DTT | dithiothreitol |

| | |
|----------|---|
| ECL | enhanced chemiluminescence |
| ECPL | Escheria coli phage lysat |
| EDTA | ethylendiamintetraacetic acid |
| FACS | fluorescent activated cell sorter |
| FADD | Fas associated death domain |
| FAS | fatty acid synthase |
| FCS | fetal calf serum |
| FITC | fluorsceinisothiocyanate |
| GADD 153 | growth arrest & DNA damage inducible protein 153 |
| GRP | glucose regulated protein |
| HEPES | N-(2-hydroxyethyl)piperazine-N´-(2-ethansulfonicacid) |
| HRP | horse raddish peroxidase |
| HSP | heat shock protein |
| IgG | immunoglobuline G |
| IgM | immunoglobuline M |
| IgY | immunoglobuline Y |
| IPTG | isopropyl β -D-thiogalactoside |
| JC-1 | 5,5´,6,6´,-tetrachloro-1,1´,3,3´ tetraethylbenzimidazolyl-carbocyanine iodide |
| JNK | c-Jun N-terminal kinase |
| kDa | kilodalton |
| LB | Luria bertani |
| MALDI-MS | matrix-assisted laser desorption/ionisation mass spectrometry |
| MAPK | mitogen activated protein kinase |
| MAPKK | MAPK kinase |
| MAPKKK | MAPKK kinase |
| MEK | MAPKK |
| MEKK | MAPKKK |
| MMLV-RT | moloney murine leukemia virus reverse transcriptase |

| | |
|-----------|--|
| mRNA | messenger RNA |
| MW | molecular weight |
| MWCO | molecular weight cutoff |
| NB | Neuroblastoma |
| NB-p260 | supposed 260 kDa antigen on NB cells |
| NBT | nitrobluetetrazoliumchloride |
| NHBTL | normal human brain tissue lysate |
| NHEK | normal human keratinocytes |
| NHLF | normal human lung fibroblasts |
| PAGE | polyacrylamide gel electrophoresis |
| PARP | poly(ADP-ribose) polymerase |
| PBS | phosphate buffered saline |
| PI | propidiumiodide |
| PVDF | polyvinylendifluoride |
| RPMI 1640 | Roswell Park Memorial Institute culture medium 1640 |
| RT-PCR | reverse transcriptase polymerase chain reaction |
| SAPK | stress-activated protein kinase |
| SDS | sodium dodecyl sulfate |
| TBS | Tris buffered saline |
| TEMED | N,N,N',N'-tetramethyl-ethylendiamine |
| TNF | tumor necrosis factor |
| TNFR | TNF receptor |
| TRAF | TNF receptor associated factor |
| Tris | tris-(hydroxymethyl)-aminomethan |
| Tween-20 | polyoxyethylen-sorbitanmonolaureat |
| v/v | volume percent (volume per volume) |
| w/v | weight percent (weight per volume) |
| X-Gal | 5-bromo-4-chloro-3-indolyl- β -D-galactoside |
| zVAD-fmk | benzoylcarbonyl-Val-Ala-Asp-(OMe) fluoromethylketone |

II. List of Figures

| | |
|---|----|
| Figure 1: Schematic pathways for caspase activation and apoptosis .. | 20 |
| Figure 2: Determination of cerulenin-mediated apoptosis by Annexin V-FITC and propidium iodide in different tumor and normal cell lines | 66 |
| Figure 3: Determination of cerulenin-mediated apoptosis by PARP cleavage | 68 |
| Figure 4: Purification of FAS from LAN-1 cells | 70 |
| Figure 5: Determination of FAS expression and activity in tumor and normal cell lines | 73 |
| Figure 6: Correlation analysis of FAS expression and FAS activity | 74 |
| Figure 7: Cerulenin-mediated inhibition of FAS activity (I) | 75 |
| Figure 8: Cerulenin-mediated inhibition of FAS activity (II) | 76 |
| Figure 9: Lack of inhibition of PARP cleavage in LAN-1 and HaCaT cells by palmitate | 78 |
| Figure 10: Expression of p53 in p53 wild-type cell lines after treatment with cerulenin | 80 |
| Figure 11: Expression of p53 in p53 mutated cell lines after treatment with cerulenin | 81 |
| Figure 12: Expression of GADD 153 after treatment with cerulenin | 82 |
| Figure 13: Expression of p21 in p53 wild-type cell lines after treatment with cerulenin | 83 |
| Figure 14: Expression of p21 in p53 mutated cell lines after treatment with cerulenin | 84 |
| Figure 15: Expression of Bax in p53 wild-type cell lines after treatment with cerulenin | 85 |
| Figure 16: Expression of Bax in p53 mutated cell lines after treatment with cerulenin | 86 |

| | |
|--|-----|
| Figure 17: Investigation of PARP cleavage and expression of p53 and the p53 inducible genes p21/WAF and Bax after treatment with etoposide in the p53 wild-type cell lines SK-N-SH and A-172 and the p53 mutated cell line HaCaT | 89 |
| Figure 18: Time-dependent cleavage of PARP in LAN-1 and HaCaT cells after treatment with cerulenin | 91 |
| Figure 19: Inhibition of PARP cleavage by the broad range caspase inhibitor zVAD-fmk in LAN-1 and HaCaT cells | 92 |
| Figure 20: Expression of Bax in LAN-1 and HaCaT cells after treatment with cerulenin..... | 93 |
| Figure 21: Cerulenin-induced cytochrome C release into the cytosol in LAN-1 and HaCaT cells | 94 |
| Figure 22: Assessment of the mitochondrial potential in LAN-1 cells following cerulenin treatment | 95 |
| Figure 23: Assessment of the mitochondrial potential in HaCaT cells after treatment with cerulenin | 96 |
| Figure 24: Cleavage of caspase 9 in LAN-1 and HaCaT cells after exposure to cerulenin | 97 |
| Figure 25: Cerulenin-induced activation of caspase 3 in LAN-1 and HaCaT-cells | 98 |
| Figure 26: Presence of caspase 8 in LAN-1 and HaCaT cells | 99 |
| Figure 27: Purification of NB-p260 from LAN-1 NB cells | 102 |
| Figure 28: Immunoreactivity of the NB-p260 purification procedure against anti-NB IgM antibodies | 103 |
| Figure 29: Generation of low molecular weight fragments of NB-p260 by endoproteinase Lys-C digestion | 105 |
| Figure 30: Generation of high molecular weight fragments of NB-p260 by endoproteinase Lys-C digestion | 106 |
| Figure 31: Immunoreactivity of the NB-p260 purification procedure against a monoclonal anti-ABP-280 antibody | 108 |
| Figure 32: Separation of NB-p260 by hydroxyapatite chromatography | 109 |

| | |
|---|-----|
| Figure 33: Immunoreactivity of NB-p260 separated by hydroxyapatite chromatography against an anti-ABP-280 antibody and purified human anti-NB IgM | 110 |
| Figure 34: Inhibition of anti-NB IgM induced apoptosis by purified NB-p260 | 114 |
| Figure 35: Investigation of cell surface expression of ABP-278 and ABP-280 in intact LAN-1 NB cells by biotinylation analysis | 116 |
| Figure 36: Cell surface expression of heat shock proteins hsp 60, hsp 70 and hsp 90 on LAN-1 cells | 117 |
| Figure 37: Biotinylation analysis of cell surface expression of heat shock proteins hsp 60, hsp 70 and hsp 90 on LAN-1 cells .. | 118 |
| Figure 38: Purification of hsp 60 from LAN-1 cells | 119 |
| Figure 39: Purification of hsp 70 from LAN-1 cells | 120 |
| Figure 40: Purification of hsp 90 from LAN-1 cells | 121 |
| Figure 41: Evaluation of the cDNA size in the different fractions after separation by gelfiltration | 124 |
| Figure 42: Evaluation of cDNA inserts of grp 75 positive plaques by restriction analysis | 126 |
| Figure 43: Structural comparison between ABP-278 and ABP-280 | 144 |
| Figure 44: Model for the induction of apoptosis by human anti-NB IgM antibodies | 150 |

III. List of Tables

| | | |
|----------|--|-----|
| Table 1: | N-terminal sequence information of fragments generated by endoproteinase Lys-C digestion of purified NB-p260 | 107 |
| Table 2: | Identification of ABP-278 by MS fingerprint | 112 |
| Table 3: | Identification of ABP-278 by N-terminal sequence analysis | 113 |
| Table 4: | Reactivity of patient sera against heat shock proteins hsp 60, hsp 70 and hsp 90 | 122 |

1. Introduction

Neuroblastoma

Neuroblastoma (NB) is a malign tumor of the autonomous nervous system and occurs almost exclusively in infancy independent of sex. At the time of diagnosis 75 % of the patients are under age of four. 7.3 % of all tumors and 15 % of all tumor casualties are due to the NB (Siegel & Sato, 1986). That makes the NB the third most frequent solid tumor in infancy after leukemia and cerebral tumors (Erttmann et al., 1990; Ater et al., 1998). The incidence in the United States is approximately one in 7,000 (Ater et al., 1998). The NB is an embryonal tumor originating from the adrenal medulla and autonomic ganglia in the chest and the abdomen. The designation of the NB according to the International Neuroblastoma Staging System (INSS) divides patients into four stages I - IVS. The system is helpful to estimate outcome and tends to define two broad groups of patients. Stages I, II and IVS have a favorable outcome with little or no treatment, whereas stage III or IV have a poor prognosis despite treatment (Evans et al., 1971). The classification is related to different parameters, one is the expansion and the distribution of tumor tissue before and of possible residual tissue after initial surgical intervention (Brodeur et al., 1993). Another important parameter is the amplification of the MYCN gene. Normally, only a single copy of MYCN resides on chromosome 2, while advanced stages show a high correlation with amplification of MYCN (Schwab et al., 1983; Brodeur et al., 1984). Although, the absence of MYCN amplification does not necessarily indicate a favorable outlook, its presence in children over one year of age is a very firm indicator of poor outcome. The possibilities of cure are in particular dependent of the corresponding stage and approach up to 100 % in the early stages I and II and decrease to 20 %

in the advanced stages III and IV (Evans et al., 1971). The therapy of NB is very difficult, especially in advanced stages of the disease with widespread metastases to liver, bone, lymph nodes and bone marrow. Current therapy includes chemotherapy, radiation, and high dose chemotherapy with subsequent bone marrow transplantation. More recently, immunotherapy has been added using monoclonal antibodies to the GD₂ glycolipid antigen that is heavily expressed by NB cells (Bosslet et al., 1989; Cheung et al., 1998). Over the last 30 years, significant therapeutic progress has been made with an increase in the five-year relative survival rate from approximately 25 % to approximately 55 %. However, the overall lethality is still approximately 60 %, and over the past decade, no improvement in the five-year survival rate of NB patients has been made (Pinkerton 1993; Harras 1996). Accordingly, the search for new modalities of therapy based on a rational understanding of the biology of the tumor is of great significance.

The biology of NB includes some unusual characteristics. It has been reported that the adrenal glands of infants who died during the first year of age contained small NBs at much higher frequency than would be expected based on the incidence of the disease (Beckwith et al., 1963). These observations are corroborated by the results of large screening programs initially established in Japan in newborns for catecholamine metabolites which serve as tumor markers. Here, too, the frequency of the increased excretions of catecholamine metabolites was significantly higher than expected based on the incidence of NB (Ajiki et al., 1998). One possible explanation for this observations is the phenomenon of spontaneous regression which is defined as partial or complete regression of tumors without therapy. Another interesting observation is that spontaneous regression of clinically manifest tumors has been repeatedly observed, especially in patients with stage IVs which is defined by metastases limited to skin, liver, and/or bone marrow

(Siegel & Sato, 1996). As a matter of fact, NB is the human tumor usually referred to as the tumor with the highest rate of spontaneous regression, topping 90 % in the stage IVs.

The mechanisms involved in the spontaneous regression and/or the development into clinically manifest tumors are not understood. There are several theories explaining the mechanisms for spontaneous regression. One possibility is the differentiation of tumor cells (Pahlman et al., 1990; Hellström et al., 1976) into benign ganglioneuroma or Schwann cell tumors (Adam et al., 1981). In some cases, complete lysis of the neoplastic cells was observed resulting only in necrotic tissue. The molecular mechanisms for the lysis are not understood although cell-mediated (Reynolds et al., 1989, d'Uscio et al., 1991) as well as antibody-mediated mechanism have been proposed (Hellström et al., 1968, Bolande 1991; Bolande et al., 1990). Antibody-mediated mechanisms may include antibody-dependent cellular cytotoxicity (ADCC) as well as complement-mediated cytotoxicity. Because NB cells are frequently characterized by the absence of the complement regulatory proteins CD55 and CD59, they are particularly susceptible to complement lysis (Cheung et al., 1988). More recently, apoptosis has been observed in NBs (Pritchard et al., 1998).

Anti-NB IgM antibodies

Recently, in our group the presence of natural anti-NB IgM antibodies in sera of healthy individuals including children and adults has been described. These antibodies elicit effective killing of human NB cells in vitro by both complement activation and induction of apoptosis (David et al., 1999). This observations were paralleled by in vivo studies in nude rats with human NB xenografts where treatment with the IgM fraction from a healthy adult with a high titer of natural anti-NB IgM caused

inhibition of tumor growth (David et al., 1996). In contrast, sera of NB patients frequently contain significantly lower titers of anti-NB IgM antibodies or even lack these antibodies. It is currently unclear whether the natural anti-NB IgM antibodies play a role in the spontaneous regression of NB or which other roles these antibodies may have in the biology of the adrenal medulla and the pathogenesis of NB.

Certainly intriguing is the observation that the natural anti-NB IgM antibodies induce apoptosis in their target cells since there are only a few systems known where apoptosis is induced by antibodies. The induction of apoptosis is apparently mediated by binding of these antibodies to a 260 kDa protein, termed NB-p260, which is recognized only by anti-NB IgM positive sera but not by anti-NB IgM negative sera (David et al., 1996). The structural characterization of NB-p260 proved to be extremely difficult since the purified protein autodegrades rapidly. This spontaneous autodegradation appears to be the consequence of an internal proteolytic activity which could not be inhibited by a multitude of protease inhibitors and made N-terminal protein sequence analysis impossible. Hence the identification of this 260 kDa cell surface receptor though difficult is currently the most important task.

Immunoblot analysis with the anti-NB IgM revealed an additional but weaker activity against two proteins with molecular weights of approximately 85 kDa that were subsequently identified as heat shock proteins hsp 90 α and hsp 90 β . Moreover, purified NB-p260 and spontaneous degradation products of purified NB-p260 showed reactivity against a monoclonal anti-hsp 90 antibody. In addition, monoclonal anti-hsp 90 antibodies were able to inhibit the binding of anti-NB IgM antibodies to a certain amount, although only a weak reduction in cytotoxicity was observed (David 1996). Whether hsp 90 related sequences are part of NB-p260 or whether hsp 90 may itself function as a further apoptosis inducing receptor in the immune response in NB is currently unknown.

Cerulenin mediated cytotoxicity

During the purification of the NB-p260 another IgM reactive protein with an apparent molecular weight of 220 kDa was copurified and subsequently identified as human fatty acid synthase (FAS) (Heiligtag 1998). Mammalian FAS is a multifunctional enzyme complex containing seven different enzymatic functions on a single chain polypeptide. The active FAS consists of two monomeric FAS subunits and catalyzes the synthesis of long-chain fatty acids, predominantly palmitic acid, from acetyl-CoA and malonyl-CoA.

Previous investigations have shown that tumor cells express elevated levels of FAS and that FAS therefore might be an exploitable target to fight tumors (Kuhajda et al., 1994; Pizer et al., 1996; Rashid et al., 1997). Furthermore the fungal antibiotic cerulenin which is a noncompetitive inhibitor of FAS proved to be cytotoxic to different tumor cell lines and it has been hypothesized that the inhibition of FAS is responsible for the cytotoxic effects of cerulenin (Pizer et al., 1996 and 1999). However, the focus of this research did not include the investigation of the underlying signal transduction pathways that are induced by cerulenin, although the induction of apoptosis has been proposed as possible mechanism (Pizer et al., 1996). Moreover it is currently not clear whether the inhibition of FAS is indeed the (only) reason for the cytotoxic effects of cerulenin or whether other mechanisms might be involved.

Apoptosis

In general two different forms of cell death are distinguished, apoptosis and necrosis.

Apoptosis, also termed programmed or physiological cell death plays a crucial role in the normal development and homeostasis of all higher organisms (Verhagen et al., 1999). Induction of apoptosis activates

defined intracellular pathways eventually leading to cell death that is defined by a variety of specific characteristics (Raff 1998). Necrosis on the contrary is an uncontrolled passive process as response to acute injuries of a cell resulting in its lysis. The cytoplasmatic cell content that is released upon lysis induces an inflammatory reaction (Wyllie 1997).

Cells undergoing apoptosis show a sequence of morphological features including cellular shrinkage, membrane blebbing and formation of the so called apoptotic bodies and condensation of chromatin. Biochemically, these relatively early alterations are associated with the translocation of phosphatidylserine residues to the extracellular side of the plasma-membrane and the activation of a calcium-dependent endonuclease which cleaves genomic DNA into multiples of internucleosomal fragments (Schulze-Osthoff et al., 1998; Cohen 1993; Oberhammer et al., 1993). Both alterations are used to distinguish between apoptosis and necrosis. The externalization of phosphatidylserine residues is used to identify (early) apoptotic cells by their binding to Annexin V (Fasok et al., 1992; Vermes et al., 1995) whereas the degradation of the DNA into characteristic 200 kb fragments yields the typical apoptotic DNA ladder which can be visualized by agarose gelelectrophoresis (Park et al., 1998; Oberhammer et al., 1993). Eventually the so called execution phase is initiated by the activation of caspases who are responsible for a variety of the biochemical and morphological changes that are associated with the apoptotic process (Cohen 1997; Budihardjo et al., 1999).

Caspases are a family of highly conserved cysteine proteases with a specificity for aspartic acid residues in their substrates. They are constitutively expressed in most cells as single chain proenzymes residing in the cytosol. Activation into fully functional proteases takes place by dividing the chain into a large and small subunit before a second cleavage removes the N-terminal prodomain. Two of each subunits assemble into the active tetramer (Green 1998; Wolf & Green, 1999). Depending on the

succession of activation caspases can be divided in effector and initiator caspases. Initiator caspases are directly or indirectly responsible for the activation of the effector or downstream caspases, that in turn activate or cleave further caspases and substrates like Poly(ADP-ribose)polymerase (PARP) (Cryns et al., 1999; Lazebnik et al., 1994). The cleavage of PARP into its characteristic fragments of 89 and 24 kDa is a hallmark of apoptosis in almost every system (Lamarre et al., 1988; Boulares et al., 1999).

Apoptosis can be divided into two general pathways that usually converge on the activation of downstream caspases or key substrate cleavage like PARP (Figure 1) (Green 1998; Sun et al. 1999). The first general apoptotic pathway involves the ligation of death receptors by their ligands such as the FasR/FasL or the TNFR/TNF system. Upon binding of the ligand adaptor proteins are recruited that bind through death domain motifs to corresponding cytoplasmatic regions of the death receptor. This adaptor molecules then bind through the so called Death Effector Domains to their counterparts in the caspases resulting in the formation of the so called apoptosom in which the aggregated procaspase transactivate. The active caspase, in general caspase 8, subsequently acts to cleave and activate the downstream caspases eventually leading to cell death (Green 1998; Nagata 1999; Uckun et al., 1992; Fulda et al., 1998; Sun et al., 1999). In the second pathway, the release of cytochrome C from the mitochondria into the cytosol is triggered by various forms of cellular stress. Induction of DNA damage for example results in the upregulation of the tumor suppressor protein p53 which is a transcriptional inducer of the bax gene. The Bax protein is a proapoptotic member of the Bcl-2 family which consist of a variety of pro- and anti-apoptotic proteins. Their relative ratios are crucial for the response to a given apoptotic stimulus. Bax translocates and inserts into the mitochondria presumably inducing the release of cytochrome C,

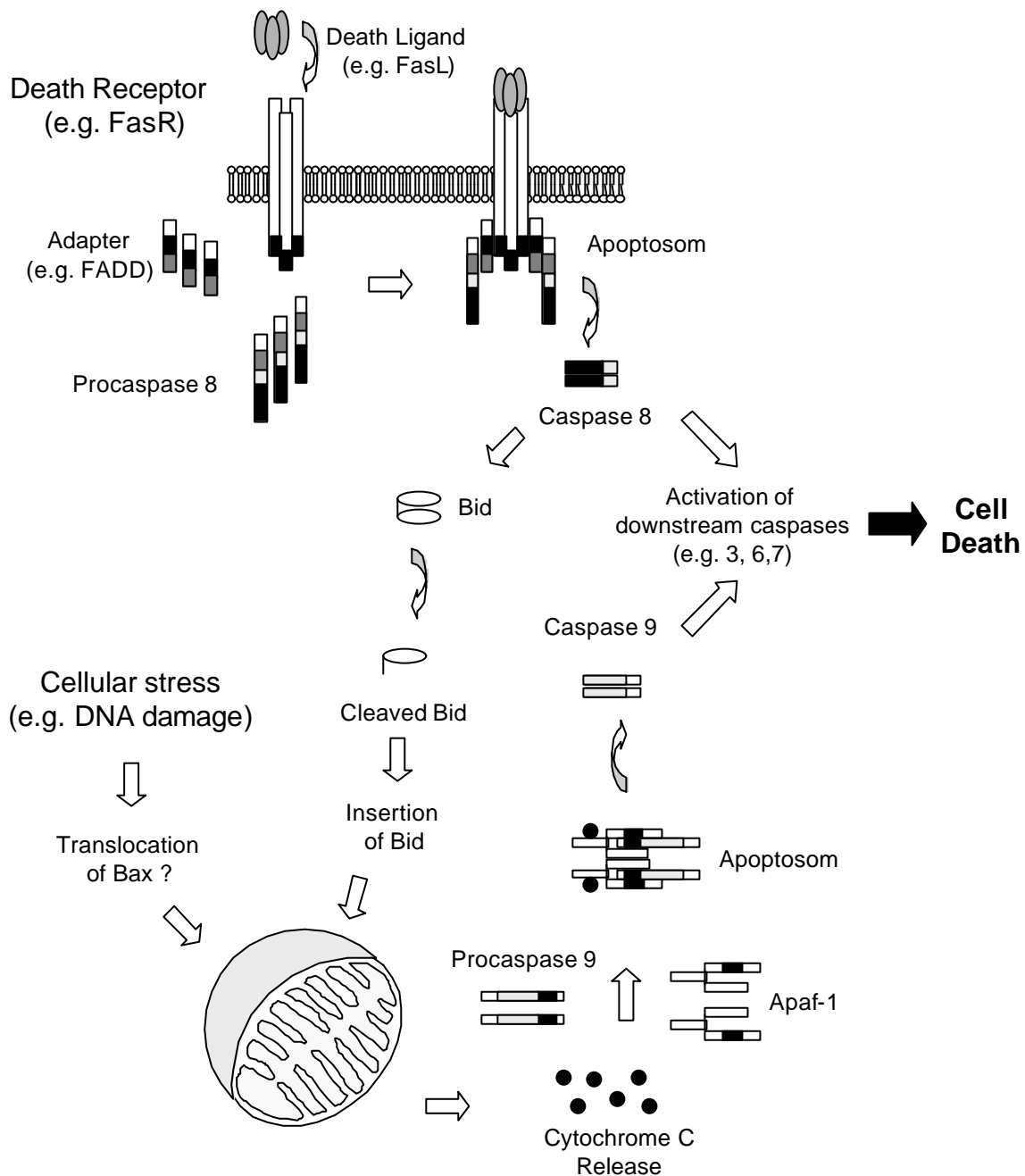


Figure 1: Schematic pathways for caspase activation and apoptosis

The first pathway involves the ligation of death receptors to their ligands. The thereby activated receptor bind adaptor molecules through corresponding Death Domains. The adaptor molecules subsequently bind to the Death Effector Domains of procaspase 8 through their own Death Effector Domains leading to the transactivation of caspase 8. Caspase 8 then cleaves and activates downstream caspases.

In the second pathway various forms of cellular stress trigger the mitochondrial release of cytochrome C, which binds to Apaf1, which in turn self-associates and binds procaspase 9. In this apoptosom transactivation of procaspase 9 into the active caspase 9 follows, and caspase 9 then cleaves and activates downstream caspases.

Cross-talk between the two pathways involves the cleavage of Bid by caspase 8. The C-terminal fragment of Bid then inserts into the mitochondria and induces the release of cytochrome C.

although the mechanism is still unclear (Lakin & Jackson 1999; Goping et al., 1998; Gross et al., 1998; Mignotte and Vayssiere, 1998). The released cytochrome C binds to Apaf1, which in turn self-associates and binds procaspase 9, resulting in the formation of an apoptosom. Transactivation of the complexed procaspase 9 to active caspase 9 follows, and the caspase then cleaves and activates downstream caspases thereby converging with the death receptor pathway (Green 1998; Wolf & Green 1999; Cohen et al., 1999). Cross-Talk between the two pathways can occur through Bid, a proapoptotic member of the Bcl-2 family, which is cleaved by activated caspase 8 (e.g., by ligation of death receptors) whereby a C-terminal fragment is produced that in turn induces the release of cytochrome C from the mitochondria. Cytochrome C subsequently functions to activate Apaf1 and procaspase 9 (Green 1998; Li et al., 1998; Luo et al., 1998).

Aims of this work

1. Analysis of the cerulenin-induced cytotoxicity and initial characterization of the involved signal transduction pathway.
2. Identification of the NB-p260 antigen and further putative apoptosis-mediating receptors in the IgM mediated apoptotic pathway

2. Materials

2.1. Cell lines

Human NB cell lines were obtained from R.C. Seeger (LAN-1, University of California, Los Angeles) (Juhl et al., 1990), N.-K.V. Cheung (NMB-7, Memorial Sloan-Kettering Cancer Center, New York) (Cheung et al., 1985), R. Wada (SH-SY5Y) (Kazmi et al., 1986) and the American Type Culture Collection (IMR-32, SK-N-SH, ATCC, Rockville, MD, USA). The human melanoma cell line SK-MEL-93-2 has been described elsewhere (Ollert et al., 1993). The colon cancer cell line WiDr was by courtesy of H. Kalthoff (University of Kiel, Germany) (Smith et al., 1993). The breast cancer cell lines MCF7 and SK-BR-3, the skin carcinoma cell line A431 and the glioblastoma cell line A-172 were purchased from the American Type Culture Collection (ATCC, Rockville, MD, USA). The transformed keratinocyte cell line HaCaT was kindly provided from the Department of Dermatology (University Hospital of Hamburg, Germany) (Boukamp et al., 1988). Normal human epidermal keratinocytes (NHEK) and normal human lung fibroblasts (NHLF) were from Clonetics (Walkersville, MD, USA).

2.2. Materials for cell culture

The culture medium RPMI 1640 with 2 mM glutamine as well as Trypsin-EDTA were obtained from Biofluids (Biosource International, Rockville, MD, USA). Penicillin, streptomycin and fetal calf serum were purchased from Gibco Life Technologies (Grand Island, NY, USA). Fibroblast growth medium FGM-2 bullet kit, keratinocyte growth medium KGM-2 bullet kit, Trypsin neutralizing solution, Trypsin/EDTA solution, HEPES buffered saline solution for the cultivation of the normal human cell lines were obtained from Clonetics (Walkersville, MD, USA).

2.3. Sera

Normal human serum was obtained by cubital vene puncture of healthy donors. The clotting took place with help of glass pearls in 50 ml centrifuge tubes (E&K Scientific, Saratoga, CA, USA) for approximately 3 h at room temperature. After 15 min of centrifugation at 2500 rpm the sera was obtained, aliquoted and stored at -80°C. Sera of NB patients was available by courtesy of Dr. S. Engler from the University Hospital of Kiel, Germany.

2.4. Antibodies

The various monoclonal, polyclonal and secondary antibodies were purchased from the following companies:

2.4.1. Monoclonal Antibodies

All monoclonal antibodies were of mouse origin if not otherwise indicated.

Chemicon (Temecula, CA, USA):

anti-filamin 90 (clone MAB1680), anti-filamin 190 (clone MAB1678)

MBL (Watertown, MA, USA):

anti-caspase 8 (clone 5F7)

Oncogene (Boston, MA, USA):

anti-MDM 2 (clone IF2), anti-p21 (clone EA10)

PharMingen (San Diego, CA, USA):

anti-p53 (clone DO-7)

Santa Cruz (Santa Cruz, CA, USA):

anti-GADD 153

Stressgen (Victoria, Canada):

anti-hsp 27 (clone G3.1), anti-hsp 60 (clone LK-2), anti-hsp 70 (clone N27F3-4), anti-hsp 90 (rat, clone 16F1), anti-grp 75 (clone 30A5)

Transduction Laboratories (San Diego, CA, USA):

anti-fatty acid synthase (clone 23), anti-filamin (clone 5)

2.4.2. Polyclonal Antibodies

Polyclonal antibodies were of rabbit origin if not mentioned otherwise.

Clontech (Walkersville, MD, USA):

anti-cytochrome C

Oncogene (Boston, MA, USA):

anti-cyclin G1, anti-activated p38-MAPK , anti-activated JNK

Pharmingen (San Diego, CA, USA):

anti-caspase 3

Roche (Indianapolis, IN, USA):

anti-Bcl-2, anti-PARP

Santa Cruz (Santa Cruz, CA, USA):

anti-caspase 9

Sigma (St. Louis, MO, USA):

anti-actin

Transduction Laboratories (San Diego, CA, USA):

anti-Bax

2.4.3. Secondary Antibodies

Amersham Pharmacia Biotech (Piscataway, NJ, USA):

sheep anti-mouse-IgG-HRP, Streptavidin-HRP

Dianova (Hamburg, Germany):

goat anti-mouse IgG-DTAF, goat anti-rabbit IgG-DTAF, goat anti-rat
IgG-DTAF

Pierce (Rockford, IL, USA):

rabbit anti-goat-HRP

Sigma (St. Louis, MO, USA):

goat anti-mouse IgG-AP, goat anti-rabbit IgG-AP, goat anti-rabbit IgG-
HRP, goat anti-rat IgG-AP, goat anti-human IgM-AP

2.5. Chemicals

If not otherwise listed below all chemicals were purchased by either Sigma (St. Louis, MO, USA) or by Fisher (Pittsburgh, PA, USA)

Alexis (San Diego, CA, USA):

PD 169,316, SB203580, Doxorubicin, Etoposide

Amersham Pharmacia Biotech (Piscataway, NJ, USA):

Agarose, NZCYM - broth, (1-¹⁴C)- sodiumacetat, CNBR-activated

Sepharose 4B

Biomol (Plymouth Meeting, PA, USA):

bongkrecic acid

BioRad (Hercules, CA, USA):

Acrylamid/Bisacrylamid (30%, 37.5:1), TEMED, SDS-PAGE Molecular

Weight Standard (broad range), Bromphenolblue, β -Mercaptoethanol

Chemicon (Temecula, CA, USA):

Chemiblot™ Molecular Weight Marker

Calbiochem (San Diego, CA, USA):

zVAD-fmk, Calpeptin

MBI Fermentas (St. Leon-Rot, Germany):

Xho I, Pst I

Molecular Probes (Eugene, OR, USA):

JC-1 (5,5',6,6'-tetrachloro-1,1',3,3'-tetraethylbenzimidazolylcarbo-
cyanine iodide)

Pierce (Rockford, IL, USA):

monomeric Avidin, D-Biotin, Sulfo-NHS-LC-Biotin

Roche (Indianapolis, IN, USA):

Complete™, endoproteinase Lys-C, Arg-C, Asp-N, Glu-C, trypsin
(sequencing grade)

Transduction Laboratories (San Diego, CA, USA):

Annexin V-FITC

2.6. Buffers and Solutions

Further buffers and solutions are listed in the corresponding sections in the Material part.

PBS (Phosphate Buffered Saline):

137 mM NaCl
2.7 mM KCl
6.5 mM Na₂HPO₄
1.5 mM K₂HPO₄
pH 7.4

TBS (Tris Buffered Saline):

20 mM Tris-HCl
500 mM NaCl
pH 7.5

TTBS is TBS with 0.1%
Tween-20

LB Broth:

10 g NaCl
10 g tryptone
5 g yeast extract
ad 1 l dH₂O
pH 7.0
autoclave

LB Agar:

10 g NaCl
10 g tryptone
5 g yeast extract
20 g agar
ad 1 l H₂O
pH 7.0
autoclave

NZY Broth:

5 g NaCl
2 g MgSO₄ • 7 H₂O
5 g yeast extract
10 g NZ amine
ad 1 l dH₂O
pH 7.5
autoclave

NZY Agar:

5 g NaCl
2 g MgSO₄ • 7 H₂O
5 g yeast extract
10 g NZ amine
15 g agar
ad 1 l H₂O
pH 7.5
autoclave

NZY Top Agar:

1 l NZY Broth
7 g agarose
autoclave

SM buffer:

5.8 g NaCl
2.0 g $\text{MgSO}_4 \cdot 7 \text{H}_2\text{O}$
50 ml 1 M Tris-HCl
5 ml 2% (w/v) gelatine
ad 1 l dH_2O
pH 7.5

TE buffer:

10 mM Tris-HCl
1 mM Na_2EDTA
pH 7.9
autoclave

4 x Separating gel buffer:

1.5 M Tris-HCl
0.4 % SDS
pH 8.8

50 x TAE buffer:

2 M Tris-acetate
50 mM Na_2EDTA
pH 8.5
autoclave

10 x TBE buffer:

0.89 M Tris-HCl
0.89 M boric acid
1 mM Na_2EDTA
pH 7.9

4 x Stacking gel buffer:

0.5 M Tris-HCl
0.4 % SDS
pH 6.8

3. Methods

3.1. Tissue Culture

3.1.1. Cultivation of cells

All tumor cell lines were cultivated in culture media (RPMI 1640 with 2 mM glutamine, 10% heat inactivated fetal calf serum, 100 U/ml penicillin and 100 µg/ml streptomycin). The normal human keratinocyte cell line was cultivated in basal keratinocyte growth medium-2 supplemented with 30 µg/ml BPE, 1 ng/ml human recombinant Erythrocyte Growth Factor, 5 µg/ml Insulin, 0.5 µg/ml Hydrocortisone, 1 µl/ml Transferrin, 1 µl/ml Epinephrine and 1 µl/ml GA-1000. The normal human fibroblast cell line was cultivated in basal fibroblast medium-2 supplemented with 1 ng/ml human recombinant Fibroblast Growth Factor, 5 µg/ml Insulin, 50 µg/ml Gentamycin, 50 ng/ml Amphotericin-B and 2 % fetal bovine serum.

For subcultivation of all tumor cell lines the old culture media was discarded and the cells were rinsed once with wash media (RPMI 1640 with 2 mM glutamine without the other supplements). The cells were subsequently detached with a trypsin-EDTA solution and after detachment of the cells fresh culture media was added to neutralize the trypsin. For subcultivation of the normal human cell lines the cells were washed with HEPES buffered saline solution, detached with a trypsin-EDTA-solution and added to a trypsin neutralizing solution. All cell lines were afterwards centrifuged at 1000 rpm for 5 minutes (Centra GP8R, IEC, Needham Heights, USA) and resuspended in fresh culture medium. Incubation took place under 5 % CO₂, 90 % humidity and 37°C (Stericult Incubator, Scientific, Bohemia, USA) in cell culture flasks (Nalgene Nunc, Rochester, USA). All steps were performed under a sterile hood (Steril Gard Hood, Modell VBM-400, Baker, USA).

3.1.2. Determination of the cell number

The number of cells was determined after diluting the cell suspension with an equal aliquot of a trypanblue solution (0.4 % (w/v) in PBS-buffer) by counting in a Neubauer counting chamber (Fisher) under a microscope. The number of cells per ml was calculated by multiplication of the median of the four quadrants with 1×10^4 with regard to the dilution factor. The relation of blue-coloured cells to the total amount of cells yielded the vitality of the cells.

3.1.3. Longterm storage of cells

For longterm storage cells were resuspended in 90 % (v/v) fetal calf serum and 10 % DMSO (v/v) (Sigma) in a concentration between 5×10^6 and 1×10^7 cells/ml. The cells were frozen overnight at -20°C , then for 24 h at -80°C and finally transferred into liquid nitrogen. For thawing the frozen cells were thawed in a 37°C waterbath, immediately transferred into the appropriate culture medium, centrifuged and cultivated.

3.2. Protein Biochemistry

3.2.1. Preparation of cell extracts

Cells were washed with RPMI 1640, detached with trypsin-EDTA, fresh culture media was added and the cells were centrifuged for 5 min at 1000 rpm. The pellet was resuspended in PBS and washed once. Depending on the purposes the cell extracts were used for three different extractions methods were applied. Usually cells were resuspended in lysis-buffer A and vortexed for approximately 30 seconds. The DNA was then pelleted by centrifugation for 5 min at 14.000 rpm (Eppendorf Centrifuge 5417R, Brinkmann, Westbury, USA). Sixfold reduction sample buffer was added and the extracts were stored at -80°C until further use. In case complete cell extracts were used, the cells were resuspended in lysis-buffer B and solubilized by sonication (Ultrasonic Liquid Processor XL2020 Sonicator, Heat Systems, Farmingdale, USA). Six-fold reduction sample buffer was directly added and the extracts were stored at -80°C. Cell extracts that were used for purification were prepared in the following manner. 5×10^8 cells were resuspended in 30 ml lysis-buffer C. To solubilize the proteins the structure of the DNA was destroyed using a syringe. The DNA was first pelleted at 8000 rpm for 10 min and then centrifuged for further 10 min at 14000 rpm to remove still present DNA. Cell extracts were directly used for purification of proteins.

Lysis-buffer A:

20 mM Tris-HCl
150 mM NaCl
5 mM Na₂EDTA
1 % Triton-X-100
1 % Complete™
pH 8.3

Lysis-buffer B:

20 mM Tris-HCl
150 mM NaCl
5 mM Na₂EDTA
1 % SDS
1 % Complete™
pH 8.3

Lysis-buffer C:

20 mM Tris-HCl
75 mM NaCl
5 mM Na₂EDTA
1 % Triton-X-100
1 % Complete™
pH 8.3

3.2.2. Purification of proteins

For purification of the different proteins (for details see 3.2.2.1 - 3.2.2.7.) LAN-1 cells were lysed in 10 ml lysis buffer B per 1×10^8 cells and cell extracts prepared accordingly to 3.2.1.. 40 ml cell lysate was then applied to a 10 ml anion exchange chromatography column (HighQ, BioRad). The different proteins were eluted with varying NaCl concentrations in buffer A, buffer exchanged against buffer B or C (PD-10, Amersham Pharmacia Biotech) and applied to a 10 ml cation exchange chromatography (EconoS, BioRad). The third column was usually a 5 ml hydroxyapatite column (CHTII, BioRad) except for hsp70 where an ADP-agarose matrix (Sigma) was used. The fractions containing the target protein were pooled and concentrated by ultrafiltration using centrifugal devices with an appropriate molecular weight cut off (Millipore, Bedford, USA). Final purification to homogeneity was achieved by preparative gelelectrophoresis using a Prep Cell (Prep Cell Model 491, BioRad). The separating gel concentrations varied in dependence of the molecular weight of the target protein, stacking gel concentrations were always 4% (v/v). If not otherwise indicated all purification steps took place at 4°C. The applied flow rates were 1 ml/min (Peristatic pump P1, Amersham Pharmacia Biotech) and fractions were collected in 2.5 ml aliquots (Model 2110, BioRad). The purification process was controlled by SDS-PAGE under reducing conditions and Coomassie or silverstaining.

Buffer A:

20 mM Tris-HCl
5 mM Na₂EDTA
75 mM NaCl
0.1 % Triton-X-100
0.1 % Complete™
pH 8.3

Buffer B:

50 mM sodium-phosphate
0.1 % Triton-X-100
0.1 % Complete™
pH 6.5

Buffer C:

10 mM sodium-phosphate
0.1 % Triton-X-100
0.1 % Complete™
pH 6.5

3.2.2.1. Purification of fatty acid synthase (FAS)

Human fatty acid synthase (FAS) was eluted from the anion exchange column in a step gradient between 175 mM and 225 mM NaCl in buffer A, buffer exchanged against buffer B and subsequently applied to the 10 ml cation exchange chromatography column. The breakthrough containing the FAS was directly applied to the hydroxyapatite chromatography column. Elution of FAS was achieved by a step gradient between 50 mM and 160 mM sodiumphosphate in buffer B. The FAS containing fractions were pooled and concentrated by ultrafiltration (100 kDa MWCO) and further purified to homogeneity by preparative SDS-PAGE using a 3.5 % separating gel.

3.2.2.2. Purification of NB-p260

The NB-p260 was eluted from the anion exchanger between 175 mM and 225 mM NaCl in buffer A, buffer exchanged to buffer B and applied to the cation exchanger. The NB-p260 containing breakthrough was applied to the hydroxyapatite column where separation from FAS was achieved with a step gradient from 160 to 350 mM sodiumphosphate in buffer B. Separation of the ABP-278 component of the NB-p260 was achieved by introducing an additional step between 160 and 225 mM sodiumphosphate. The protein containing fractions were pooled, concentrated (50 kDa MWCO) and finally purified by preparative gelelectrophoresis using a 3.15 % separating gel.

3.2.2.3. Purification of heat shock protein 27 (hsp27)

Hsp27 was eluted between 75 and 100 mM NaCl from the anion exchange column and buffer exchanged to buffer C. Elution from the cation exchange column was achieved using a step gradient between buffer C and buffer B with 100 mM NaCl. The fractions were applied to the hydroxyapatite column, eluted in the breakthrough and were subsequently concentrated (MWCO 30 kDa). Final purification was done by preparative gelelectrophoresis using a separating gel concentration of 13 %.

3.2.2.4. Purification of heat shock protein 60 (hsp 60)

A gradient between 150 and 250 mM NaCl yielded hsp 60 from the cation exchanger. After buffer exchanging to buffer C, hsp 60 was applied to the cation exchange column where it came in the breakthrough. The breakthrough was afterwards directly applied to the hydroxyapatite column where hsp 60 was eluted between 150 und 225 mM sodiumphosphate in buffer B. Hsp 60 containing fractions were pooled, ultrafiltrated (50 kDa MWCO) and finally purified through a 8.8% separating gel by preparative gelelectrophoresis.

3.2.2.5. Purification of heat shock protein 70 (hsp 70)

Hsp 70 was eluted between 100 and 150 mM NaCl form the cation exchange column. After buffer exchange to buffer C hsp 70 was eluted in a step gradient between 0 and 1 M NaCl in buffer B. Subsequently hsp 70 was purified by ADP agarose. For approximately 1 ml of ADP agarose matrix 60 µg of ADP agarose were equilibrated overnight in binding buffer. Hsp 70 containing fractions were then buffer exchanged against binding buffer, added to the ADP agarose matrix and incubated overnight on a

rotating shaker (ATR, Laurel, USA) at 4°C. The matrix was afterwards transferred in a 2 ml column (Pierce) and washed thoroughly (about 10 column volumes) first with binding buffer and second with washing buffer. Afterwards another washing step followed using washing buffer. Elution buffer was done with washing buffer containing 3 mM ADP. The hsp 70 containing breakthrough was pooled, concentrated (30 kDa MWCO) and eventually purified to homogeneity through a 7.5 % separating gel by preparative gelelectrophoresis.

| <u>Binding buffer:</u> | <u>Washing buffer:</u> | <u>Elution buffer:</u> |
|--------------------------------|------------------------|------------------------|
| 20 mM Tris-Acetat | Binding buffer | Binding buffer |
| 20 mM NaCl | 0.5 M NaCl | 0.5 M NaCl |
| 15 mM β -Mercaptoethanol | | 3 mM ADP |
| 3 mM $MgCl_2$ | | |
| 0.1% Complete™ | | |
| pH 7.5 | | |

3.2.2.6. Purification of heat shock protein 90 (hsp 90)

Hsp 90 was eluted with a gradient between 250 and 325 mM NaCl from the anion exchanger, subsequently buffer exchanged to buffer C and applied to the cation exchanger. The hsp 90 containing breakthrough was applied to the hydroxyapatite chromatography column and hsp 90 was eluted by a step gradient between 200 and 250 mM sodiumphosphate in buffer B. The hsp 90 containing fractions were pooled, concentrated (100 kDa MWCO) and purified to homogeneity by preparative SDS-PAGE using a separating gel of 6 %.

3.2.3. SDS-polyacrylamid-gelelectrophoresis (SDS-PAGE)

SDS-PAGE was performed in accordance with the original method described by Lämmli (Lämmli, 1970).

Gelelectrophoresis in a minigel-apparatus (LKB 2050, MIDGET, Amersham Pharmacia Biotech) was performed to control the various steps of the purification procedures as well as for Western blotting analysis. The dimensions of the separating gel were approximately 9 x 6 x 0.75 cm, the ones for the stacking gel 9 x 2 x 0.75 cm. The concentration of the separating gel varied between 7.5 and 13% in dependence of the size of the proteins, the concentration of the stacking gel was on principle 4%. A 30 % acrylamid-solution with 0.81 % (w/w) N,N'-bismethylen-acrylamid was used as stock solution. Samples were boiled with 6-fold reducing sample buffer and run at 170 V in electrophoresis buffer.

Separating gel:

375 mM Tris-HCl
x % acrylamid (w/v)
0.1 % SDS (w/v)
0.05 % TEMED (v/v)
0.05 % APS (w/v)
pH 8.8

Stacking gel:

125 mM Tris-HCl
4 % acrylamid (w/v)
0.1 % SDS (w/v)
0.05 % TEMED (v/v)
0.06 % APS (w/v)
pH 6.8

6-fold reducing sample buffer:

375 mM Tris-HCl
300 mM DTT
30 % glycerine (v/v)
12 % SDS (w/v)
0.006% bromphenolblue (w/v)

Electrophoresis buffer:

25 mM Tris-HCl
192 mM glycine
0.1% SDS (w/v)
pH 8.3

3.2.4. Storage of gels

Gels were dried in a drying system between two cellophan foils for 24 h (SE 1200 Easy Breeze Air Gel Dryer, Amersham Pharmacia Biotech).

3.2.5. Staining of proteins with Coomassie Brilliant Blue R-250

After finishing the gelelectrophoresis the stacking gel was stained in the staining solution for 20 min and afterwards destained in the destaining solution. The destained gels were stored in dH₂O until drying.

Staining solution:

0.25 % CBB R-250 (w/v)
45 % methanol (v/v)
45 % dH₂O (v/v)
10 % acetic acid (v/v)

Destaining solution:

45 % methanol (v/v)
45 % dH₂O (v/v)
10 % acetic acid (v/v)

3.2.6. Staining of proteins with silvernitrate

After electrophoresis the separating gels were fixed for 30 to 60 min depending on their polyacrylamid-concentration in the fixing solution. The gels were then transferred for 1 h or overnight in the incubation solution, washed three times in ddH₂O and were afterwards stained for 30 min in staining solution. Finally the gels were rinsed in dH₂O and developed in the developing solution until a sufficient staining was accomplished. The development was stopped by transferring the gels in the stop and storage solution.

Fixing solution:

30 % ethanol (v/v)
15 % acetic acid (v/v)
55 % dH₂O

Incubation solution:

500 mM sodium acetate
14 mM sodium dithionite
25 % ethanol (v/v)
0.5 % glutardialdehyde, 25%

Staining solution:

6 mM silvernitrate
0.03 % formaldehyde, 30% (v/v)

Developing solution:

262 mM sodium carbonate
0.03 % formaldehyde, 30% (v/v)

Stop and storage solution:

50 mM Na₂EDTA

3.2.7. Determination of protein concentrations

For determination of protein concentrations the BCA-Assay (Smith et al., 1985) in a microtiter plate was used. Therefore 10 μ l of the sample were added to 200 μ l solution C (50 parts solution A and 1 part solution B) and the mixture was incubated for 30 min at 37°C. The plate was then cooled to room temperature and the samples measured at 550 nm using a Plate Reader (HTS 7000 Plus, Perkin Elmer, Meriden, CO, USA). A serial dilution of bovine serum albumin was used for the calibration curve. BSA was dissolved and diluted in the same buffer in which the samples were present. All measurements were done at least in duplicate.

Solution A:

1 % BCA (w/v)
2 % Na₂CO₃ •H₂O (w/v)
0.16 % sodium tartrate (w/v)
0.4 % NaOH (w/v)
0.95 % NaHCO₃ (w/v)
pH 11.25

Solution B:

4 % CuSO₄•5 H₂O (w/v)

3.2.7. Electrophoretic transfer of proteins

The transfer sandwich, the sponges and the filter papers were equilibrated for approximately 10-15 min in transfer buffer. PVDF membranes were used as transfer membranes and prepared according to the supplier's instruction (Immobilon-P, Millipore). After finishing the SDS-PAGE the separating gel was equilibrated for 5 min in transfer buffer, the sandwich assembled and inserted in the transfer chamber (TE Series Transphor Electrophoresis Unit, Amersham Pharmacia Biotech). Transfer took place under ice cooling at a voltage of 50 V. Transfer times were dependent of the size of the proteins and varied between 30 min to 3 h.

Transfer buffer:

10 mM CAPS
10 % methanol (v/v)
pH 11

3.2.9. Expression of FAS in different cell lines

Cell extracts of various tumor cell lines (LAN-1, NMB-7, IMR-32, SK-N-SH, HaCaT, A431, WiDr, SK-MEL 93-2, MCF-7, SK-BR-3) and the normal human cell lines NHEK and NHLF were prepared as described earlier (see 3.2.1.). Protein concentrations were measured in duplicate by BCA-assay, readjusted to approximately 800 $\mu\text{g/ml}$, measured again in triplicate by BCA-assay and eventually adjusted to a final concentration of 633 $\mu\text{g/ml}$. For quantification experiments 10 μg of each cell extract in triplicate and a serial dilution of purified FAS (10 to 400 ng) as internal standard were separated on 7.5 % polyacrylamide gels. The proteins were then electrophoretically transferred (2 hours, 50 Volt) onto PVDF-membranes and immunoblotted against a monoclonal mouse anti-FAS antibody (Transduction Laboratories). The blots were developed by chemiluminescence and subsequently analyzed by 1D Image Analysis Software (Version 3.0, Eastman Kodak, Rochester, USA).

3.2.10. Expression of hsp 60, hsp 70 and hsp 90 in different cell lines

Expression of hsp 60, hsp 70 and hsp 90 was analyzed in a variety tumor cell lines (LAN-1, NMB-7, IMR-32, SK-N-SH, SY5Y, HaCaT, A431, WiDr, SK-MEL 93-2), the normal human cell lines NHEK and NHLF and normal human brain tissue lysate (Imgenex, San Diego, CA, USA). Cell extracts and determination of protein concentrations was done as mentioned earlier (see 3.2.1. and 3.2.9.). For quantification experiments 5 μg of each cell extract in triplicate and a serial dilution of the purified hsp (12.5 to 300 ng) as an internal standard were separated on 7.5 % polyacrylamide gels and then electrophoretically transferred for 1 h and 50 V onto PVDF-membranes. The membranes were probed with monoclonal antibodies against hsp 60 (mouse), hsp 70 (mouse) and hsp 90 (rat) (Stressgen), developed by chemiluminescence and analyzed by 1D Image Analysis Software (Version 3.0, Eastman Kodak).

3.2.11. Screening of patient sera for immunoreactivity against heat shock proteins hsp 60, hsp 70 and hsp 90

To evaluate immunoreactivity of patient sera against against the heat shock proteins hsp 27, hsp 60, hsp 70 and hsp 90 100 ng of each of the purified proteins were separated by 10 % SDS-PAGE for hsp 60, hsp 70 and hsp 90 and 13 % SDS-PAGE for hsp 27, respectively, and electrophoretically transferred onto PVDF-membranes (60 min, 50 V). Reactivity against the various proteins was then determined by probing with different patient sera in 1:20 dilutions.

3.2.12. Labeling of cell surface proteins with Sulfo-NHS-LC-Biotin

For labeling of cell surface proteins the membrane impermeable biotin derivate Sulfo-NHS-LC-Biotin (Pierce) as well as subconfluent cells were used to minimize biotinylation of internal proteins. 1.5×10^8 cells were washed once with PBS buffer and then biotinylated for 30 min at 4°C using 30 µg Sulfo-NHS-LC-Biotin in 1 ml PBS buffer for 1×10^7 cells. The cells were afterwards washed twice with wash media, detached with a cell scraper and cell viability was checked with trypan blue. Cells were only used if cell viability was smaller 5 %. The cells were then pelleted for 5 min at 1000 rpm (Centra GP8R, IEC) and washed for two more times with RPMI 1640 including supplements. Finally cell extracts were prepared as described earlier (see 3.2.1.) using 5 ml lysis-buffer.

3.2.13. Isolation of biotin-labeled proteins by monomeric avidin

For isolation of biotinylated proteins a monomeric avidin matrix (Pierce) was chosen to allow elution of the biotinylated proteins under mild conditions. A 3 ml monomeric avidin matrix was prepared following the supplier's instruction and transferred into a 4 ml column (Econo-column,

BioRad) which was connected to a peristaltic pump (P1, Amersham Pharmacia Biotech) and a fraction collector (Model 2110, BioRad). 4 ml of biotinylated sample were applied to the column. After the sample had entered the matrix, the column was closed and incubated for 30 min at room temperature to allow efficient binding of biotinylated proteins. Then the column was washed first with PBS including 0.1% Tween-20 and second with PBS containing 1 M NaCl to elute non-biotinylated and non-specific bound proteins. After absorbance at $\lambda = 280$ nm has reached baseline again, biotinylated proteins were eluted with 0.1 M Glycin-HCl, pH 2.8.

3.2.14. Generation of internal fragments of NB-p260 by endoproteinase Lys-C digestion

Endoproteinase Lys-C (sequencing grade, Roche) is a serine protease which cleaves peptid bonds C-terminal to Lysin. Digestion was performed in electrophoresis buffer in which the NB-p260 was present after the purification procedure. For generation of low molecular weight fragments endoproteinase Lys-C : NB-p260 ratios of 1:20, 1:50 and 1:100 were incubated for 5, 10 and 15 h with or without adding new enzyme every five hours. For generation of high molecular weight fragments the NB-p260 was incubated for 2, 4 and 6 h with endoproteinase Lys-C at ratios of 1:50 and 1:100. In both cases incubation took place at 25°C under shaking (Thermocycler 5436, Eppendorf). To terminate the digestion reactions reducing sample buffer was added and the samples were boiled for 10 min. Samples were then stored until further use at -80°C.

3.2.15. Amino acid sequencing

Protein(fragments) for N-terminal sequencing were separated by SDS-PAGE and electrophoretically transferred onto a PVDF-membrane (Immobilon P^{SQ}, Millipore). The membrane was subsequently washed with dH₂O, stained for approximately 60 seconds in staining solution and was then destained for 30 min in destaining solution. After thorough washing, the membrane was airdried, relevant bands cut out and stored at -20°C until N-terminal sequencing was performed.

N-terminal sequencing was done by automatized Edman degradation in a liquid-phase-sequenator (ABI 476A, Applied Biosystems, Weiterstadt, Germany) with a connected data analysis program (Model 610A, version 1.2). Sequencing was performed by courtesy of Dr. M. Teppke (Department of Biochemistry and Molecular Biology, University of Hamburg, Germany). Sequenced bands were evaluated with the SWISS-PROT data base.

Staining solution:

0.1% CBB R-250 (w/v)
40 % methanol (v/v)
59 % dH₂O (v/v)
1 % acetic acid (v/v)

Destaining solution:

50 % methanol (v/v)
50 % dH₂O (v/v)

3.2.16. Protein identification by Toplab

Commercial protein identification of the non-ABP-280 reactive NB-p260 compound was performed by Toplab GmbH (Martinsried, Germany). To that end the non-ABP-280 reactive NB-p260 compound was purified as described earlier (see 3.2.2.2). The purified protein was then again separated by SDS-PAGE (7.5 %), stained with Coomassie Brilliant Blue 250 and the protein containing bands were cut out. The bands were thoroughly washed with ddH₂O and subsequently send in ddH₂O to Toplab for further manipulations.

At Toplab an in-gel digest with endoproteinase Lys-C was performed and the resulting peptides were separated by RP-HPLC (HP 1100, Hewlett Packard, Germany). A MALDI-MS fingerprint was then carried out from selected HPLC fractions and one fraction was subjected to N-terminal sequence analysis by Edman degradation (Procise 492, PE Biosystems, Germany).

3.3. Immunology

3.3.1. Immunoblotting

After finishing the electrophoretic transfer membranes were washed once in washing buffer and unspecific protein binding sites were blocked for 1 h in 5 % non fat dry milk in washing buffer. The membranes were washed once again and then incubated in the first antibody in an appropriate dilution in 5 % non fat dry milk in washing buffer for two hours at room temperature or overnight at 4°C. Afterwards the membranes were washed three times for 10 min in washing buffer before incubation in the second antibody in an appropriate dilution in washing buffer with 5% non fat dry milk took place for 2 h. After washing for three times again, the membranes were developed by either using chemiluminescent-development (HRP: SuperSignal West Pico Chemiluminescent Substrate, Pierce; AP: Immun-Star™ Substrate, BioRad) or color-development (NBT/BCIP). In case of chemiluminescent development the membranes were incubated for 5 min in the substrat solution (in case of HRP: 1 part luminol/enhancer : 1 part peroxidase solution) and exposed for varying times depending on the quality of the used antibodies and the amount of the corresponding antigen. Films were then developed between 10 sek to 1 min, rinsed in water and fixed for 7 min. The fixed films were washed for 20 min and airdried. For color development membranes were incubated in the color development solution until a sufficient staining was achieved. The membranes were then washed in dH₂O and airdried. With asterix (*) marked immunoblots in chapter 4.4.5. were done by Dr. David.

Washing buffer:

50 mM Tris-HCl
150 mM NaCl
0.3 % Tween-20 (v/v)
pH 8.0

Color development solution:

0.1 M Tris-HCl
0.004 M MgCl₂
0.01 % NBT (w/v)
0.005 % BCIP (w/v)
pH 9.5

3.3.2. Purification of human IgM antibodies

For purification of human anti-NB IgM antibodies sera of donors with a cytotoxicity greater than 80 % against human NB cells were used. To that end 15 ml of sera were first purified by gelfiltration using a Sephacryl S-300 HR matrix (Amersham Pharmacia Biotech) with a volume of 620 ml (dimensions: 100 x 5 cm). The sera was loaded directly on the gel filtration matrix and subsequently washed into the matrix with buffer 1. Separation was achieved using the same buffer at a flow rate of 0.17 ml/min. Fractions were collected in 4 ml aliquots and an elution profile was recorded by measuring the absorption at a wavelength $\lambda = 280$ nm (Shimadzu UV160U, Japan). The IgM containing fractions were pooled and applied to a 30 x 1.5 cm anion exchange chromatography column in buffer 1 (Macro Prep High Q, BioRad). After washing thoroughly with buffer 1, elution took place by using a linear NaCl gradient (0-1 M NaCl) in buffer 1 at a flow rate of 2 ml/min. Fractions were again collected in 4 ml aliquots. The IgM containing fractions were pooled and concentrated by ultrafiltration (Amicon ultrafiltration unit 8010, Diaflo ultrafilter XM 300, Amicon, Witten/Ruhr, Germany) to a final concentration of 1 or 2 mg/ml. The concentrated IgM antibodies were finally sterile filtrated using a cellulose acetate filter (Millex-Ha sterile filter 0.45 μ m, Millipore), aliquoted and stored until further use at -20°C.

Buffer 1:

30 mM sodiumphosphate
pH 7.0

3.3.3. Inhibition of anti-NB IgM-induced apoptosis by NB-p260

To verify the function of the NB-p260 as apoptosis inducing receptor cytotoxic anti-NB IgM antibodies were preadsorbed on immobilized NB-p260 and the nonbound IgM fraction was analyzed for induction of apoptosis.

To that end 1 cm² nitrocellulose membrane (BioRad) was cut into small pieces and incubated with purified NB-p260 (50 µg) in 0.2 ml of 50 mM Tris-HCl, pH 8.0 for 2 h at 4°C. After washing for three times with TBS buffer, the membrane pieces were blocked for 2 h in 10 % (w/v) nonfat dry milk in TBS buffer. The membrane pieces were washed once again before preadsorption of 80 µl purified cytotoxic anti-NB IgM antibodies (1 mg/ml) took place for 2 h at 4°C. The supernatant containing the nonbound IgM fraction was subsequently evaluated for its ability to induce apoptosis (see 3.4.1.). Control experiments were performed by incubating anti-NB IgM antibodies with nitrocellulose pretreated with nonfat dry milk only (negative control) and by induction of apoptosis with non preadsorbed anti-NB IgM antibodies. The extent of apoptosis was measured by cytofluorometric analysis (FACScan, Becton Dickinson, Germany) using Annexin V and propidium iodide (see 3.4.2.).

3.3.4. Serological screening of recombinant cDNA expression libraries (SEREX)

To identify antigens that are reactive against human polyclonal anti-NB IgM an approach called serological screening of recombinant cDNA expression libraries (SEREX) was employed using a cDNA library that was constructed from LAN-1 cells (see 3.5.1.). The used vector contains an IPTG inducible β -galactosidase promotor that is positioned 5' upstream of the inserted cDNA. Induction with IPTG leads to the expression of a fusion protein containing the translated cDNA insert. These recombinant proteins can then be identified using suited antisera.

For identification of positive clones/plaques approximately 5×10^4 cells were plated on 150 mm² NZY agar plates and incubated at 37°C until small plaques were visible. Membranes were in parallel treated with 10 mM IPTG, airdried and then applied to the plates. The plates were incubated overnight at 37°C. Subsequently the plates were cooled for about 30 min at 4°C to further harden the NZY Top Agar. The membranes and the plates were accordingly marked and washed 5 times with TBS buffer. After blocking for at least two hours the membranes were immersed in the first antisera solution overnight at 4°C. The membranes were subsequently washed for three times with washing buffer (see 3.2.1.) and incubated for 2 h with the second antibody-AP conjugate in an appropriate dilution. After washing again two times with washing buffer and one time with 0.1 M Tris-HCl the membranes were developed using BCIP-NBT color development.

Positive plaques were picked, immersed in 500 μ l SM buffer and 20 μ l chloroform and incubated overnight at 4°C overnight to release the phage particles. The picked plaques were screened for two further rounds using about 100 to 500 plaques per 85 mm² plate to receive a monoclonal phage stock which was stored at 4°C.

3.3.5. Preabsorption of IgM antibodies at E.coli phage lysate (ECPL)

Polyclonal sera usually contain antibodies that are cross reactive with either E.coli or phage proteins. Hence it is necessary to preabsorb these antibodies at E.coli phage lysate (ECPL) in order to screen a cDNA library. Therefore purified anti-NB IgM antibodies (see 3.2.2.) were preabsorbed using different matrices.

- a. To prepare a matrix coupled to E.coli proteins a 20 ml culture of XL-1 Blue MRF' cells were grown overnight, pelleted for 20 min at 2000 rpm and resuspended in 10 ml buffer 1. Five mg of a lysozyme solution (25 mg/ml ddH₂O) was added and the suspension was incubated for 20 min at room temperature to allow the breakdown of the bacterial cell walls. 20 µl of DNase I and 100 µl Triton-X-100 were added and the suspension was incubated for further 60 min at room temperature. The DNA was then pelleted for 30 min at 50000 x g and the supernatant buffer exchanged against buffer 1.
- b. For the preparation of a matrix coupled to E.coli and phage proteins 20 ml XL1-Blue MRF' cells were infected with a non recombinant λ ZAP phage stock and grown short before cell lysis occurred (usually about 4 h). Protein extracts were done as described under 3.3.5.a and buffer exchanged against buffer 1.

The protein containing supernatant was then further depleted of any residual DNA by anion exchange chromatography. To this end the respective supernatants were applied to a 5 ml anion exchange chromatography (HighQ, BioRad) in buffer 1. Elution was performed in two steps. First a linear gradient between buffer 1 and buffer 1 containing 0.5 M NaCl was applied before final elution was done with buffer 1 containing 1 M NaCl. The purification process was monitored by reading

the absorbance at 260 nm and 280 nm and the ratio was used to determine the DNA content of the various fractions. Coomassie staining was used to doublecheck these results. The protein containing fractions were afterwards buffer exchanged to coupling buffer and subsequently measured for protein concentrations by BCA assay. For both preparations 20 ml matrices of CNBr-activated Sepharose 4B were prepared according to the manufacturer's instructions (Amersham Pharmacia Biotech). 5 g of the freeze-dried matrix were suspended in 50 ml 1 mM HCl and the matrix was then washed for 15 min with 1 l of 1 mM HCl. The matrices were subsequently incubated overnight with 100 mg protein of the respective supernatants in 30 ml of coupling buffer at 4°C on a rotating shaker. The matrices were afterwards pelleted at 1000 rpm for 5 min. After washing with 100 ml coupling buffer and blocking non occupied binding sites with blocking buffer for 2 h at room temperature, the matrices were washed with three cycles of washing buffers 1 and 2 and finally resuspended and stored in TBS buffer containing 0.2 % sodiumazide. Coupling efficiencies were checked both by reading the absorbance at 280 nm and by Coomassie staining of the protein containing supernatant before and after coupling.

Buffer 1:

50 mM sodium carbonate
0.1 % Tween 20 (v/v)
pH 9.0

Coupling buffer:

0.1 M sodium carbonate
0.5 M NaCl
pH 8.3

Blocking buffer:

0.2 M glycine-HCl
pH 8.0

Washing buffer 1:

0.1 M sodium acetate
0.5 M NaCl
pH 4.0

Washing buffer 2:

0.1 M Tris-HCl
0.5 M NaCl
pH 8.0

- c. A commercially available E.coli lysate coupled to a matrix was purchased from Pierce transferred into a 5 ml column and subsequently used for preadsorption.

Preadsorption of anti-NB IgM antibodies was performed by incubation of the antibodies with the prepared matrices at 4°C overnight on a rotating shaker. The non-bound IgM antibodies were then recovered, probed for reactivity against both LAN-1 cell extracts and ECPL and stored for further use at 4°C with 0.1% sodiumazide as conservative.

3.3.6. Cytofluorometric Binding Assays

Flow cytometry is a method to investigate single cells in solution. In this context the fluorescence of cells was measured using fluorescence marked secondary antibodies. Cells were detached and washed twice with ice cold PBS buffer. 5×10^5 cells were then incubated in 100 μ l PBS buffer containing the primary antibody for 60 min at 4°C. After washing twice with PBS buffer the cells were resuspended in 100 μ l PBS containing the secondary antibody conjugated to DTAF (1:50 dilution) and incubated for further 60 min at 4°C. Subsequently the cells were washed twice with PBS and resuspended in 300 μ l PBS for measurement. For determination and exclusion of dead cells propidium iodide in a final concentration of 1 μ g/ml was added directly before measurement.

To determine for unspecific binding of the secondary antibody controls were run without first antibody incubation. Usually 5000 cells were measured with a FACScan and analyzed with LysisII, version 1.1 (Becton Dickinson, Germany).

3.4. Apoptosis

3.4.1. Induction of apoptosis with human anti-NB IgM

For induction of apoptosis with anti-NB IgM antibodies cells were detached at subconfluency and incubated at 37°C for indicated times at a concentration of 2×10^5 cells/ml in supplemented RPMI 1640 media in the presence or absence of IgM antibodies. For induction of apoptosis with anti-NB IgM antibodies a concentration of 100 µg/ml was used. Control experiments were performed by incubation with 100 µg/ml IgM antibodies of a negative donor or buffer only.

3.4.2. Induction of apoptosis with cerulenin

For induction of apoptosis with cerulenin cells were plated for 18 h prior to addition of cerulenin using 0.5 ml RPMI 1640 with supplements per 10^5 cells. Cerulenin (5 mg/ml in DMSO) was then added to yield concentrations of 5, 10 or 15 µg/ml and incubated for indicated times. Control experiments were done by incubating with 2.5 µl DMSO/ml media only.

3.4.3. Cytofluorometric determination of apoptotic cells

Quantification of apoptotic cells was performed by FACScan analysis (Becton Dickinson). For Annexin V staining, cerulenin-treated cells were washed in PBS, incubated with Annexin V-FITC and propidium iodide for 15 min at room temperature. Annexin V-positive cells that did not take up propidium iodide were identified as early apoptotic, whereas Annexin V-positive cells that could also be stained with propidium iodide were classified as late apoptotic. If not indicated otherwise, the percentage of both cell populations was used to calculate the extent of apoptosis after subtraction of corresponding background values.

3.4.4. Assessment of the mitochondrial potential (ΔY_m)

Changes in the mitochondrial membrane potential were measured by flow cytometry using the cationic lipophilic dye JC-1 (5,5',6,6'-tetrachloro-1,1',3,3'-tetraethylbenzimidazolyl-carbocyanine iodide) according to the supplier's instructions (R&D Systems, Minneapolis, USA). JC-1 aggregates in intact mitochondria producing a red fluorescence (590 nm). Upon depolarisation of the mitochondrial potential (and the pH) JC-1 dissociates resulting in green fluorescence (525 nm) of the monomeric state (Salvioli et al., 1997). Hence the depolarization of the mitochondrial potential is indicated by a decrease in the red fluorescence and an increase in the green fluorescence. After incubation with or without cerulenin for indicated times 1×10^6 cells were pelleted and subsequently resuspended in reaction buffer, JC-1 was added to a final concentration of 10 μ M and incubated at 37°C, 5 % CO₂ for 20 minutes. Both red (FL-2) and green (FL-1) fluorescence emissions were analyzed using a FACScan and the software Cell Quest (Becton Dickinson).

3.4.5. Detection of cytochrome C release

For detection of cytochrome C release 4×10^6 cells were incubated for indicated times with or without cerulenin (15 μ g/ml). Cells were subsequently harvested and mitochondrial and cytosolic fractions were separated with the ApoAlert Cell Fractionation Kit according to the supplier's instructions (Clontech). To this end cells were resuspended in 400 μ l wash buffer, centrifuged 5 min for 3500 rpm and suspended in 200 μ l Fractionation Buffer Mix. The cells were then incubated for 10 min on ice before they were homogenized with a 200 μ l dounce tissue grinder (Fisher, Pittsburgh, USA). Nuclei were separated by centrifugation for 10 min at 2500 rpm. The supernatant was afterwards centrifuged for 25 min at 10000 rpm. The pellet (mitochondrial fraction) was resuspended in 50 μ l reducing sample buffer, while the supernatant (cytosolic fraction) was treated with sixfold reducing sample buffer. Samples were then analyzed for cytochrome C release.

3.5. Molecular Biology

3.5.1. RNase decontamination of equipment and buffers

RNase's are extremely stable and therefore great care is necessary to prevent any contaminations with them or to inactivate them in a proper way, respectively. Water and buffers were incubated overnight at 37°C with 0.1% diethylpyrocarbonate (DEPC) as RNase inhibitor and subsequently autoclaved to decompose the DEPC as long as not RNase free components were used. All pipette tips and reaction tubes were RNase free single use commodities. Pipettes and benches were cleaned with RNase Away (MβP, San Diego, CA, USA).

3.5.2. Construction of a cDNA library

A cDNA library of LAN-1 cells was constructed using the λ ZAP Express System (Stratagene, La Jolla, CA, USA).

3.5.2.1. Isolation of Poly(A)⁺ RNA

Isolation of polyadenylated mRNA was done with the QuickPrep Micro mRNA Purification Kit (Amersham Pharmacia Biotech) according to the supplier's instruction. 1×10^7 cells were suspended in 0.4 ml of extraction buffer by vortexing. The sample was then diluted by adding 0.8 ml of elution buffer, mixed and centrifuged for 1 min at 10000 rpm. The supernatant was added to 1 ml of pelleted Oligo (dT)-Cellulose and resuspended by inverting the tube. The Oligo (dT)-cellulose and the bound poly(A)⁺ RNA were subsequently pelleted by centrifugation for 15 seconds at 10000 rpm. The pellet was washed five times with 1 ml of High-Salt buffer and then two times with 1 ml of Low-Salt buffer.

The resin was resuspended in 0.3 ml of Low-Salt buffer, transferred to a MicroSpin Column and washed for three more times. The column was then centrifuged for 10 sec and the effluent was discarded. Elution was done by two elutions steps with 0.2 ml elution buffer prewarmed to 65°C. The mRNA was afterwards precipitated for 1 h at -20°C by adding 10 µl of glycogen solution, 40 µl of potassium acetate solution and 1 ml of 95 % ethanol. The precipitated mRNA was collected by centrifugation for 14000 rpm at 4°C for 15 min and resuspended in an appropriate amount of DEPC-treated water.

3.5.2.2. cDNA synthesis

For the construction of the cDNA the λ ZAP Express cDNA Synthesis Kit (Stratagene) was used. Poly(A)⁺ RNA corresponding to 2×10^7 LAN-1 cells dissolved in 37.5 µl DEPC-treated water were used as starting material. The following reagents were combined and gently mixed:

- 5 µl 10x first strand buffer
- 3 µl first strand methyl nucleotide mixture
- 2 µl linker primer (1.4 µg/µl)
- 1 µl RNase Block Ribonuclease Inhibitor (40 U/µl)
- 37.5 µl poly(A)⁺ RNA in DEPC-treated water

The linker primer contained a Xho I restriction site to allow a sense orientation (EcoR I \rightarrow Xho I) of the finished cDNA in the λ ZAP vector with regard to the lacZ promoter. To protect the cDNA against a later following Xho I digestion dCTP was substituted against 5-methyl dCTP in the first-strand nucleotide mixture to hemimethylate the cDNA. The primers were allowed to anneal for 10 min at room temperature before 1.5 µl of MMLV-RT (50 U/µl) was added. The reaction mixture was incubated for 1 h at 37°C and then placed on ice.

During the second strand synthesis RNase H was used to nick the RNA bound to the first-strand cDNA thereby producing a multitude of fragments which served as primers for DNA polymerase I. The original mRNA was thereby translated into second-strand cDNA. The following precooled components for second strand synthesis were subsequently added:

- 20 μ l second-strand buffer
- 6 μ l second strand dNTP mixture
- 16 μ l sterile distilled water
- 2 μ l RNase H (1.5 U/ μ l)
- 11 μ l DNA polymerase I (9.0 U/ μ l)

The reaction mixture was incubated for 2.5 h at 16°C and the tubes placed on ice afterwards. Temperatures above 16°C were not acceptable due to the risk of formation of unclonable hairpin structures. For blunting of the uneven cDNA termini 23 μ l of blunting dNTP mix and 2 μ l of cloned Pfu DNA polymerase (2.5 U/ μ l) were added and the mixture was incubated for 30 min at 72°C. The cDNA was extracted twice with phenol-chloroform [1:1 (v/v)] and precipitated overnight at -20°C with 20 μ l of 3 M sodium acetate and 400 μ l of 95 % ethanol. The precipitated cDNA was collected by centrifugation at 14000 rpm at 4°C for 60 min, washed once with 70 % ethanol and airdried.

To allow for directional cloning of the cDNA in the λ ZAP vector EcoR I adaptors were ligated to the blunt termini. The pellet was therefore resuspended in 8 μ l of a solution containing the EcoRI adaptors and incubated at 4°C for 1h to allow the complete solution of the pellet. The following components were then added:

- 1 μ l 10 x ligase buffer
- 1 μ l 10 mm rATP
- 1 μ l T4 DNA ligase (4 u/ μ l)

The ligation reaction was performed over 2 days at 4°C. The ligase was subsequently heat inactivated at 70°C for 30 min.

After cooling the mixture to room temperature the adapters were phosphorylated by adding the following components:

- 1 μ l 10 x ligase buffer
- 2 μ l 10 mM rATP
- 6 μ l sterile water
- 1 μ l T4 polynucleotide kinase (10 U/ μ l)

After phosphorylation for 30 min at 37°C, the kinase was heat inactivated for 30 min at 70°C. To produce the cohesive end the EcoR I adapter and the residual linker primer from the 3' end of the cDNA were released by a Xho I digestion. 28 μ l of Xho I buffer supplement and 3 μ l of Xho I (40 U/ μ l) were added, the mixture was incubated for 1.5 h at 37°C and the cDNA afterwards precipitated overnight by adding 5 μ l of 10 x STE buffer and 125 μ l of 95 % ethanol. The cDNA was collected by centrifugation at 14000 rpm at 4°C for 60 min, the dried pellet resuspended in 14 μ l of 1 x STE buffer and mixed with 3.5 μ l of column loading dye.

To separate the finished cDNA from the linker primer and the EcoRI adapter a size separation was done using Sepharose CL-2B gel filtration media. A 1ml pipet was used as column and connected with a tube to a syringe which served as buffer reservoir. The gel filtration matrix was equilibrated in 1x STE buffer, filled into the column until approximately 0.5 cm under the point where the pipet and the syringe joined. The matrix was thoroughly washed and the cDNA sample was then applied directly on top of the column bed. Fractions were collected in 100 μ l aliquots. The different fractions were afterwards extracted twice with 100 μ l phenol-chloroform [1:1 (v/v)] and precipitated overnight at -20°C by adding 200 μ l of 95 % ethanol. After collecting the cDNA by centrifugation, the pellet was washed once with 70% ethanol and then resuspended in 3.5 μ l of sterile water. The quantity of the cDNA was subsequently checked by an ethidium bromide plate assay (see 3.5.2.), the size by running an agarose gelelectrophoresis (see 3.5.5.)

3.5.2.3. Construction of the cDNA library in the λ ZAP Express vector

After determining the size and quantity of the cDNA in the different fractions the best suited fractions were used for ligation into the λ ZAP Express Vector using the following components:

- 1.0 μ l λ ZAP Express Vector
- 0.5 μ l 10 x ligase buffer
- 0.5 μ l 10 mM rATP (pH 7.5)
- 1.0 μ l resuspended cDNA (approximately 100 ng cDNA)
- 1.5 μ l sterile water
- 0.5 μ l T4 DNA ligase (4 U/ μ l)

The ligation reaction was performed over 2 days at 4°C. 2 μ l of each ligation reaction was then added to packaging extract (Gigapack III Gold packaging extract, Stratagene) and packaging was allowed to take place for 2 hours at room temperature. The packaging reaction was stopped by adding 500 μ l of SM-buffer and 20 μ l of chloroform. The cell debris was sedimented by centrifugation and the supernatant containing the phage was checked for titer as well as efficiency of the packaging process by blue white screening (see 3.5.5.).

The packaging reactions were therefore plated in the E.coli strain XL1-Blue MRF' by adding 1 μ l of the undiluted stock and 1 μ l of a 1:10 dilution of the λ phage to 200 μ l of the host cells ($OD_{600} = 0.5$). The various suspensions were incubated for 15 min at 37°C before the following components were added:

- 3 ml NZY Top Agar (melted and prewarmed to 50°C)
- 15 μ l 0.5 M IPTG (in dH₂O)
- 50 μ l X-gal (250 mg/ml in DMF)

The suspensions were immediately plated onto 85 mm² NZY agar plates and cooled for 15 min to harden the NZY Top Agar. The plates were then incubated overnight at 37°C.

To achieve a large stable library with a high titer the primary library was amplified by adding 5×10^4 pfu to 600 μ l of XL1-Blue MRF' cells at an $OD_{600} = 0.5$ in 10 mM $MgSO_4$. Plating was done as described before (see above) using 8 ml NZY Top Agar and 150 mm² plates. All in all 1×10^6 plaques were amplified. After overnight growth the plates were overlaid with 10 ml of SM-buffer for 24 h to allow the phages to diffuse into the SM-buffer. The bacteriophage suspension was then recovered, 5 % (v/v) chloroform was added and the suspension was incubated for 15 min at room temperature to kill any residual cells. The cell debris was afterwards pelleted by centrifugation for 10 min at 2000 rpm. After addition of 0.3% (v/v) chloroform the supernatant was aliquoted and stored at 4°C and -80°C, respectively.

3.5.2.4. Assessment of the cDNA library

To assess the quality of the constructed cDNA library regarding the size of the inserted cDNA approximately 500 plaques were plated. 10 of these plaques were picked and the phages in vivo excised (see 3.5.2.). The resulting phagemids were plated on LB-kanamycin plates, single colonies were then picked and mini preps prepared (see 3.5.3). The isolated phagemid DNA was resuspended in 20 μ l TE buffer and subjected to a restriction digestion with the restrictions enzymes Xho I and Pst I (M β B). Therefore the following components were combined and incubated for 1 h at 37 °C .

- 4 μ l resuspended phagemid
- 0.5 μ l Xho I
- 0.5 μ l Pst I
- 1 μ l 10 x buffer red
- 4 μ l sterile water

Analysis of the restriction digest was done by agarose gelelectrophoresis.

3.5.3. In vivo excision

In vivo excision of the λ ZAP Express Vector leads to formation of the pBK-CMV phagemid vector. For in vivo excision the plaque of interest was picked and transferred to 500 μ l SM-buffer and 20 μ l chloroform. The solution was incubated overnight to release the phage particles. 250 μ l of the phage stock ($>1 \times 10^5$ phage particles) were combined with 200 μ l XL1-Blue MRF' cells ($OD_{600} = 1.0$) and 1 μ l ExAssist helper phage ($>1 \times 10^6$ pfu/ μ l) in Falcon 2059 propylene tubes (Fisher) and incubated for 15 min at 37°C. 3 ml of NZY Broth was added and the tubes were incubated overnight at 37°C and 220 rpm. After heating the tubes for 20 min at 70°C the cell debris was pelleted at 1000 x g for 15 min. The excised pBK-CMV phagemid containing supernatant was transferred into a new tube. To plate the excised phagemids 10 and 100 μ l, respectively, were added to 200 μ l XL1-Blue cells ($OD_{600} = 1.0$) and incubated for 15 min at 37°C. 300 μ l of NZY Top Agar was then added and the tubes were incubated for further 45 min at 37°C. Afterwards 200 μ l of each cell mixture was plated on LB-kanamycin plates and the plates were incubated overnight at 37°C. Colonies were then selected for preparation of plasmid preps.

3.5.4. Plasmid DNA isolation

For isolation of plasmid DNA the method of alkalic lysis was used (Sambrook et al., 1989).

A single colony was picked from an LB Agar kanamycin plate, transferred into 3 ml of LB agar with 50 µg/ml kanamycin and incubated overnight at 37°C and 220 rpm. The cell suspension was then pelleted by centrifugation for 2 min at 20000 x g and resuspended in 200 µl of solution I. After transfer to a 1.5 ml tube 400 µl of solution II were added, the tube was softly shaken and incubated for 5 min at room temperature to lyse the bacterial cells and denaturate the genomic DNA. 300 µl of solution III was added to precipitate the genomic DNA and most of the proteins. The suspension was incubated for 5 min on ice and afterwards centrifugated for 8 min at 14000 x g. The plasmid DNA containing supernatant was extracted twice with phenol/chloroform [1:1 (v/v)]. The plasmid DNA was precipitated for 30 min at 4°C by adding an equal volume of isopropanole. After centrifugation for 10 min at 4°C and 14000 x g the plasmid DNA was washed with 70 % (v/v) ethanol, airdried for approximately 20 min and resuspended usually in 20 µl sterile ddH₂O. Contaminating RNA was removed by digestion with 1 µl RNase A (10 mg/ml) for 30 min at 37°C. The plasmid DNA was either directly used or stored at -20°C.

Solution I:

50 mM glucose
25 mM Tris-HCl
10 mM Na₂EDTA
pH 8.0

Solution II:

0.2 M NaOH
1% SDS (w/v)

Solution III:

3 M potassium acetate
1 % SDS (w/v)
pH 5.2

3.5.5. Ethidium bromide plate assay

The incorporation of ethidium bromide into (c)DNA can be used to quantify the amount of (c)DNA present in a sample. To quantitate the amount of (c)DNA present in a sample the incorporation of ethidium bromide was measured using UV visualization for quantification. DNA samples of known concentrations were used as comparative standards. To that end 30 ml of 0.8 % (w/v) agarose in TAE buffer was boiled and cooled to 50°C. 10 µl of an ethidium bromide stock solution (10 mg/ml) was added and the agarose solution was poured in 85 mm petri dishes. After the agarose has hardened 0.5 µl of a serial dilution of the standard (10-200 ng/µl) as well as of the samples were spotted on the plate. The samples were absorbed into the plate for 15 min and subsequently quantified visually using a UV light box.

3.5.6. Blue white screening

The multiple cloning site in the λ ZAP vector is part of the lacZ-gen of *E. coli* that codes for the C-terminal domain of β -galactosidase. Induction with IPTG leads to expression of the C-terminal domain of β -galactosidase. Infection of the phage in an *E. coli* strain, such as XL1-Blue MRF', that expresses the N-terminal domain leads to the formation of the active enzyme (α -complementation). Growth on agar plates that contain the β -galactosidase substrate result in the cleavage of the substrate by the active enzyme thereby producing a blue color. Insertion of (c)DNA in the multiple cloning site prevents expression of the active C-terminal domain and therefore the formation of the blue color. Hence blue plaques contain non recombinant phages whereas white plaques contain recombinant phages.

3.5.7. Agarose gel electrophoresis

The electrophoretic separation of DNA fragments was performed on horizontal agarose gels with agarose-concentrations between 0.8 and 1.5% (w/v) containing 1 µg/ml ethidium bromide. The agarose was therefore boiled in 50 ml TAE buffer in a microwave. After cooling to approximately 60°C ethidium bromide was added and the gel was poured in the casting stand (DNA Plus Mini Agarose Gel System, USA Scientific, Ocala, USA). After the gel was hardened, the chamber was filled with sufficient TAE buffer to cover the gel. 5-fold loading buffer was added to the samples and the samples were subsequently loaded. Electrophoresis was done at a voltage of 100 V for 45 - 60 min. Bands were visualized by an UV-Transilluminator (FBTIV-816, Fisher) and documented (Photo documentation camera FB-PDC-34, Fisher).

Loading buffer (5x):

100 mM EDTA
20 % Ficoll 400 (v/v)
0.025 % Bromphenolblue (v/v)

3.5.8. Cultivation and storage of bacterial cell cultures

Bacterial glycerol stocks were streaked on LB agar plates containing 12.5 µg/ml tetracycline and grown overnight at 37°C. The plates were wrapped with Parafilm and were viable for approximately one month when stored at 4°C. For growth of liquid cultures a single colony was inoculated in the appropriate media (10 mM MgSO₄, 0.2% (w/v) maltose in LB Broth for XL1- Blue MRF'; NZY Broth for XL0LR) overnight at 30°C and 200 rpm to a maximum OD₆₀₀ = 1.0. The cells were then collected at 500 x g for 10 min and resuspended in half of the original volume with sterile 10 mM MgSO₄. Cells were usable for approximately one week and were

diluted to an $OD_{600} = 0.5$ directly before use. For longterm storage glycerol stocks were made and frozen at -80°C . Therefore 1 ml of an overnight culture was mixed with 150 μl glycerol, deepfrozen in liquid nitrogen and then transferred to -80°C .

3.5.9. DNA sequencing

Sequencing of double-stranded DNA was performed by the method of Sanger (Sanger et al., 1977) under non-radioactive conditions using the ALFExpress DNA Sequencer and the AutoRead Sequencing Kit (Amersham Pharmacia Biotech) according to the supplier's instruction.

Plasmid DNA was prepared out of a 10 ml culture (see 3.5.3.) and suspended in 32 μl water. To denaturate the DNA 8 μl of 2 M NaOH were added and the solution was incubated for 10 min at room temperature. The solution was then neutralized by adding 7 μl 3 M sodium acetate and 4 μl of ddH_2O . 120 μl 100 % ethanol were added and the DNA was precipitated at -20°C for 15 min. The DNA was subsequently pelleted and washed once with 70 % (v/v) ethanol. The pellet was airdried and resuspended in 20 μl of ddH_2O . 2 μl of Cy5-labeled T3 and T7 primers (1 pmol), respectively, as well as 2 μl of annealing buffer were added.

T3 primer: 5' Cy5-AATTAACCCTCACTAAAGGG 3'

T7 primer: 5' Cy5-GTAATACGACTCACTATAGGGC 3'

The annealing reaction was preheated at 65°C for 5 min and then incubated at 37°C for 10 min. The tubes were afterwards placed for at least 10 min at room temperature. After adding 1 μl of extension buffer and 3 μl of DMSO the sequencing reactions were immediately performed. 2.5 μl of the four different nucleotid mixes were pipetted in four corresponding tubes and put on 37°C .

2 µl of diluted T7 DNA Polymerase [1:1 (v/v)] with enzyme dilution buffer] were then added to the annealing reaction and the mixture was thoroughly mixed. Immediately 4.5 µl of this solution was added to each nucleotid mix. The reaction was allowed to take place for 5 min before 5 µl of the stop solution was added. The reactions were heated for 3 min at 90°C and kept on ice until sequencing was performed. 6 µl of each reaction were loaded into the appropriate wells of the sequencing gel. The DNA fragments were subsequently separated by size and according to the fluorescence labeling transcribed into the corresponding DNA sequence.

The 0.5 mm sequencing gel was run for 800 min with a geltemperatur of 42°C and a voltage of 1500 V. Analysis was performed with the Alf Manager 3.01 Software (Amersham Pharmacia Biotech) and the MacDNAsis Software (Hitachi, USA).

Annealing buffer:

1 M Tris-HCl
0.1 M MgCl₂
pH 7.6

Enzyme dilution buffer:

20 mM Tris-HCl
5 mM DTT
0.1 mg/ml BSA
5 % glycerol

Extension buffer:

304 mM citric acid
324 mM DTT
40 mM MnCl₂
pH 7.5

Stop solution:

100 % deionized formamid (v/v)
5 mg/ml Dextran Blue 2000

Nucleotid mixes (e.g. A-mix):

5 µM ddNTP
1 mM dATP
1 mM dCTP
1 mM dTTP
1 mM dGTP
1 mM c7dGTP
50 mM NaCl
40 mM Tris-HCl
pH 7.6

Sequencing gel:

6 % acrylamid, 40% (w/V)
6 M urea
5.8 % 10 x TBE buffer
0.08 % TEMED (w/v)
0.04 % APS (w/v)

3.6. Radioactive Methods

3.6.1. Measurement of endogenous FAS activity

For measurement of endogenous FAS activity 1×10^5 cells were plated in triplicate in 24-well plates in 0.5 ml of culture media (E&K Scientific). After 18 hours of growth 0.5 μCi of ^{14}C -acetat were added to each well and incubation was continued for 2 hours at 37°C . The cells were harvested with a cellscraper and washed with PBS. The cells were subsequently lysed in 50 μl hypotonic lysis buffer at room temperature. The lipids were extracted for 30 min by adding 1 ml chloroform/methanol [2:1 (v/v)] and separated from the insoluble DNA and proteins by centrifugation at 14000 rpm for 10 min. The lipid containing phase was then extracted for three times with PBS and subsequently added to 2 ml of scintillation solution (Scintisafe™ EconoSafe, Fisher) in 5 ml polyethylen vials (Packard, Meriden, CO, USA). ^{14}C -labeled lipids in the samples were detected and quantified using the Packard Liquid Scintillation Counter Tricarb 2900 TR (Packard).

Hypotonic lysis buffer:

1 mM DTT
1 mM Na_2EDTA
20 mM Tris-HCl
pH 7.5

3.6.2. Inhibition of endogenous FAS activity by cerulenin

To test the ability of cerulenin to inhibit endogenous FAS activity 1×10^5 cells were plated in triplicate in 24-well plates (E&K Scientific) and grown for 15 h. Then treatment for 3 h with cerulenin (5 mg/ml in DMSO) in concentrations of 5, 10, and 15 $\mu\text{g/ml}$ took place. ^{14}C -Acetat was subsequently added and cells were incubated for two further hours. Extraction of lipids and quantification of ^{14}C -incorporation in lipids was performed as described in 3.6.1..

4. Results

4.1. Cerulenin-mediated apoptosis

Although the cytotoxic effect of cerulenin has been shown in different tumor cells, the involved molecular mechanisms are currently not clear. Therefore this investigations were focussed on the following topics. First, it was examined whether the cerulenin induced cytotoxicity is due to the induction of apoptosis or necrosis and whether the cytotoxicity is mediated by the function of cerulenin as inhibitor of FAS. Then further potential targets of cerulenin, e.g. its DNA damaging potential were investigated. Finally, the involved signal transduction pathway and in particular the involvement of mitochondria and the caspase family was evaluated. Since these were the first investigations regarding the molecular mechanisms of the cerulenin-induced cytotoxicity a broad range approach using a variety of different NB cell lines as well as other tumor cell lines was performed to obtain a comprehensive overview.

4.1.1. Induction of apoptosis by cerulenin

The cytotoxic effects of cerulenin were investigated in ten different tumor cell lines (LAN-1, IMR-32, NMB-7, SK-N-SH, HaCaT, A431, SK-MEL-93-2, WiDr, SK-BR-3 and MCF7) and the two normal human cell lines NHEK (normal human epidermal keratinocytes) and NHLF (normal human lung fibroblasts). Dramatic morphological changes with typical signs of apoptosis such as membrane blebbing and loss of adherence were observed in all four neuroblastoma cell lines (LAN-1, IMR-32, NMB-7 and SK-N-SH) as well as in HaCaT and A431 cells after 12 hours of incubation with 15 µg/ml of cerulenin. Less prominent morphological changes were seen in SK-MEL-93-2, MCF7, and SK-BR-3 cells, whereas WiDr cells and normal keratinocytes and fibroblasts showed no signs of apoptosis (not shown).

4.1.1.1. Annexin V assay

The externalization of phosphatidylserine residues by Annexin V assay in the tumor cell lines LAN-1, SK-N-SH, HaCaT, SK-BR-3 and WiDr as well as normal human keratinocytes and normal fibroblasts were then exemplarily used to confirm the morphological observations that cerulenin induces apoptosis in different tumor cell lines (Figure 2).

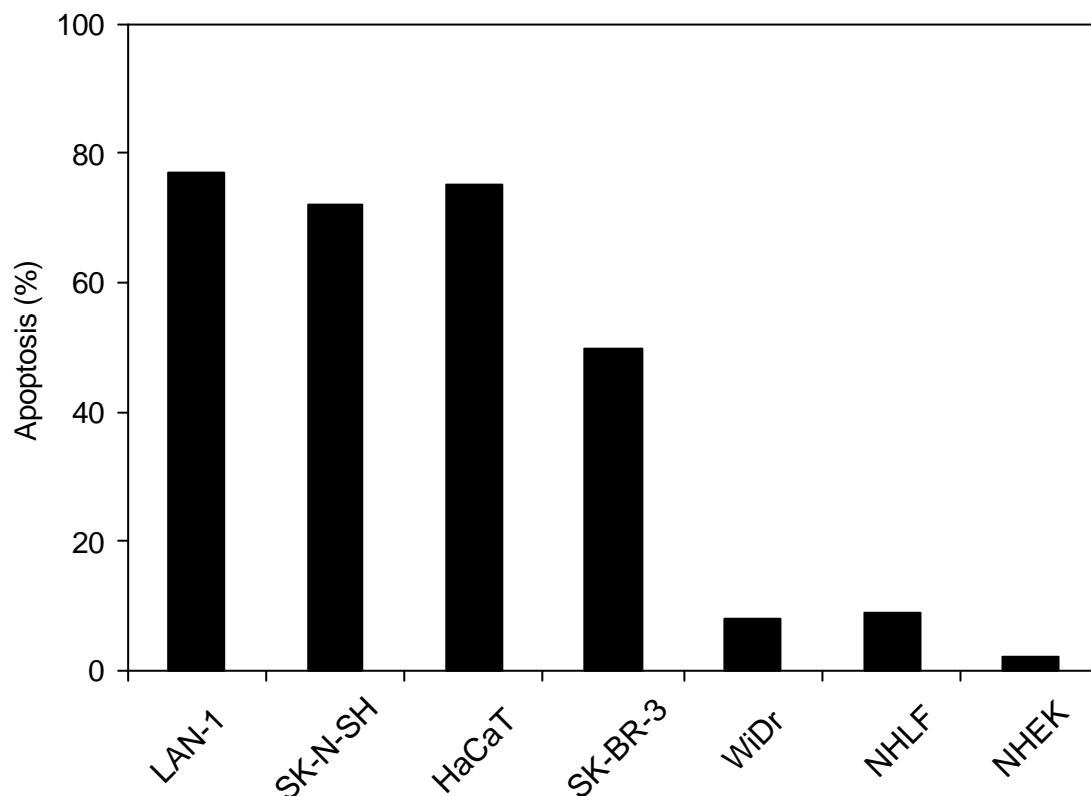


Figure 2: Determination of cerulenin-mediated apoptosis by Annexin V-FITC and propidium iodide in different tumor and normal cell lines

The extent of apoptosis in the tumor cell lines LAN-1, SK-N-SH, HaCaT, SK-BR-3 and WiDr as well as in the normal cell lines NHEK and NHLF after treatment for 18 h with 15 µg/ml cerulenin was determined by cytofluorometry after staining with Annexin V-FITC and propidium iodide. To calculate the extent of apoptosis the percentage of both early apoptotic (Annexin V-FITC positive only) and late apoptotic cells (Annexin V-FITC and propidium iodide positive) after subtraction of corresponding background values was used. Facscan analysis by courtesy of Dr. David.

The NB cell lines LAN-1 and SK-N-SH as well as the transformed keratinocyte cell line HaCaT were highly sensitive to cerulenin treatment. With respect to the expression of phosphatidylserine on the cell surface cerulenin led to more than 75 % specific apoptosis in all three cell lines. The breast cancer cell line SK-BR-3 which showed minor dramatic morphological effects was less sensitive and yielded approximately 50 % specific apoptosis. In contrast, no apoptotic effects were observed after treatment of WiDr cells, normal human keratinocytes and normal human fibroblasts in accordance with the lack of morphological changes.

4.1.1.2. Cleavage of PARP

In a second set of experiments the cleavage of the nuclear enzyme poly(ADP-ribose) polymerase (PARP), which has significance as a prototype caspase substrate in apoptotic processes, into its characteristic 89 kDa fragment was investigated.

Treatment with cerulenin led to the cleavage of PARP in most of the tumor cell lines. Furthermore PARP cleavage happened in a dose-dependent manner (Figure 3). In LAN-1 and SK-N-SH cells, no signs of PARP cleavage were apparent after treatment with 5 µg/ml cerulenin, but became evident with 10 µg/ml and further increased after exposure to 15 µg/ml (Figure 3: top panel). The same results were obtained with the two other NB cell lines NMB-7 and IMR-32 (not shown). Similar dose-dependent effects were observed in HaCaT and A431 cells (Figure 3: upper middle panel). The cell lines SK-MEL-93-2 and SK-BR-3 showed a dose dependent reduction of the intact PARP, although the 89 kDa fragment was barely detectable (Figure 3: lower middle panel). The breast cancer cell line MCF7 showed no cleavage of PARP which is probably due to the fact that this cell line is deficient in caspase 3, the caspase usually responsible for PARP-cleavage (not shown).

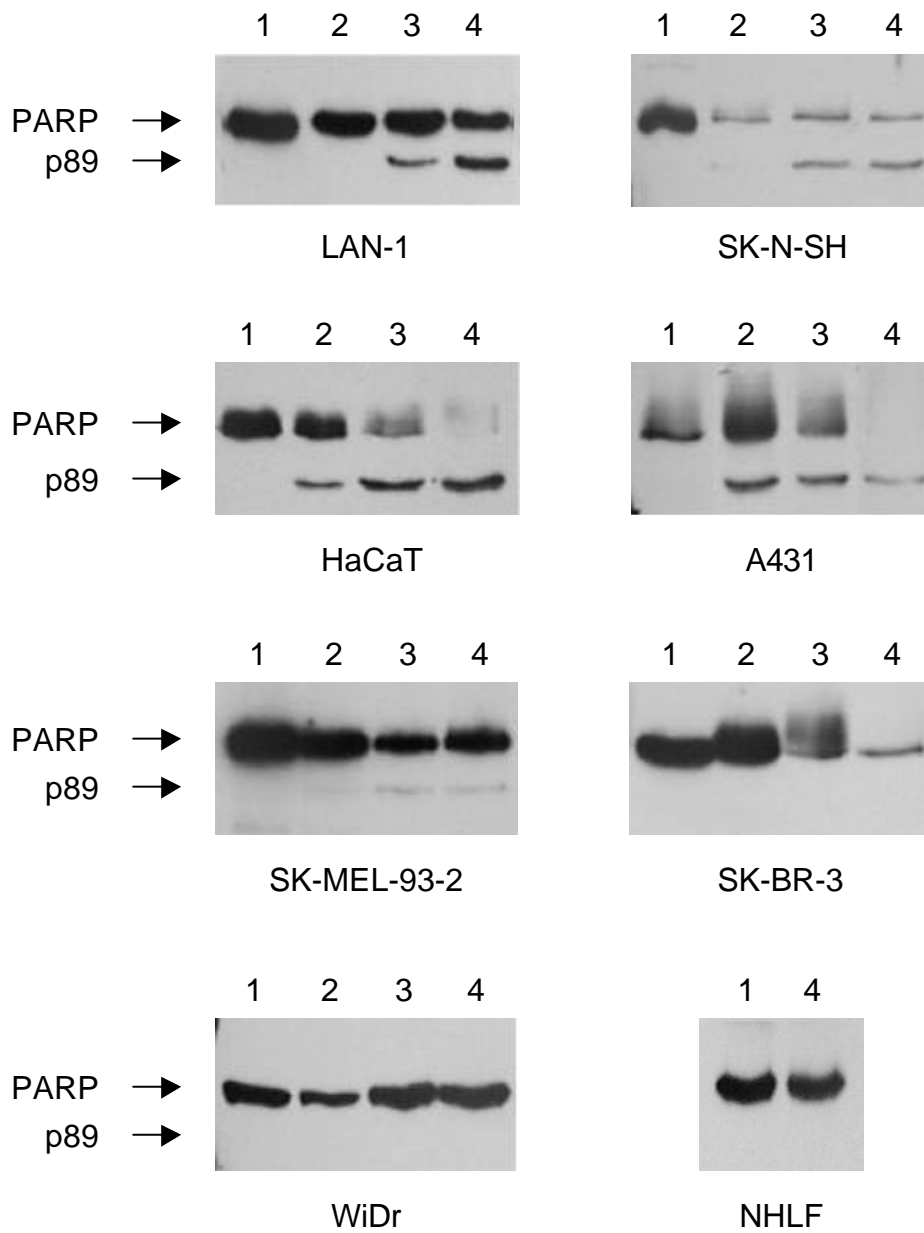


Figure 3: Determination of cerulenin-mediated apoptosis by PARP cleavage

The tumor cell lines LAN-1, SK-N-SH, HaCaT, A431, SK-MEL-93-2, SK-BR-3 and WiDr as well as the normal human cell line NHLF were exposed to different concentrations of cerulenin for 18 hours. Cleavage of PARP was determined by immunoblot analysis against a polyclonal rabbit anti-PARP antibody using the ECL system for development.

- Lane 1: Controls treated with DMSO
- Lane 2: Treatment with 5 µg/ml cerulenin
- Lane 3: Treatment with 10 µg/ml cerulenin
- Lane 4: Treatment with 15 µg/ml cerulenin

WiDr and NHLF cells were completely refractory to treatment with cerulenin, which was confirmed by both the absence of PARP cleavage and by unchanged amounts of intact PARP (Figure 3: lower panel). NHEK could not be evaluated due to lack of detectable PARP.

4.1.2. Investigation of FAS as potential target of cerulenin

Cerulenin (2,3-Epoxy-4-oxo-7,10-dodecadienamide) is known as a specific inhibitor of FAS. Therefore it has been hypothesized that the inhibition of FAS by cerulenin confers the cerulenin-induced cytotoxicity and that the expression/endogenous activity of FAS correlates with the susceptibility to cerulenin. To investigate this hypothesis the expression as well as the endogenous activity of FAS were investigated in 10 different tumor cell lines as well as in two normal cell lines. In addition the inhibition of FAS activity in the same cell lines by different concentrations of cerulenin was investigated. Furthermore the ability of palmitate, the end product of the FAS pathway, to rescue cells from cerulenin-induced cytotoxicity was evaluated.

4.1.2.1. Purification of FAS

FAS from LAN-1 cell extracts (Figure 4 A: Lane 1) was purified using a combination of anion exchange, cation exchange, and hydroxyapatite chromatography and preparative SDS-PAGE. In the first step FAS was eluted from the anion exchange chromatography column in a step gradient between 150 and 250 mM NaCl (Figure 4 A: Lane 2). After buffer exchange and application to the cation exchange chromatography column FAS was recovered in the breakthrough (Figure 4 A: Lane 3).

Subsequently the breakthrough was applied to the hydroxyapatite chromatography column where FAS was eluted in a step gradient between 50 and 160 mM sodium phosphate (Figure 4 A: Lane 4). After ultrafiltration of the FAS containing fractions complete purification was achieved by preparative gelelectrophoresis using a 3.15 % separating gel concentration (Figure 4 A: Lane 5).

The identity of the purified protein was confirmed by immunoblot analysis using a monoclonal antibody against FAS (Figure 4 B: Lane 1).

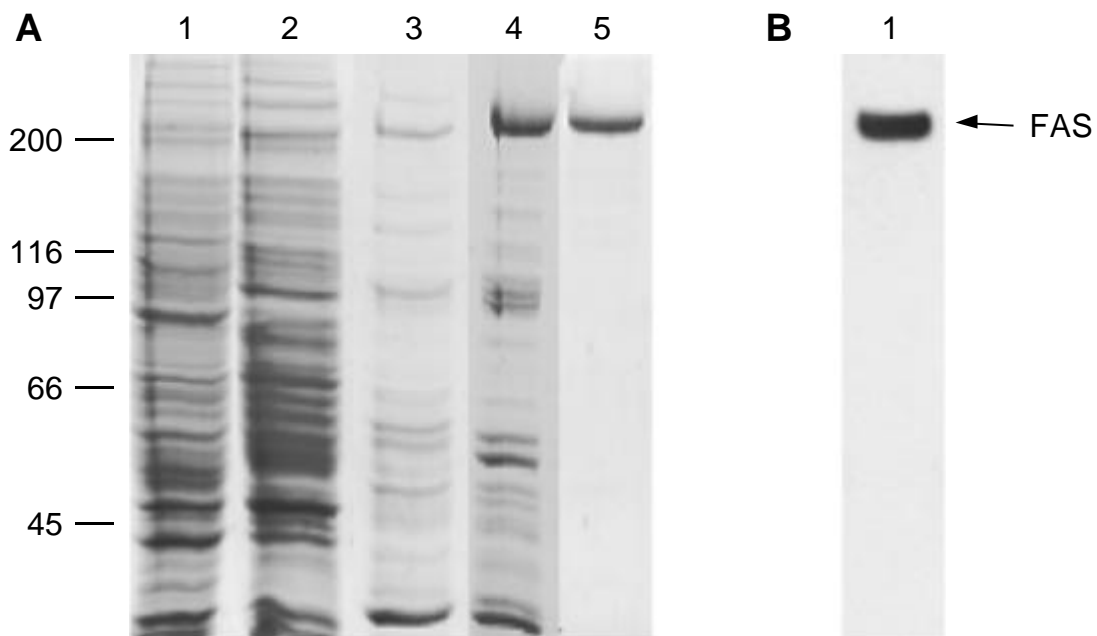


Figure 4: Purification of FAS from LAN-1 cells

A) Evaluation of the purification process of FAS by SDS-PAGE (7.5 %) under reducing conditions and Coomassie staining (Lane 1-5).

Lane 1: LAN-1 cell extracts

Lane 2: anion exchange chromatography, 150-250 mM NaCl in buffer A

Lane 3: cation exchange chromatography, breakthrough in buffer B

Lane 4: hydroxy apatite chromatography, 50-160 mM sodium phosphate in buffer B

Lane 5: preparative gelelectrophoresis, 3.15 % separating gel

B) Immunoblot analysis of the purified protein using a monoclonal mouse anti-FAS antibody. Immunodetection was done with the ECL system (Lane 1).

Lane 1: immunoblot of purified FAS

4.1.2.2. Expression of FAS in different human tumor and normal cell lines

FAS expression in ten different human tumor cell lines as well as in normal human keratinocytes and fibroblasts was determined by densitometric analysis using purified FAS as standard (Figure 5: black bars). FAS expression levels were quite heterogenous with the breast carcinoma cell line SK-BR-3 exhibiting significantly higher FAS expression than any other cell line (350 ng/10 µg cell extract). The cell lines SK-MEL-93-2, SK-N-SH, WiDr and NHLF showed rather low expression of FAS (25 and 50 ng FAS/10 µg cell extracts) whereas the cell lines HaCaT, A431, NMB-7, NHEK, MCF7, IMR-32 and LAN-1 showed a medium expression between 70 and 120 ng/10 µg of cell extracts (Figure 5).

Even different cell lines of the same tumor type (neuroblastoma) exhibited significant differences of FAS expression: LAN-1 and IMR-32 cells showed similar levels of FAS, while on the contrary the amount in NMB-7 cells was approximately 20% lower and only small amounts were seen in SK-N-SH cells, although these cell lines do not show major differences in their phenotype. Furthermore no difference in FAS expression between the cancer cell lines and the normal cells could be observed. Of particular interest in this context is the fact that normal human keratinocytes showed virtually the same extent of FAS expression as transformed keratinocytes (HaCaT) and skin carcinoma cells (A431), indicating that the change to a more cancerous phenotype has no apparent effect on FAS expression.

4.1.2.3. Endogenous FAS activity in different human tumor and normal cell lines

In addition to FAS expression endogenous FAS activity in all cell lines was investigated to see whether different FAS expression levels are accompanied by commensurate endogenous FAS activity. Evaluation of endogenous FAS activity was done by measuring the incorporation of [1-¹⁴C] acetic acid in cellular lipids. As shown in Figure 5, the endogenous FAS activity paralleled FAS expression in all cell lines (white bars). Only in SK-BR-3 cells a certain disaccordance between FAS expression and activity could be observed. As these cell line showed an extremely high expression and activity of FAS it is not clear whether the observed difference was due to some inaccuracy in the measuring procedure or due to partially functional inactivated FAS. Figure 6 demonstrates the excellent correlation between FAS expression and activity. A correlation coefficient of 0.986 was calculated with a p-value < 0.0001 including SK-BR-3 cells, thereby excluding the presence of functional inactive FAS in the different cell lines (with the possible exception of SK-BR-3).

Neither the expression of FAS nor the endogenous activity of FAS did show a correlation with the induction of apoptosis by cerulenin. The four NB cell lines showed similar induction of apoptosis but varied in their FAS expression/activity by a factor of two. SK-MEL-93-2 and SK-BR-3, the cell lines with the lowest and the highest expression and activity of FAS varying by a factor of approximately 10 exposed a rate of apoptosis that was virtually the same. Furthermore HaCaT, A431 and normal keratinocytes showed virtually the same expression and activity of FAS, but as HaCaT and A431 were highly susceptible for cerulenin treatment normal keratinocytes proved to be refractory against cerulenin treatment.

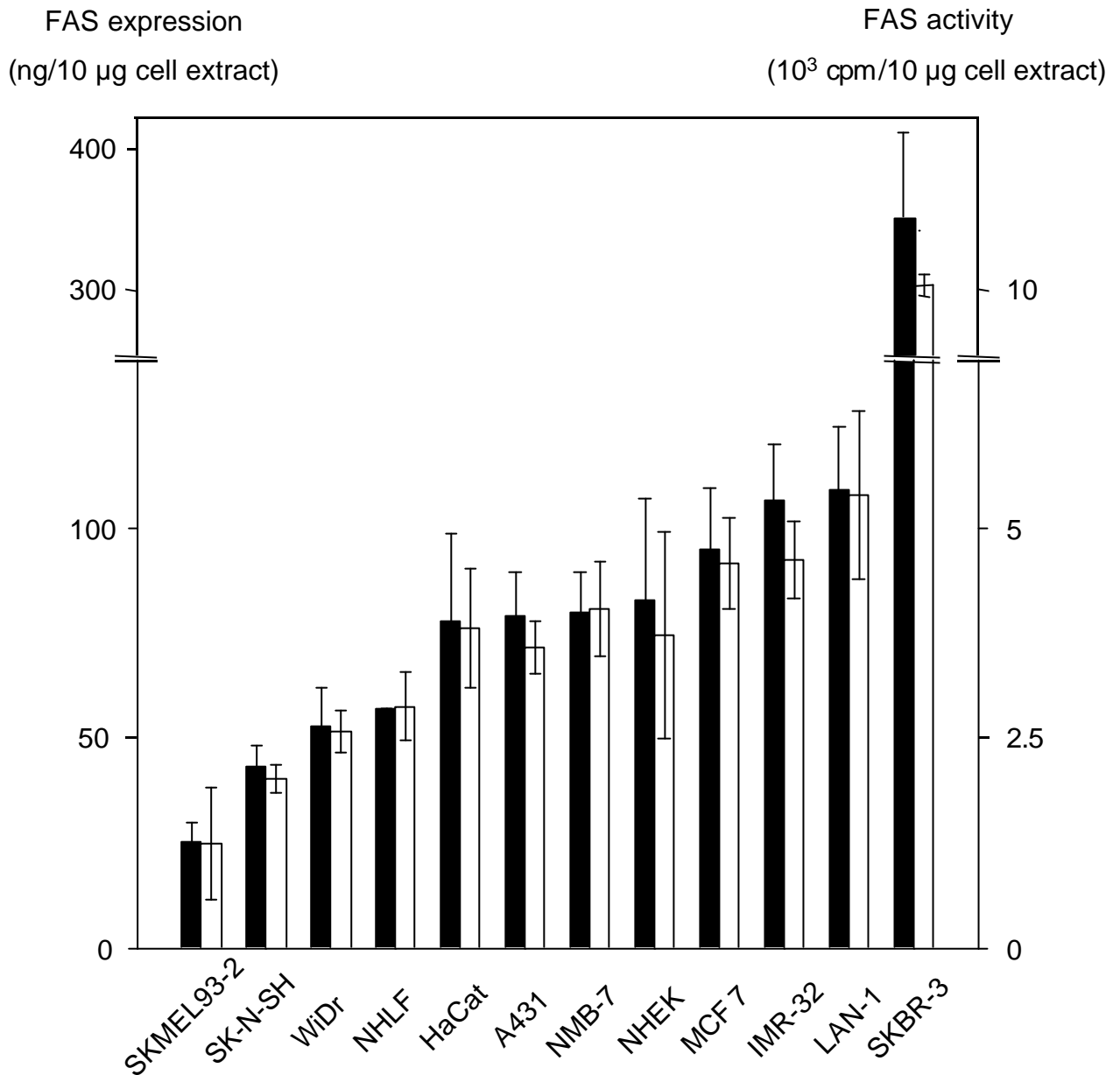


Figure 5: Determination of FAS expression and activity in tumor and normal cell lines

FAS expression and activity was examined in ten different tumor cell lines and two primary cell lines (NHEK and NHLF).

For quantitative analysis of FAS expression 10 µg of each cell extract were immunoblotted against a monoclonal mouse anti-FAS antibody. The blots were developed by chemiluminescence and subsequently analyzed with the Kodak 1D Image Analysis Software. FAS expression is represented as ng FAS per 10 µg cell extract (black bars). Endogenous FAS activity was measured by ¹⁴C-incorporation into acylglycerols in intact cells. FAS activity is expressed as cpm per 10 µg cell extracts (white bars). Data represent means of three independent experiments.

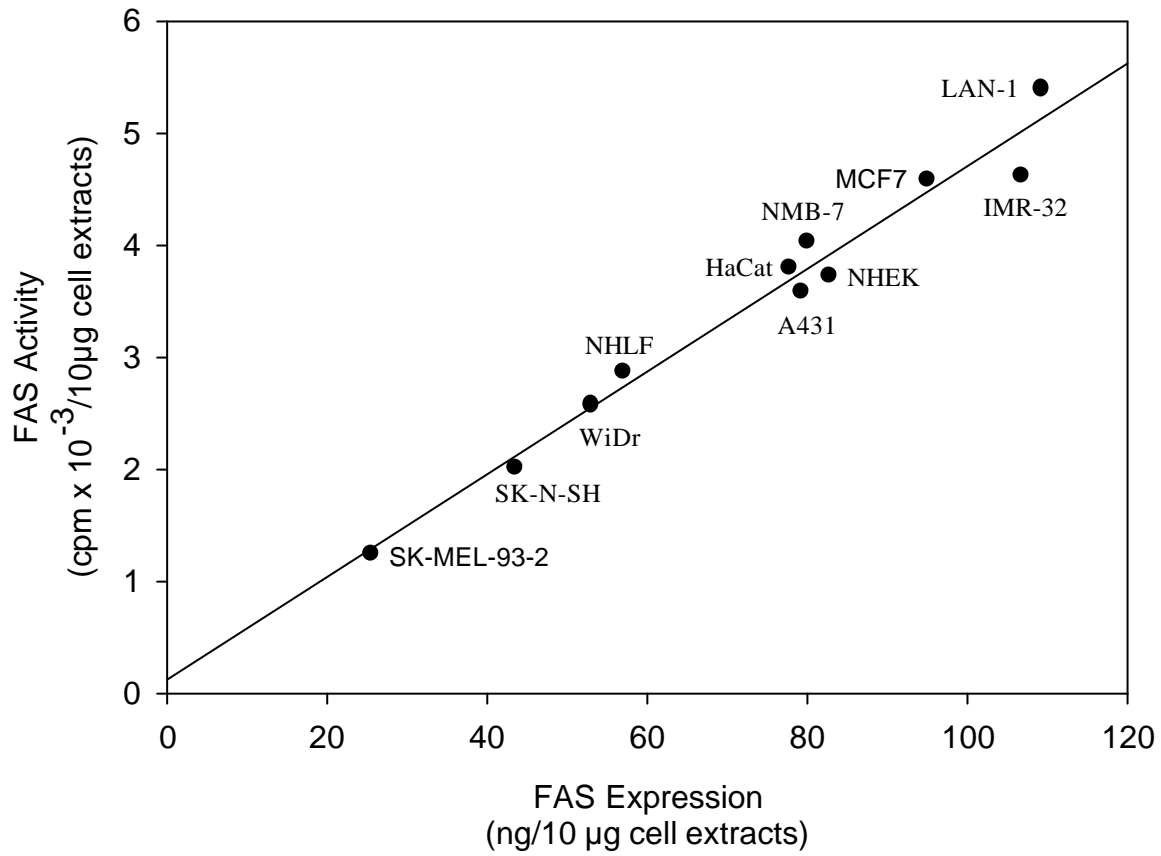


Figure 6: Correlation analysis of FAS expression and FAS activity

FAS expression (ng/10 µg cell extract) was plotted against endogenous FAS activity (cpm x 10⁻³/10 µg cell extract). SK-BR-3 cells were excluded from the graph because of the much higher FAS expression and activity.

4.1.2.4. Inhibition of FAS activity by cerulenin

To investigate the FAS inhibitory effect of cerulenin all cell lines were treated with different concentrations of cerulenin (5, 10, and 15 $\mu\text{g/ml}$) and the decrease of [$1\text{-}^{14}\text{C}$] acetic acid incorporation in fatty acids in relation to nontreated cells were measured (Figure 7 and 8). Maximum inhibition in most of the cell lines was already achieved after three hours of incubation with 5 $\mu\text{g/ml}$ cerulenin, resulting in a reduction of FAS

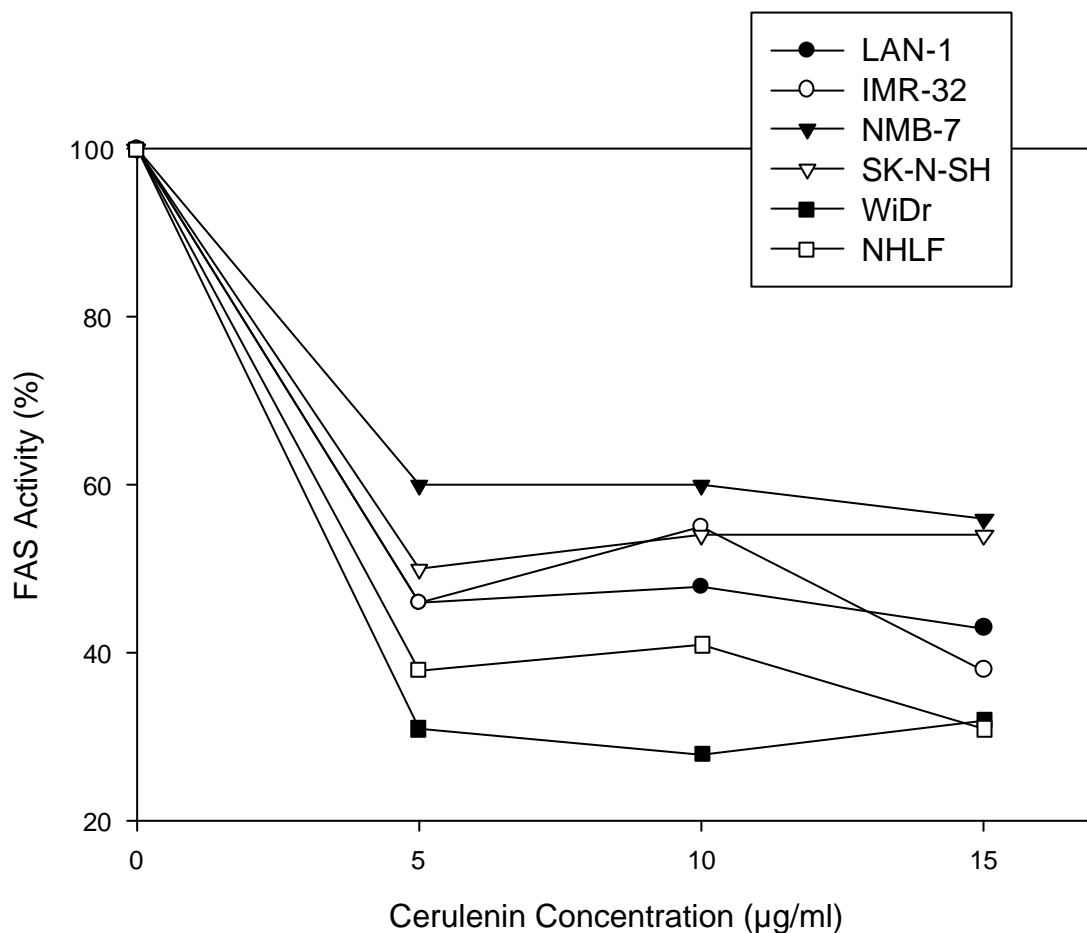


Figure 7: Cerulenin-mediated inhibition of FAS activity (I)

Investigation of inhibition of FAS activity by cerulenin in the tumor cell lines LAN-1, IMR-32, NMB-7, SK-N-SH, WiDr and the normal cell line NHLF.

Evaluation was done by measuring ^{14}C -incorporation into acylglycerols in intact cells with increasing cerulenin concentrations. FAS activity is expressed as percentage of endogenous non-inhibited FAS activity (100 %).

activity between 40 and 70 %. No further decrease in FAS activity was observed by increasing the cerulenin concentration to 10 and 15 $\mu\text{g/ml}$. Only SK-MEL-93-2 and SK-BR-3 cells exposed a notable dose-dependent response to cerulenin with a significant decrease in FAS activity from 5 to 15 $\mu\text{g/ml}$ cerulenin. As these cell lines represented the ones with the lowest and the highest FAS activity it is not likely that the magnitude of activity itself was responsible for this dose dependence.

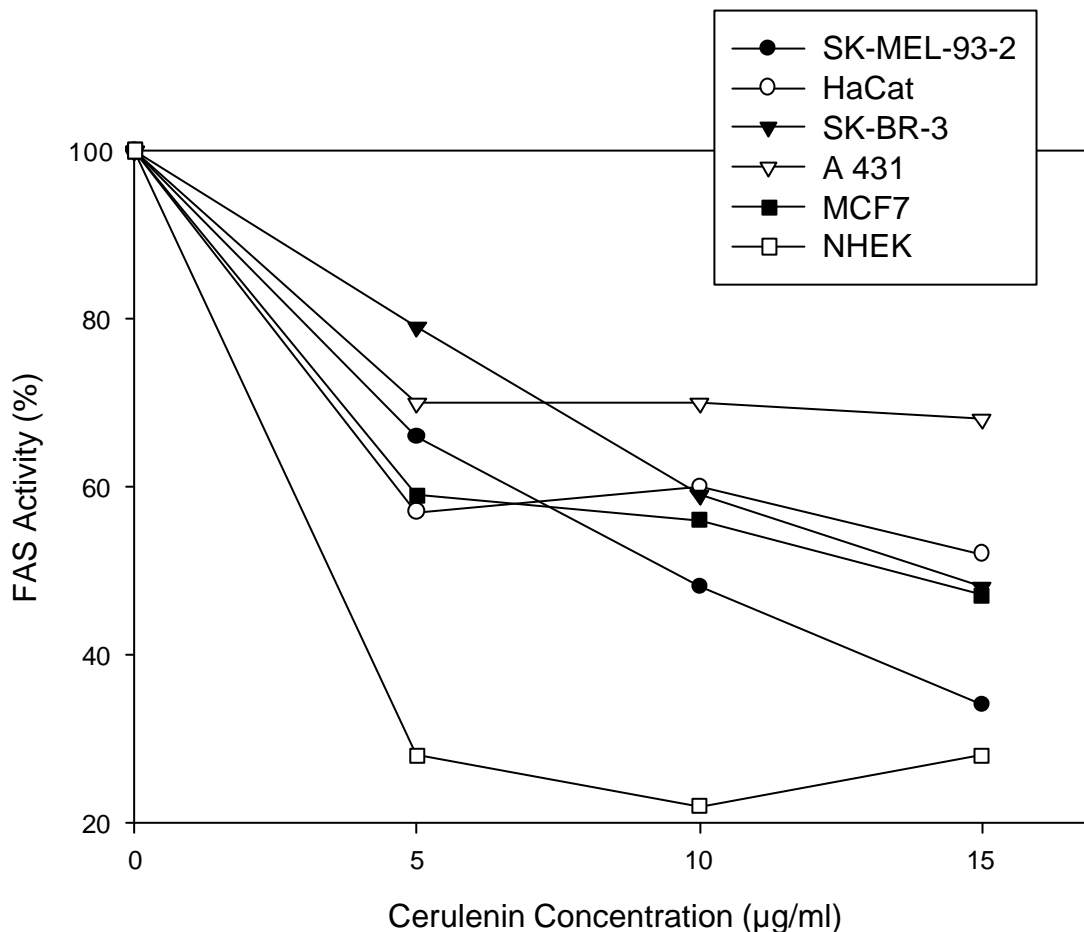


Figure 8: Cerulenin-mediated inhibition of FAS activity (II)

Investigation of inhibition of FAS activity by cerulenin in the tumor cell lines SK-MEL-93-2, HaCaT, SK-BR-3, A431, MCF7 and the normal cell line NHEK.

Evaluation was done by measuring ^{14}C -incorporation into acylglycerols in intact cells with increasing cerulenin concentrations. FAS activity is expressed as percentage of endogenous non-inhibited FAS activity (100 %).

Further reduction of FAS activity could not be achieved by extending the length of cerulenin exposure to six hours (data not shown) indicating that maximum inhibition is already accomplished after three hours of incubation. The extent of inhibition of FAS by cerulenin and the magnitude of activity of FAS itself showed no correlation as illustrated by the following examples:

1. The cell lines A431, HaCaT and NHEK which showed virtually the same FAS activity varied significantly in the inhibition of FAS with A431 exposing a reduction of approximately 30 %, HaCaT of 50 % and NHEK of about 75%.
2. The cell lines SK-MEL-93-2 and SK-BR-3 which differed by an order of magnitude in FAS activity were inhibited to similar extent.
3. The four NB cell lines all showed virtually the same dimension of inhibition although their activity varied by a factor of two.

Of particular importance was the question whether a correlation between the inhibition of FAS and the induction of apoptosis by cerulenin exist. As illustrated by the following observations such a relationship is unlikely:

1. The cell lines WiDr, NHEK and NHLF showed the highest magnitude of FAS-inhibition by cerulenin but were refractory to its cytotoxic effects.
2. The cell lines LAN-1, IMR-32, NMB-7, SK-N-SH and HaCaT which exposed the highest sensitivity against cerulenin-mediated cytotoxicity showed only a medium inhibition by cerulenin.
3. The cell line A 431 which exposed the same sensitivity against cerulenin as the five cell lines mentioned in 2. exposed one of the lowest inhibition by cerulenin.

This results strongly indicate that the induction of apoptosis by cerulenin is not due to the inhibition of FAS but that on the contrary other mechanisms of action are responsible.

4.1.2.5. Investigation of the ability of palmitate to rescue cells from cerulenin-induced apoptosis

To evaluate whether the endproduct of the FAS pathway palmitic acid was able to rescue LAN-1 or HaCaT cells from cerulenin-mediated apoptosis cells were pretreated for 2 hours with 80 μ mol palmitic acid before incubation with 15 μ g/ml cerulenin took place.

Figure 9 shows that palmitate was neither able to rescue LAN-1 cells nor HaCaT cells from cerulenin-induced apoptosis as measured by the inability of palmitate to inhibit PARP cleavage. This results further prove that cerulenin-mediated apoptosis is not mediated through FAS pathway inhibition but that other mechanisms are responsible.

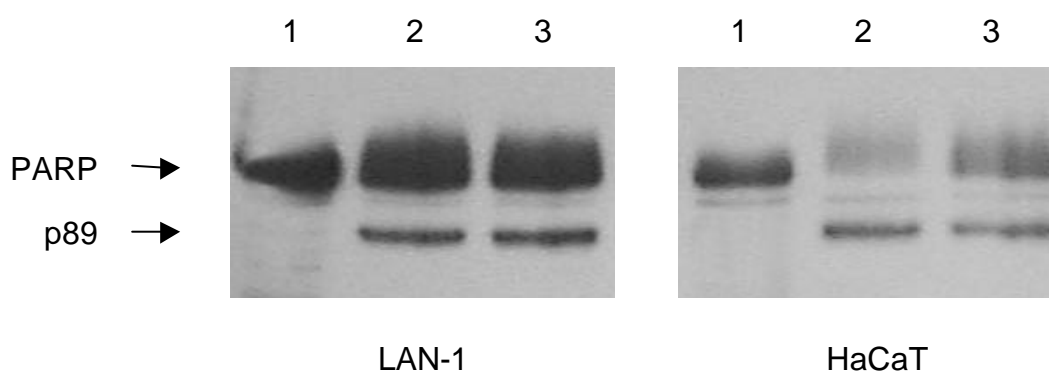


Figure 9: Lack of inhibition of PARP cleavage in LAN-1 and HaCaT cells by palmitic acid

The inhibition of PARP cleavage by palmitate was exemplarily investigated in LAN-1 (A) and HaCaT cells (B) after 18 h of incubation with 15 μ g/ml cerulenin in the presence or absence of 80 μ mol palmitate. Evaluation was done by immunoblot analysis against a polyclonal rabbit anti-PARP antibody using chemiluminescence for detection.

Lane 1: Controls treated with DMSO and palmitate for 18 h

Lane 2: Cells treated with 15 μ g/ml cerulenin for 18 h

Lane 3: Cells pretreated for 2 hours with 80 μ mol palmitate before treatment with 15 μ g/ml cerulenin took place for 18 h

4.1.3. Induction of DNA damage by cerulenin

Induction of apoptosis usually occurs through ligand binding to the corresponding death receptor or by cellular stress inducing the mitochondrial release of cytochrome C. One of the most common forms of cellular stress is the induction of DNA damage followed by (over)expression of the tumor suppressor protein p53. The induction of DNA damage is furthermore a common feature for a variety of chemotherapeutic drugs such as doxorubicin and etoposide.

The DNA damaging potential of cerulenin was first determined by its ability to induce p53 expression. In addition the expression of the growth arrest & DNA damage inducible protein 153 (GADD 153) in response to cerulenin exposure was investigated as an upregulation of its mRNA has been shown in a cDNA expression array (Weigelt 2000).

The expression of p53 and of the p53 inducible gene products p21/WAF and Bax was investigated in the different p53 wild-type cell lines (LAN-1, IMR-32, SK-N-SH, MCF7) as well as in all p53 mutated cell lines (NMB-7, HaCaT, A431, WiDr, SK-MEL-93-2 and SK-BR-3) to get the comprehensive overview of significant differences in the expression of the investigated proteins. Moreover, the p53 wild-type cell line A-172 was newly included in the investigations as functional activity of p53 in NB cell lines as well as in MCF7 cells might be impaired (Moll et al., 1998).

4.1.3.1. Expression of the tumor suppressor protein p53

The tumor suppressor protein p53 is a transcription factor which after induction migrates from the cytosol in the nucleus and causes there the expression of different genes like p21/WAF and bax. Treatment with 15 µg/ml cerulenin in the p53 wild-type cell lines LAN-1, SK-N-SH,

IMR-32, MCF7 and A-172 led to a strong induction of the p53 protein in all cell lines as shown in Figure 10. Induction of p53 was already visible after 12 h of treatment with cerulenin with a further increase after 24 h of exposure. In addition to the increased expression of p53 the induction of a further protein with an estimated molecular weight of 42 kDa was observed in SK-N-SH, IMR-32 and MCF7 cells. This 42 kDa protein is probably a recently identified new member of the p53 family, termed p53CP (Bian et al., 1997).

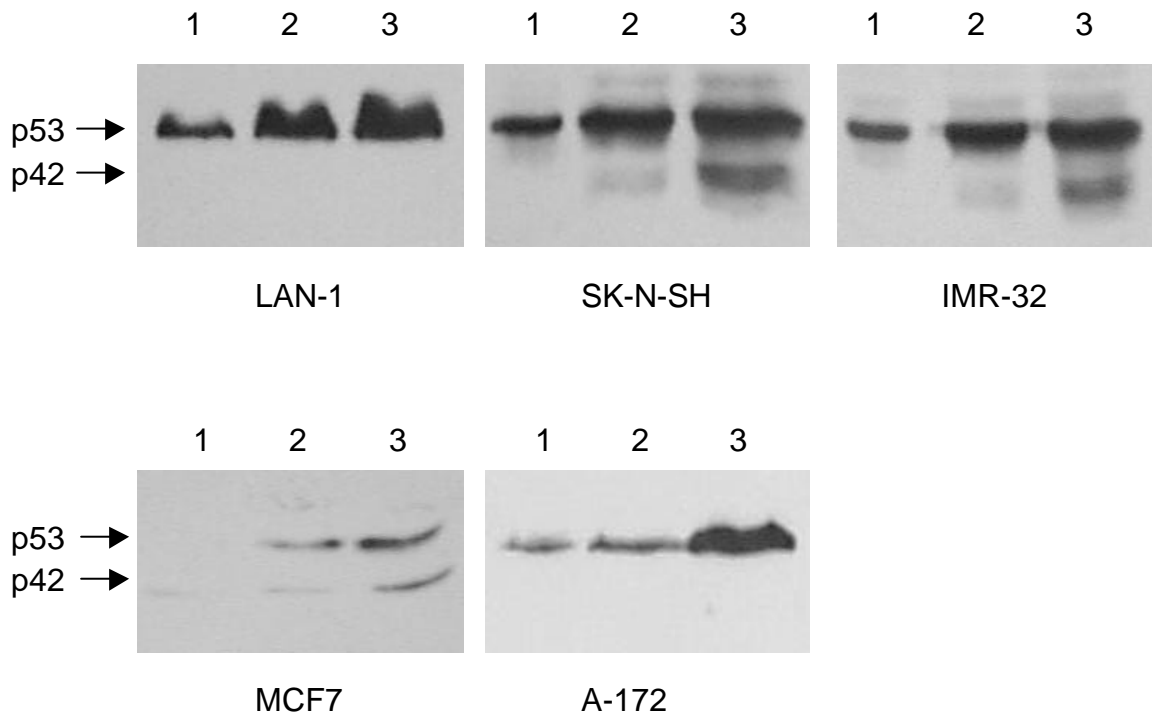


Figure 10: Expression of p53 in p53 wild-type cell lines after treatment with cerulenin

Expression of p53 after treatment with 15 $\mu\text{g/ml}$ cerulenin for indicated times was investigated in the p53 wild-type cell lines LAN-1, SK-N-SH, IMR-32, MCF7 and A-172. Evaluation was done by immunoblot analysis against a monoclonal mouse anti-p53 antibody using the ECL system for development.

Lane 1: Cells treated with DMSO alone for 24 h

Lane 2: Cells treated for 12 h with 15 $\mu\text{g/ml}$ cerulenin

Lane 3: Cells treated for 24 h with 15 $\mu\text{g/ml}$ cerulenin

As expected no induction of p53 expression could be observed in the p53 mutated cell lines NMB-7, HaCaT, A431, SK-BR-3, WiDr and SK-MEL-93-2 (Figure 11).

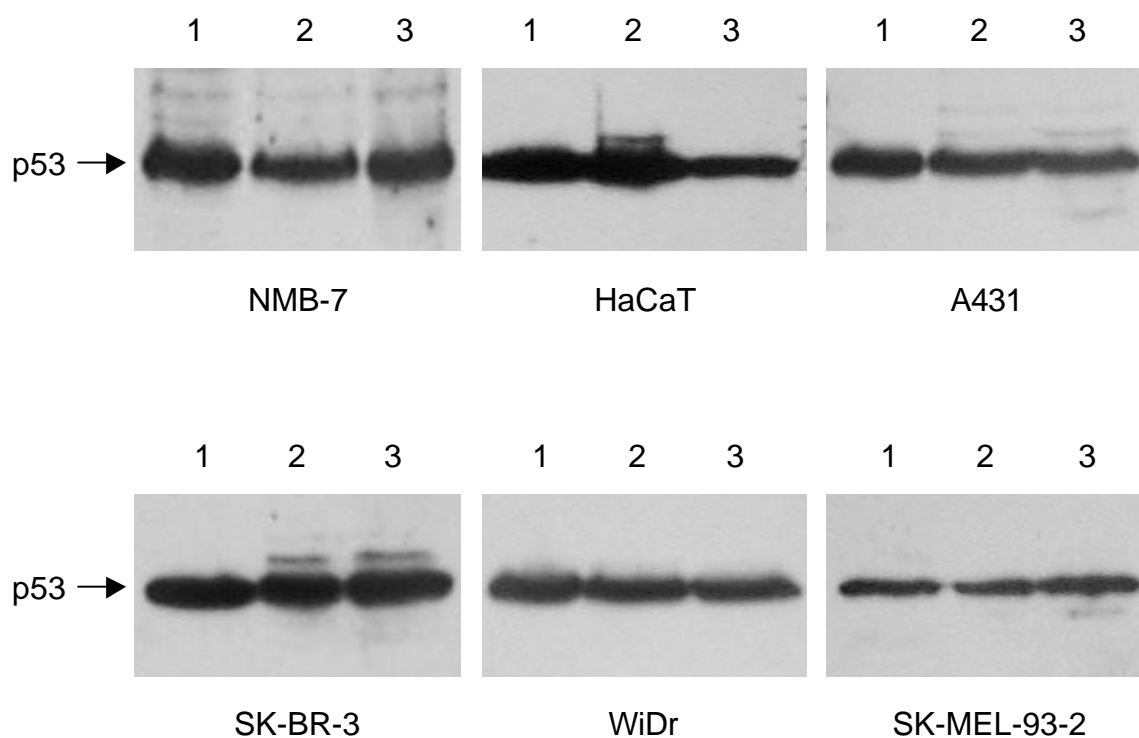


Figure 11: Expression of p53 in p53 mutated cell lines after treatment with cerulenin

Expression of p53 after treatment with 15 µg/ml cerulenin for indicated times was evaluated in the p53 mutated cell lines NMB-7, HaCaT, A431, SK-BR-3, WiDr and SK-MEL-93-2 by immunoblot analysis using a monoclonal mouse anti-p53 antibody. Detection was done with the ECL system.

Lane 1: Cells treated with DMSO alone for 24 h

Lane 2: Cells treated for 12 h with 15 µg/ml cerulenin

Lane 3: Cells treated for 24 h with 15 µg/ml cerulenin

4.1.3.2. Expression of GADD153

Results of a cDNA expression array indicated an increase in mRNA expression of the growth arrest & DANN damage inducible protein 153 (GADD 153) in LAN-1 cells (Weigelt, 2000). Hence the expression of GADD 153 was investigated exemplarily in the p53 wild-type and mutated cell lines LAN-1, HaCaT and WiDr after treatment with 15 µg/ml cerulenin. An increase in GADD 153 expression independent of the p53 status was observed in all three cell lines as early as 12 h after cerulenin treatment further proving its DNA damaging potential (Figure 12).

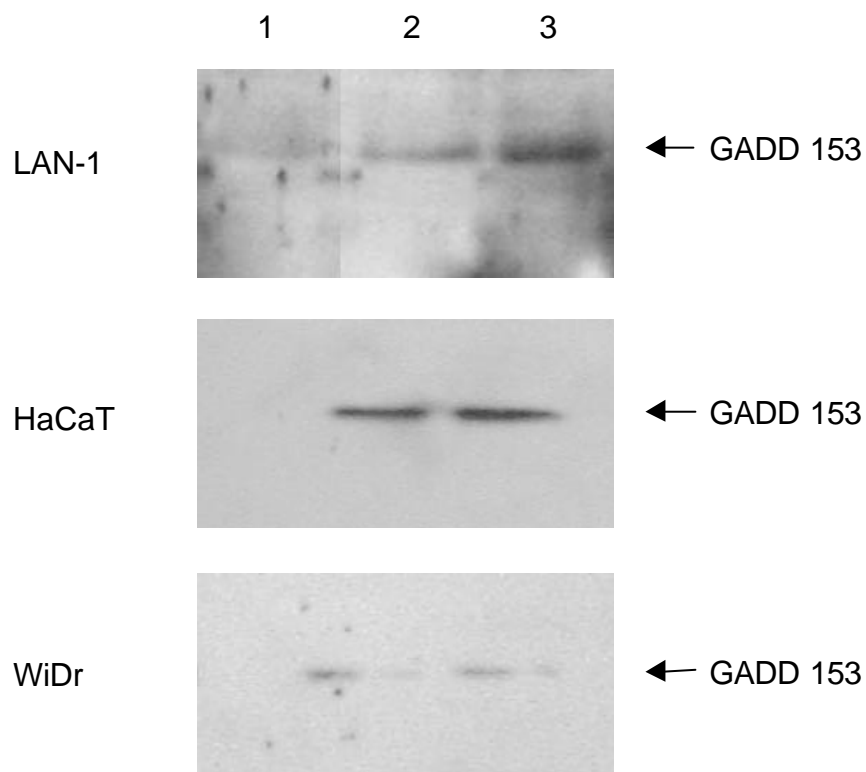


Figure 12: Expression of GADD 153 after treatment with cerulenin.

Expression of GADD 153 was investigated in LAN-1, HaCaT and WiDr cells after exposure to 15 µg/ml cerulenin by immunoblot analysis using the ECL system for development. A monoclonal mouse anti-GADD 153 antibody was used for detection of GADD 153.

Lane 1: Cells treated with DMSO alone for 24 h

Lane 2: Cells treated for 12 h with 15 µg/ml cerulenin

Lane 3: Cells treated for 24 h with 15 µg/ml cerulenin

4.1.3.3. Expression of p21/WAF

The p53 inducible cyclin-dependent kinase inhibitor p21/WAF is responsible for G1 arrest after DNA damage to allow cells to repair the DNA-damage or to prevent DNA damaged cells to divide and implement the damage in successor cells.

The exposure of the p53 wild-type cell lines LAN-1, SK-N-SH, IMR-32, MCF7 and A-172 to cerulenin surprisingly did not induce the expression of p21/WAF although this cell lines showed a strong increase in p53 expression (Figure 13). Rather the cell lines where p21/WAF was detectable under normal conditions showed a decreased expression with increased exposure times to cerulenin.

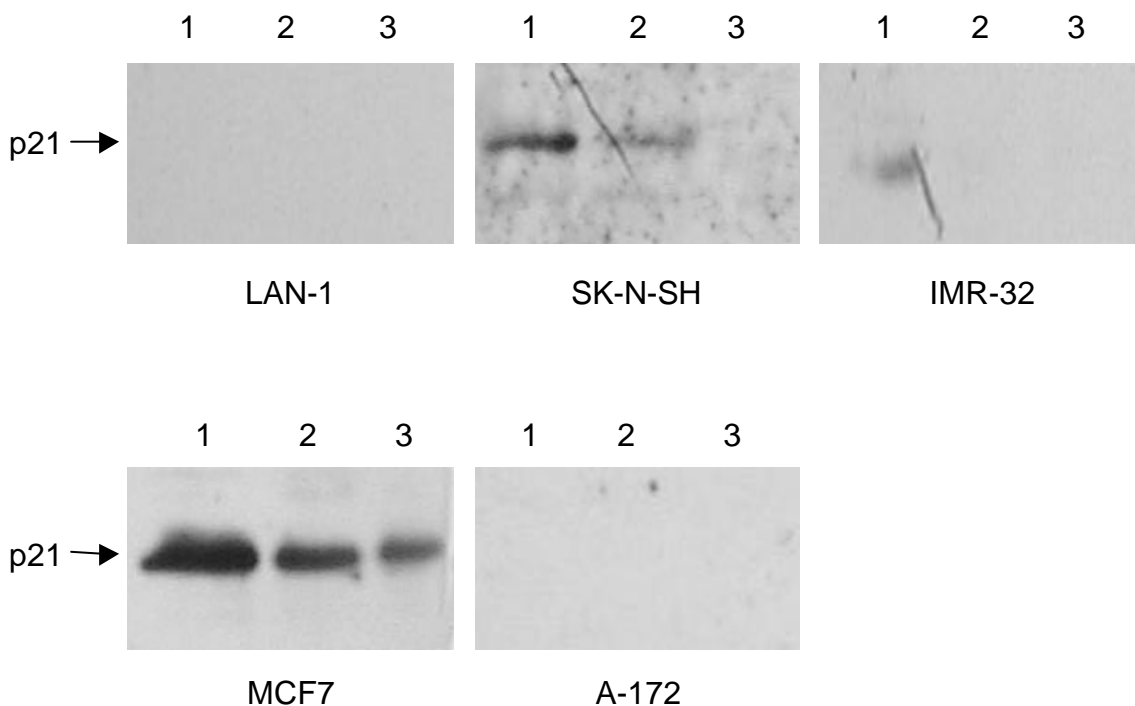


Figure 13: Expression of p21 in p53 wild-type cell lines after treatment with cerulenin

Investigation of p21 expression in the p53 wild-type cell lines LAN-1, SK-N-SH, IMR-32, MCF7 and A-172 after treatment with 15 µg/ml cerulenin for indicated times. Evaluation was done by blotting against a monoclonal mouse anti-p21 antibody and the ECL system for development.

Lane 1: Cells treated with DMSO alone for 24 h

Lane 2: Cells treated for 12 h with 15 µg/ml cerulenin

Lane 3: Cells treated for 24 h with 15 µg/ml cerulenin

On the other hand all p53 mutated cell lines (NMB-7, HaCaT, A431, SK-BR-3, WiDr and SK-MEL-93-2) showed an unexpected increase in p21/WAF protein levels after 12 h and stronger after 24 h of exposure to cerulenin (Figure 14).

The induction of p21/WAF in the p53 mutated cell lines and the decrease or non detectable expression in the p53 wild-type cell lines was puzzling and indicated that the p21/WAF expression is regulated in a p53 independent manner.

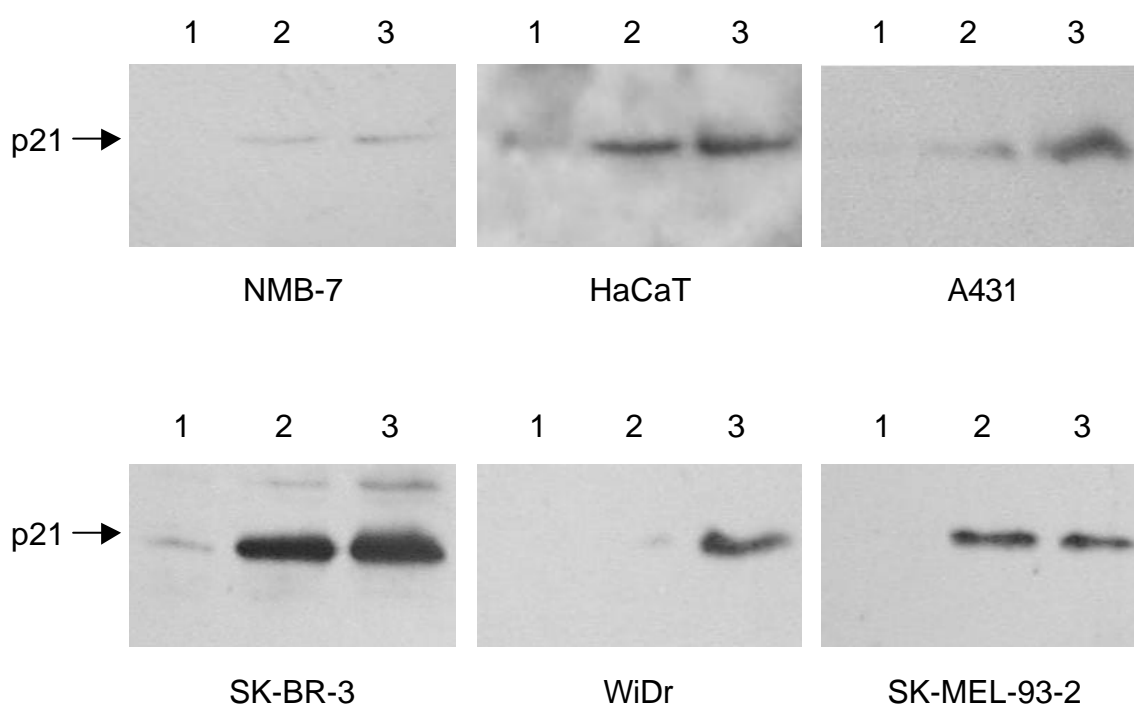


Figure 14: Expression of p21 in p53 mutated cell lines after treatment with cerulenin

Expression of p21 after treatment with 15 $\mu\text{g/ml}$ cerulenin for indicated times was evaluated in the p53 mutated cell lines NMB-7, HaCaT, A431, SK-BR-3, WiDr and SK-MEL-93-2 by immunoblotting against a monoclonal mouse anti-p21 antibody using the ECL system for development.

Lane 1: Cells treated with DMSO alone for 24 h

Lane 2: Cells treated for 12 h with 15 $\mu\text{g/ml}$ cerulenin

Lane 3: Cells treated for 24 h with 15 $\mu\text{g/ml}$ cerulenin

4.1.3.4. Expression of Bax

Bax is a proapoptotic member of the Bcl-2 family and plays an important role in the apoptotic process involving mitochondria due to its pore-forming ability.

All three p53 wild-type NB cell lines (LAN-1, SK-N-SH and IMR-32) showed a strong increase in expression of Bax protein levels after 24 h whereas no increase was observed in the p53 wild-type cell lines MCF7 and A-172 (Figure 15). The NB cell lines showed an additional band at approximately 18 kDa after 24 h of cerulenin treatment, presumably a previously described cleavage product of Bax (Wood et al., 1999).

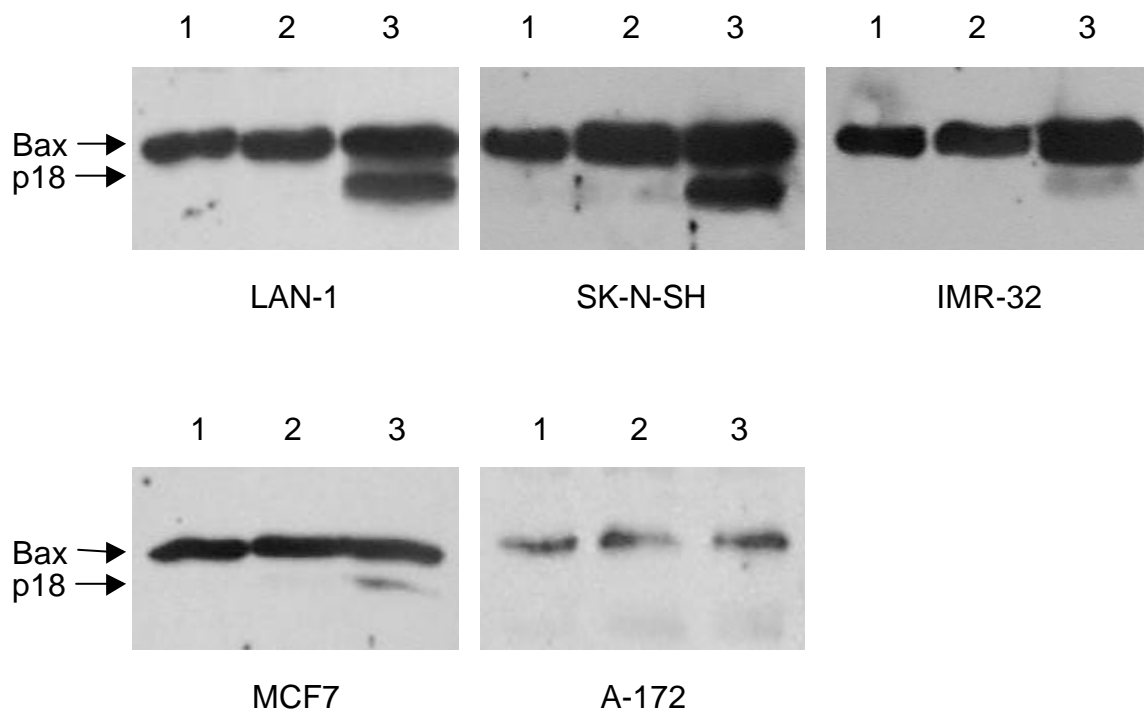


Figure 15: Expression of Bax in p53 wild-type cell lines after treatment with cerulenin

Analysis of Bax expression after treatment with 15 µg/ml cerulenin for 12 h and 24 h in the p53 wild-type cell lines LAN-1, SK-N-SH, IMR-32, MCF7 and A-172 by immunoblot analysis using a polyclonal rabbit anti-Bax antibody and the ECL system for development.

Lane 1: Cells treated with DMSO alone for 24 h

Lane 2: Cells treated for 12 h with 15 µg/ml cerulenin

Lane 3: Cells treated for 24 h with 15 µg/ml cerulenin

As shown in Figure 16 the p53 mutated cell lines SK-BR-3, WiDr and SK-MEL-93-2 did not show any differences in Bax protein levels after treatment with cerulenin. In NMB-7, HaCaT and A431 cells on the other hand an increased expression of Bax was observed after 12 h and stronger after 24 h of exposure to cerulenin. Interestingly the NB cell line NMB-7 also showed an additional band at 18 kDa after 24 h.

In summary, overexpression of Bax seemed to be independent of the p53 status and rather dependent of the type of tumor cell line. Furthermore all investigated NB cell lines (LAN-1, SK-N-SH, IMR-32 and NMB-7) showed a strong increase in Bax protein levels as well as the appearance of an 18 kDa band, presumably a cleavage product of Bax.

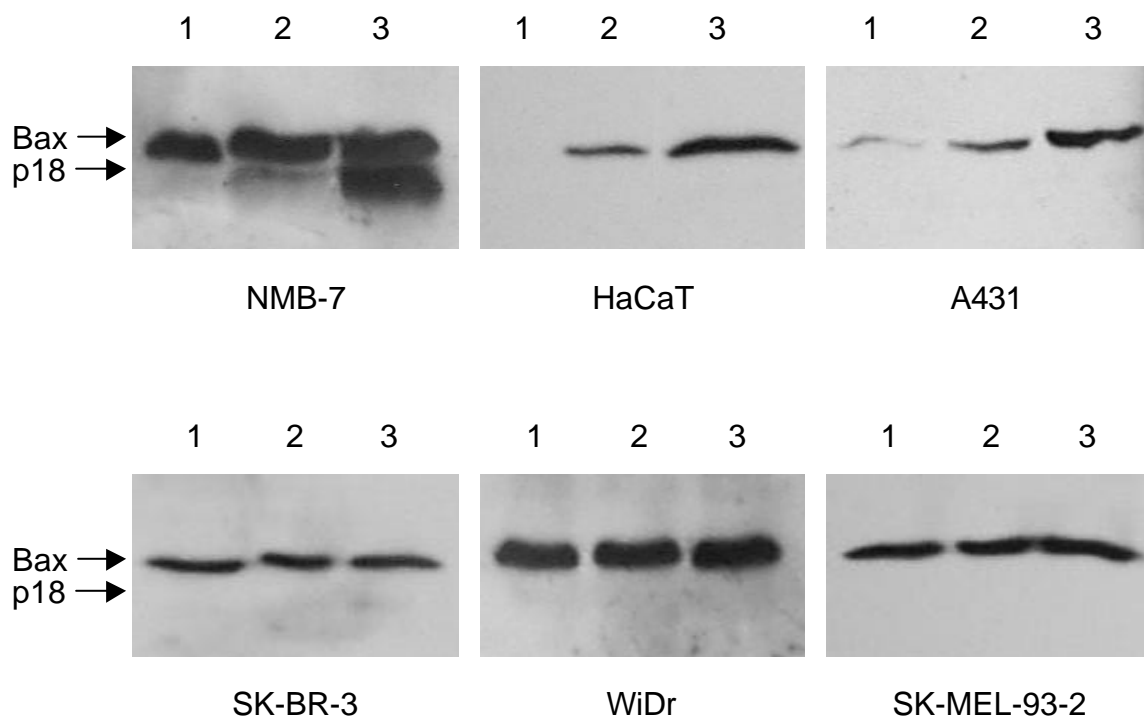


Figure 16: Expression of Bax in p53 mutated cell lines after treatment with cerulenin

Expression of Bax after treatment with 15 $\mu\text{g/ml}$ cerulenin for indicated times was investigated in the p53 mutated cell lines NMB-7, HaCaT, A431, SK-BR-3, WiDr and SK-MEL-93-2. Evaluation was done by immunoblot analysis against a polyclonal rabbit anti-Bax antibody using the ECL system for development.

Lane 1: Cells treated with DMSO alone for 24 h

Lane 2: Cells treated for 12 h with 15 $\mu\text{g/ml}$ cerulenin

Lane 3: Cells treated for 24 h with 15 $\mu\text{g/ml}$ cerulenin

4.1.4. Induction of apoptosis and DNA damage by doxorubicin and etoposide

The results obtained with cerulenin regarding the induction of p53 inducible genes were quite puzzling. Functional impairment of wild-type p53 due to impaired translocation into the nucleus has been reported for different NB cell lines and the breast cancer cell line MCF7 and might be an explanation for the lack of induction in these cell lines. But even in the p53 wild-type and p53 functional glioblastoma cell line A-172 no induction of p21/WAF and Bax was observed. It is therefore unlikely that functional impairment was the reason for the lack of induction of the p53 inducible genes.

To further evaluate this phenomenon the effects of the known DNA damaging agents doxorubicin and etoposide regarding the induction of apoptosis and DNA damage were determined by cleavage of PARP and expression of p53, p21/WAF and Bax. The p53 wild-type NB cell lines SK-N-SH, the p53 functional glioblastoma cell line A-172 as well as the p53 mutated cell line HaCaT were chosen for this approach. The commonly used NB cell line LAN-1 was refractory to treatment with both doxorubicin and etoposide and was therefore not included in this analysis. Similar results were obtained after treatment with doxorubicin (1 µg/ml) and etoposide (50 µmol) and the results with etoposide are exemplary shown (Figure 17 A-D). The induction of apoptosis by doxorubicin and etoposide was of particular importance as responses to an overexpression of p53 can result in either apoptosis or cell cycle arrest or both depending on the extent of DNA damage induced. To best compare the effects in these systems with the effects obtained after treatment with cerulenin a similar apoptotic response was most desirable. As shown in Figure 17 A cleavage of PARP was clearly visible after 24 h of incubation in all investigated cell lines indicating that the

induction of apoptosis is independent of p53 expression, a characteristic also observed after treatment with cerulenin.

Subsequently the induction of p53 and the p53 inducible gene products p21/WAF and Bax was investigated (Figure 17 B-D). A strong induction of p53 was observed in the p53 wild-type cell lines SK-N-SH and A-172, while the p53 mutated cell line HaCaT did not show an altered expression of p53 (Figure 17 B). The increases in p53 levels achieved with both doxorubicin and etoposide were comparable to the one obtained with cerulenin. Interestingly the NB cell line SK-N-SH showed the expression of an additional band of approximately 42 kDa after 24 h of treatment with both doxorubicin and etoposid. This additional band was also observed after treatment with cerulenin.

In contrast to treatment with cerulenin exposure to doxorubicin and etoposide led to a strong increase in p21/WAF expression in the p53 wild-type cell lines whereas the p53 mutated cell line HaCaT did not show expression of p21 at all (Figure 17 C). In accordance with the apparent functional activity of p53 after treatment with doxorubicin and etoposide an increased expression of Bax was observed in the p53 wild-type cell line SK-N-SH and A-172 whereas the p53 mutated cell line HaCaT showed unchanged Bax protein levels (Figure 17 D). Moreover the presumable 18 kDa Bax cleavage product was detected exclusively in the NB cell line SK-N-SH indicating that cleavage of Bax is a common feature in NB cell lines with a variety of chemotherapeutic drugs.

In summary comparable results for cleavage of PARP and induction of p53 expression were obtained with cerulenin, doxorubicin and etoposide. In sharp contrast doxorubicin and etoposide but not cerulenin were able to induce a strong increase in p21/WAF and Bax in both p53 wild-type cell lines. This results indicate that the lack of induction of p53 inducible genes after treatment with cerulenin is not due to functional impairment of p53 but due to other so far unknown mechanisms.

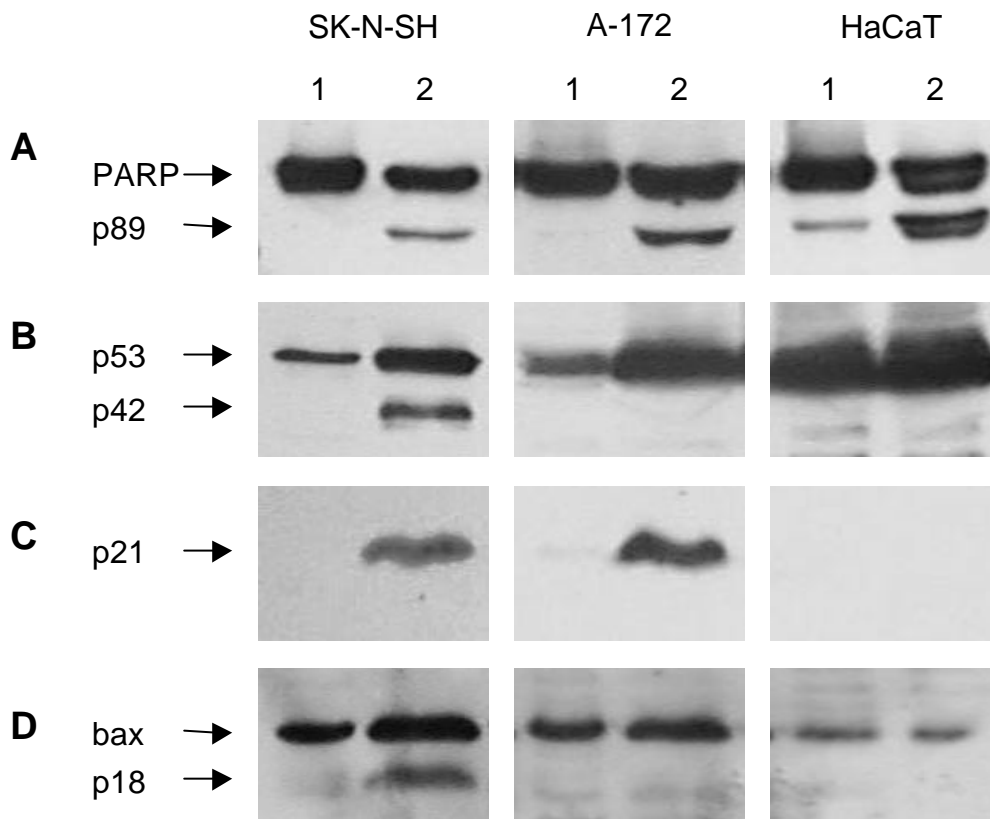


Figure 17: Investigation of PARP cleavage and expression of p53 and the p53 inducible genes p21/WAF and Bax after treatment with etoposide in the p53 wild-type cell lines SK-N-SH and A-172 and the p53 mutated cell line HaCaT

Cleavage of the intact PARP into its 89 kDa fragment and the expression of p53 and the p53 inducible genes p21/WAF and Bax were investigated after treatment with 50 μmol etoposide for 24 h in the p53 wild-type cell lines SK-N-SH and A-172 and the p53 mutated cell line HaCaT by immunoblot analysis. Detection in all cases was done with the ECL system.

- A) Cleavage of PARP into its 89 kDa fragment was determined using a polyclonal rabbit anti-PARP antibody.
- B) Expression of p53 was evaluated with a monoclonal mouse anti-p53 antibody.
- C) Expression of p21/WAF was determined with a monoclonal mouse anti-p21 antibody.
- D) Expression and cleavage of Bax was evaluated using a polyclonal rabbit anti-Bax antibody.

Lane 1: Cells treated with DMSO alone for 24 h.

Lane 2: Cells treated for 24 h with 50 μmol etoposide.

4.1.5. Cerulenin-mediated signal transduction pathway

The induction of apoptosis was verified in a host of different tumor cell lines both by Annexin V assay and PARP cleavage (see 4.4.1). Though this results clearly prove that cerulenin induces apoptosis nothing was so far known about the involved signal transduction pathway. The initial characterization of the cerulenin-mediated apoptotic pathway in particular the time dependence of the process and the involvement of mitochondria and caspases was therefore the next aim. The p53 wild-type cell line LAN-1 and the p53 mutated cell line HaCaT were chosen for this approach to further evaluate whether there are differences in the cerulenin-mediated signal transduction pathway in dependence of the p53 status.

4.1.5.1. Time dependence of PARP cleavage

The onset of apoptosis as measured by PARP cleavage was a rapid process. The characteristic cleavage product of 89 kDa was observed after nine hours of incubation with 15 µg/ml cerulenin in LAN-1 cells and increased in a time-dependent manner (Figure 18 A). Similar results were obtained with HaCaT cells where the 89 kDa cleavage product was even detectable after 6 hours of cerulenin treatment (Figure 18 B). After 24 h of incubation with cerulenin intact PARP was already completely degraded underscoring the high sensitivity of these cell lines against cerulenin.

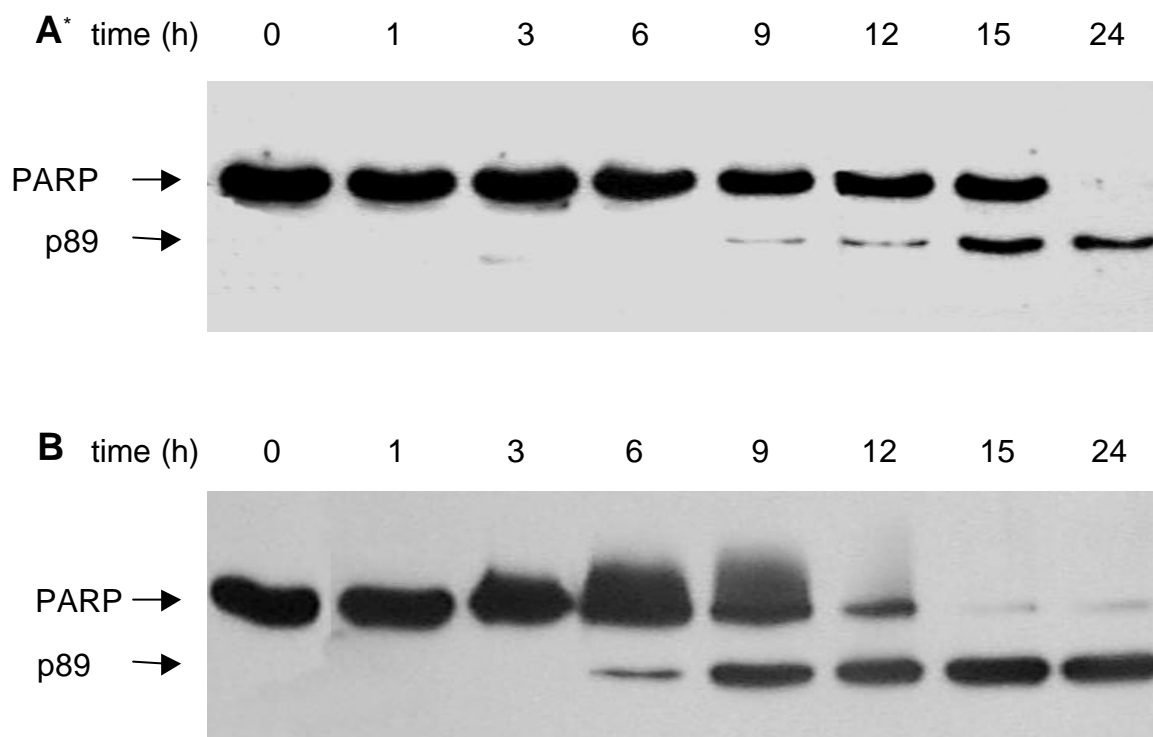


Figure 18: Time-dependent cleavage of PARP in LAN-1 and HaCaT cells after treatment with cerulenin

Cleavage of PARP after treatment with 15 $\mu\text{g/ml}$ cerulenin for indicated times was determined by immunoblot analysis in LAN-1 cells (A) and in HaCaT cells (B) against a polyclonal rabbit anti-PARP antibody using the ECL system for detection.

To evaluate whether caspases are involved in the apoptotic process upstream of PARP cleavage LAN-1 and HaCaT cells were incubated with the broad range caspase inhibitor zVAD-fmk before treatment with cerulenin took place.

As shown in Figure 19 preincubation with zVAD-fmk led to a complete inhibition of PARP cleavage in both cell lines. These results clearly show that PARP cleavage is mediated by caspases and that caspases therefore are evidently involved in the cerulenin-mediated apoptosis. Although zVAD-fmk inhibited PARP cleavage, it was not able to inhibit the commitment of cell death in LAN-1 and in a lesser extent in HaCaT cells. Even in the presence of zVAD-fmk cerulenin induced the

characteristic morphological changes of apoptosis (data not shown). These data indicate that the cerulenin-mediated apoptosis is not solely mediated through upstream caspases but that additional mediators than caspases are also involved.

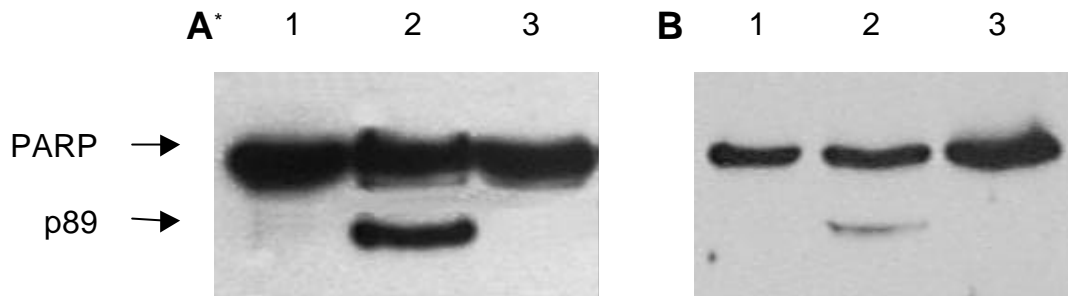


Figure 19: Inhibition of PARP cleavage by the broad range caspase inhibitor zVAD-fmk in LAN-1 and HaCaT cells

Cleavage of PARP after 18 h of incubation with 15 $\mu\text{g/ml}$ cerulenin in the presence or the absence of the broad range caspase inhibitor zVAD-fmk (75 μmol) was determined in LAN-1 cells (A) and in HaCaT cells (B). Evaluation was done by immunoblotting against a polyclonal rabbit anti-PARP antibody and the ECL system was used for immunodetection.

Lane 1: Controls treated with DMSO alone

Lane 2: Cells treated for 18 h with 15 $\mu\text{g/ml}$ cerulenin

Lane 3: Cells treated 1 h with 75 μmol zVAD-fmk prior to exposure to 15 $\mu\text{g/ml}$ cerulenin for 18 h

4.1.5.2. Involvement of mitochondria

Mitochondria have been illustrated to be involved especially in drug-induced apoptotic systems. Moreover the investigation of p53 inducible genes had shown an overexpression of the proapoptotic poreforming protein Bax in all NB cell lines as well as in HaCaT and A431 cells indicating the involvement of mitochondria in the apoptotic response (see 4.4.3.4.). To further evaluate the role of mitochondria, first, the expression of Bax was more thoroughly investigated in LAN-1 and HaCaT cells (Figure 20 A and B). In both cell lines Bax expression started to increase after 12 h of incubation with cerulenin. In parallel an additional band of approximately 18 kDa could be detected in LAN-1 but not in HaCaT cells. This 18 kDa protein first appeared after 18 h of incubation

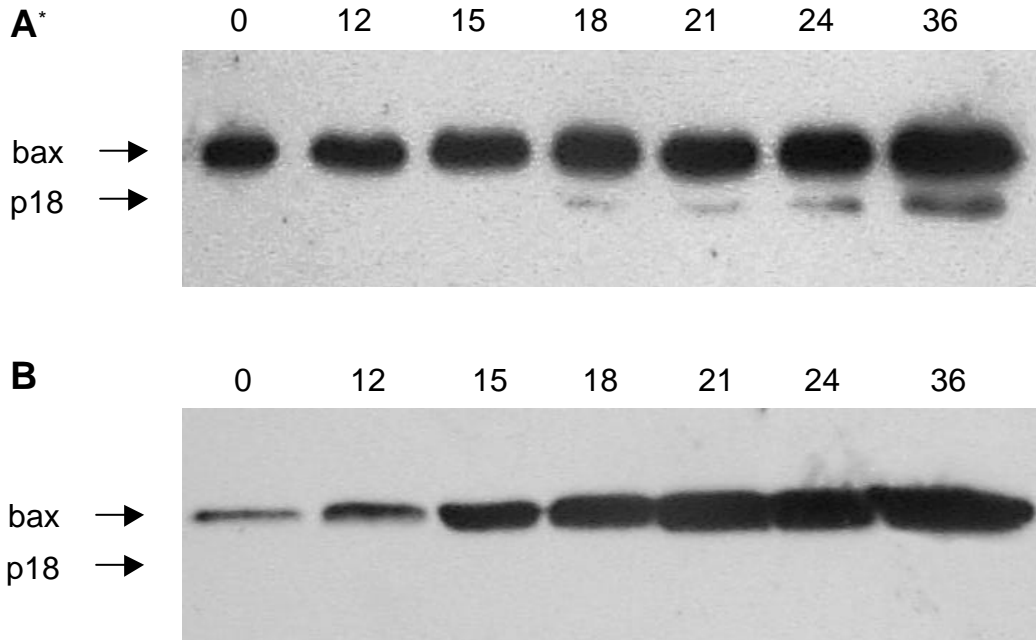


Figure 20: Expression of Bax in LAN-1 and HaCaT cells after treatment with cerulenin

Expression of Bax was determined by immunoblot analysis in LAN-1 cells (A) and in HaCaT cells (B) after treatment with 15 $\mu\text{g/ml}$ cerulenin for indicated times. A polyclonal rabbit anti-Bax antibody and the ECL system were used for immunodetection.

and increased in intensity over 36 h. Presumably this 18 kDa protein is a cleavage product of Bax which has been described previously as a more cytotoxic form than the full length 21 kDa Bax protein (Wood et al., 2000). It has been shown that the release of cytochrome C from the mitochondria into the cytosol is triggered by overexpression of Bax and represents an important mediator of drug-induced apoptosis. To evaluate whether cytochrome C is an effector molecule in the cerulenin-mediated apoptotic pathway its release in LAN-1 and HaCaT cells was investigated next. Figure 21 shows that the release of cytochrome C from the mitochondria into the cytosol is an early event. In LAN-1 cells the release could be detected already after 3 h of cerulenin treatment whereas the release in HaCaT cells was observed after 6 h.

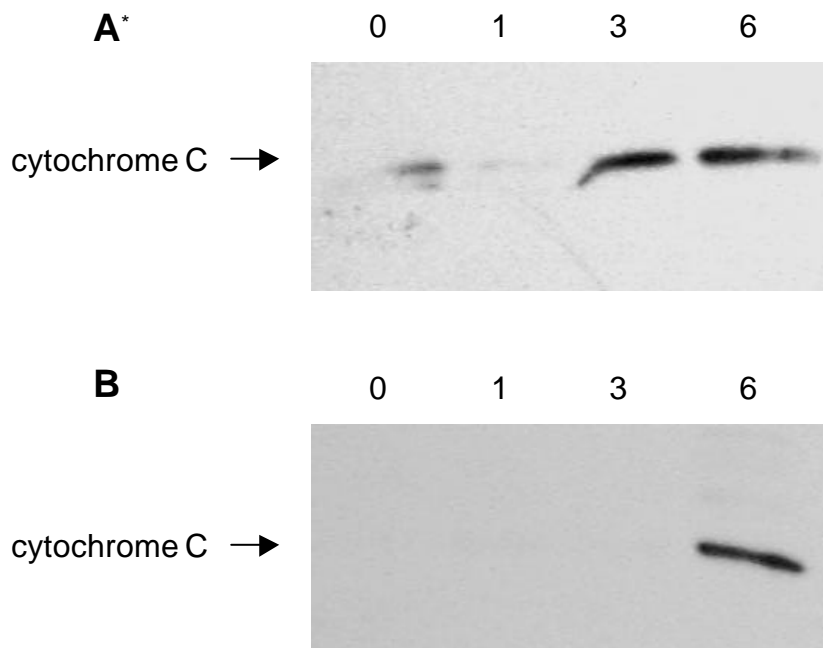


Figure 21: Cerulenin-induced cytochrome C release into the cytosol in LAN-1 and HaCaT cells

Following treatment with 15 $\mu\text{g/ml}$ for indicated time the release of cytochrome C into the cytosol was examined in LAN-1 cells (A) and in HaCaT cells (B) by immunoblot analysis against a polyclonal rabbit anti-cytochrome C antibody. The ECL system was used for detection.

Finally, changes in the mitochondrial potential following treatment with cerulenin were investigated in LAN-1 and HaCaT cells (Figure 22 and 23). As shown in Figure 22 a decrease in the mitochondrial potential in LAN-1 cells was observed as early as 18 h after incubation with cerulenin. A further decrease of the mitochondrial potential occurred in a time-dependent manner eventually leading to a complete breakdown after 36 h of incubation. On the other hand no changes in the mitochondrial potential were observed in HaCaT cells (Figure 23).

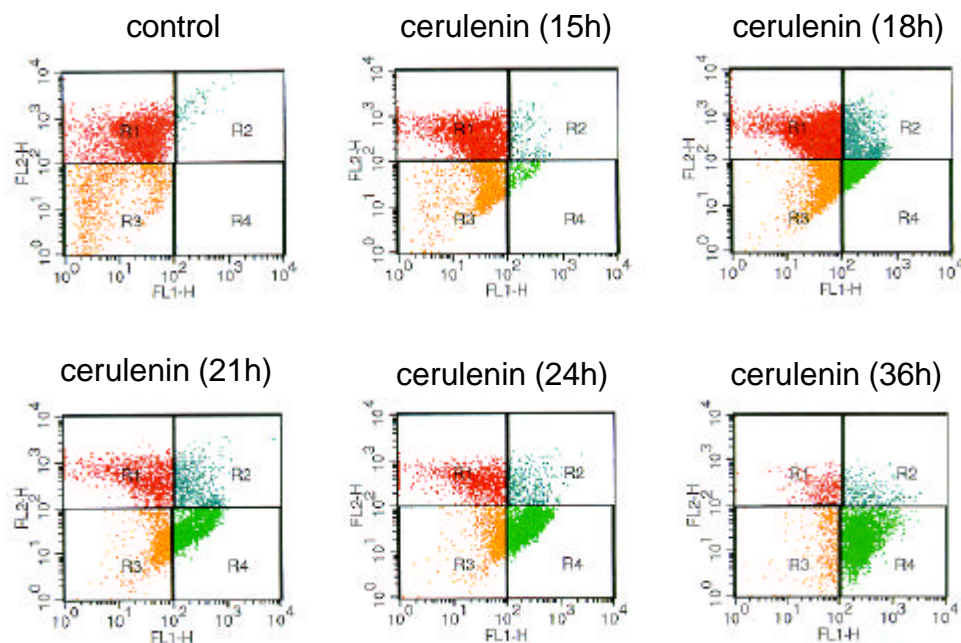


Figure 22: Assessment of the mitochondrial potential in LAN-1 cells following cerulenin treatment

LAN-1 cells were treated for indicated times with 15 $\mu\text{g/ml}$ cerulenin and the mitochondrial potential was quantified by cytofluorometric analysis. Staining was performed with the cationic lipophilic fluorochrome JC-1. Analysis by courtesy of Dr. David.

This results indicate that the mere overexpression of Bax is not sufficient for the mitochondrial breakdown as HaCaT cells showed a strong overexpression of Bax but no breakdown of the mitochondrial potential. Interestingly, the onset of the mitochondrial breakdown in LAN-1 cells correlated with the appearance of the 18 kDa cleavage product of Bax. Moreover, the further decrease in the mitochondrial potential was accompanied by increasing amounts of the 18 kDa cleavage product leading to the assumption that the generation of the 18 kDa fragment of Bax is responsible for the mitochondrial breakdown.

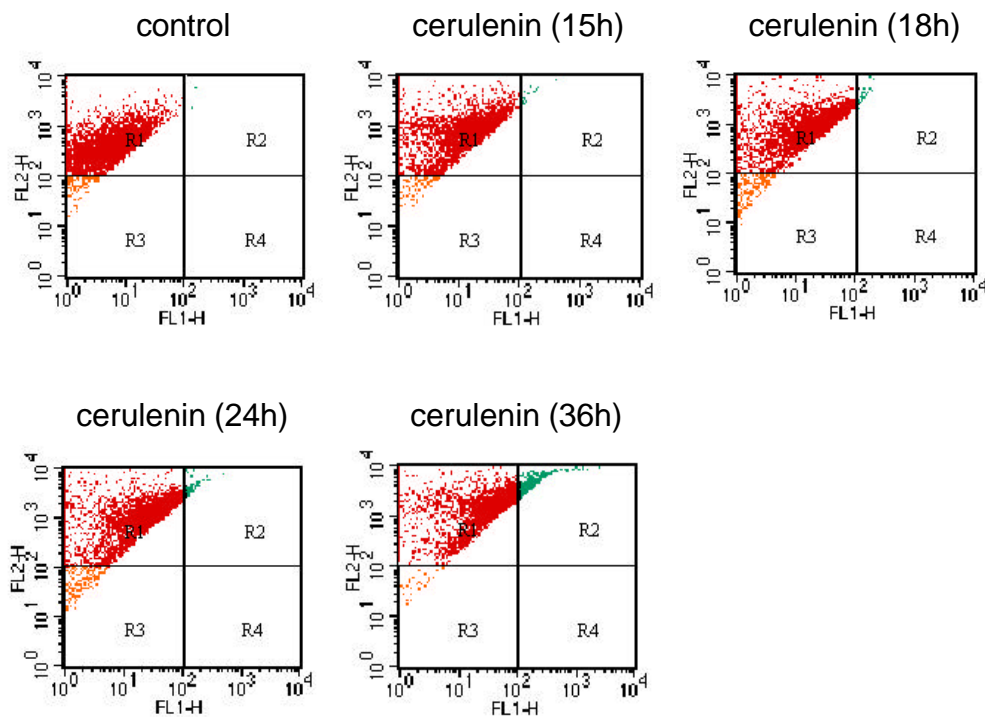


Figure 23: Assessment of the mitochondrial potential in HaCaT cells after treatment with cerulenin

HaCaT cells were treated for indicated times with 15 $\mu\text{g/ml}$ cerulenin and the mitochondrial potential was quantified by cytofluorometric analysis. Staining was performed with the cationic lipophilic fluorochrome JC-1. Analysis by courtesy of Dr. David.

4.1.5.3. Activation/Involvement of caspases

The release of cytochrome C in the cytosol is an event known to activate caspase 9 by formation of a complex of cytochrome C, APAF-1 and caspase 9 itself. Hence the activation of caspase 9 was first investigated in both cell lines after treatment with cerulenin (Figure 24). In accordance with the early release of cytochrome C into the cytosol the development of the 10 kDa cleavage product of caspase 9 was detected after 6 h in LAN-1 and HaCaT cells.

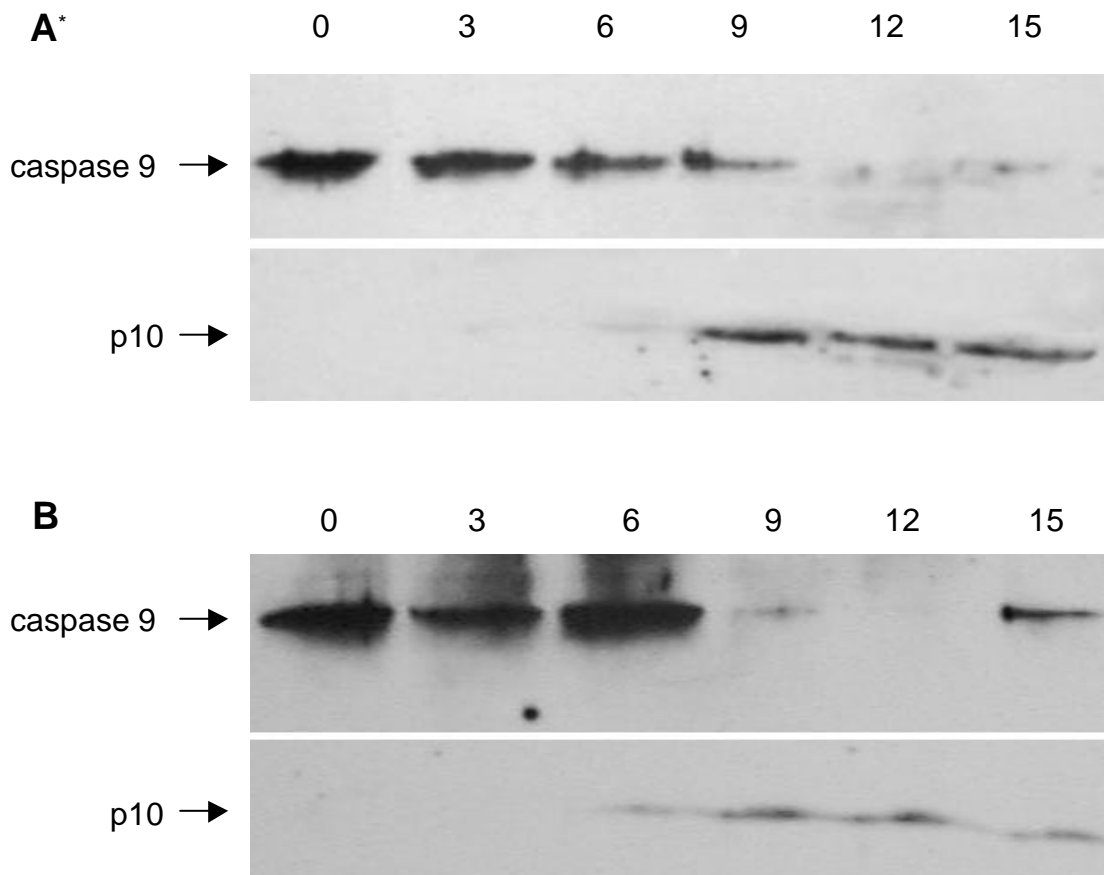


Figure 24: Cleavage of caspase 9 in LAN-1 and HaCaT cells after exposure to cerulenin

Cleavage of caspase 9 in LAN-1 cells (A) and in HaCaT cells (B) after exposure to 15 $\mu\text{g/ml}$ cerulenin for indicated times. Analysis by immunoblotting against a polyclonal rabbit anti-caspase 9 antibody using the ECL system for detection.

Caspase 3 can be activated by the active form of caspase 9 and is the caspase usually responsible for the cleavage of PARP. Therefore the activation of caspase 3 was investigated next. As shown in Figure 25 the proteolytic processing of procaspase 3 into its active 17 kDa fragment began after nine hours of cerulenin treatment in LAN-1 cells while the appearance in HaCaT cells in accordance with their earlier onset of PARP cleavage was already detectable after six hours of incubation.

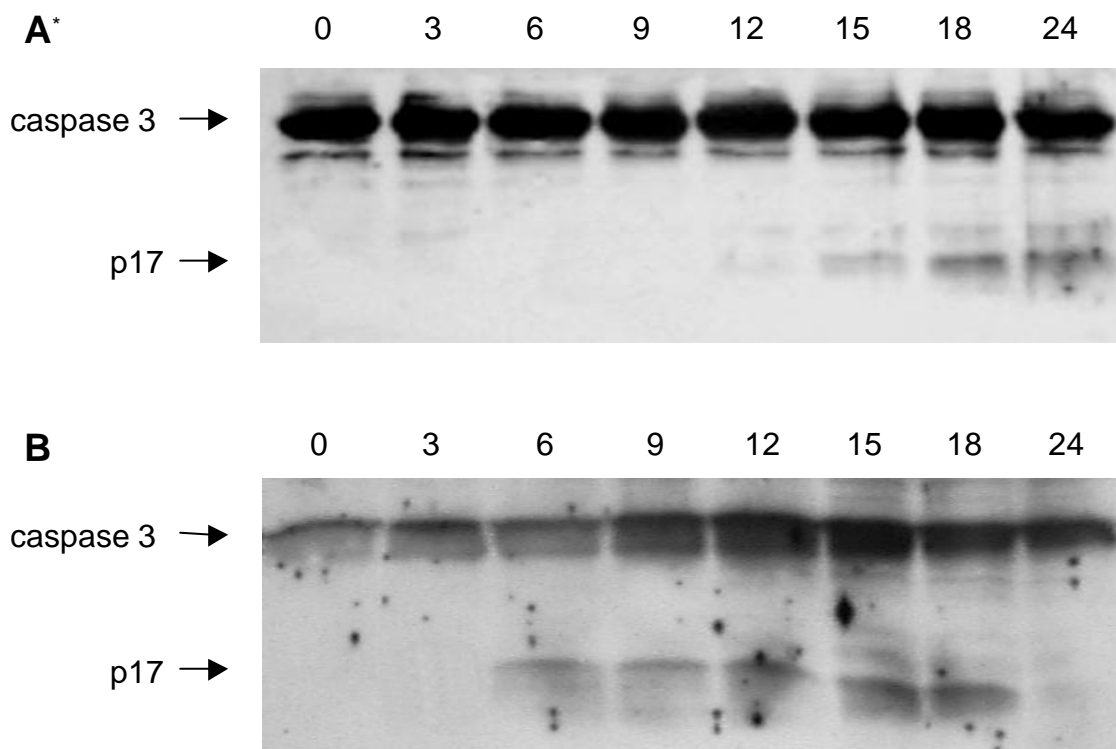


Figure 25: Cerulenin-induced activation of caspase 3 in LAN-1 and HaCaT cells

Cleavage of caspase 3 in LAN-1 cells (A) and in HaCaT cells (B) after treatment for indicated times with 15 $\mu\text{g/ml}$ cerulenin was determined by immunoblot analysis against a polyclonal rabbit anti-caspase 3 antibody using the ECL system for detection.

Caspase 8 usually functions as a receptor-mediated upstream caspase, although it has been reported that it can also be activated downstream of the mitochondria. Interestingly, it has recently been shown that caspase 8 is silenced or deleted in N-myc amplified NB cell lines. Figure 26 shows that caspase 8 expression in LAN-1 cells was undetectable whereas the two main isoforms caspase 8a and caspase 8b could be readily detected in HaCaT cells, although no activation of caspase 8 could be observed (data not shown).

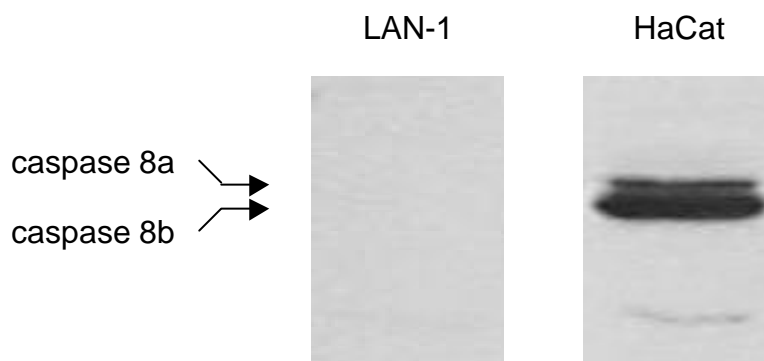


Figure 26: Presence of caspase 8 in LAN-1 and HaCaT cells

The existence of caspase 8 was examined by immunoblot analysis in LAN-1 and in HaCaT cells using a monoclonal mouse anti-caspase 8 antibody and the ECL system for detection.

4.2. IgM-mediated apoptosis and putative receptors

Previous work in our group has shown the occurrence of natural human anti-NB IgM antibodies that are capable of inducing apoptosis exclusively in human NB cells. In immunoblot analysis strong reactivity against a protein of 260 kDa, termed NB-p260, could be detected with cytotoxic sera whereas sera of NB patients showed no detection. Polyclonal antibodies raised against purified NB-p260 were able to inhibit the induction of apoptosis by anti-NB IgM or to induce apoptosis by themselves (David 1996; Weigelt 2000). The characterization of the NB-p260 proved to be extremely difficult due to its inherent instability which impeded the N-terminal sequencing of the purified protein. The purification and molecular identification of the NB-p260 protein was therefore most important. Subsequently the ability of purified NB-p260 to inhibit anti-NB IgM mediated apoptosis and its cell surface expression as a prerequisite to function as apoptosis-mediating receptor were determined.

In addition weaker reactivities were also found against a protein of approximately 90 kDa, that was later on identified as hsp 90. It has also been demonstrated that monoclonal anti-hsp 90 antibodies were able to inhibit the IgM mediated cytotoxicity to a certain amount, raising the possibility that hsp 90 might be an additional apoptosis-mediating receptor (David 1996). Yet it has still to be determined whether sera of NB patients lack reactivity against hsp 90 and whether it is expressed on the cell surface since hsp 90 can only then be involved in IgM mediated responses. Albeit hsp 60 and hsp 70 have not been identified as major antigens so far, they nevertheless were also included in this investigation since these two proteins have been implicated in a variety of immune responses including the generation of autoantibodies.

In a different approach the suitability of polyclonal anti-NB IgM for the serological analysis of a recombinant LAN-1 cDNA expression library (SEREX) to identify new potential tumor antigens was investigated.

4.2.1. Identification and characterization of NB-p260

4.2.1.1. Purification of NB-p260

According to the original purification protocol the NB-p260 was purified by sequential ion exchange chromatography, first applying the anion exchange chromatography column EconoQ followed by the cation exchanger EconoS. The NB-p260 came in the breakthrough on both columns. Complete purification was then achieved by preparative gelelectrophoresis (Heiligtag, 1998).

This protocol had two major disadvantages. First, as the NB-p260 came in the breakthrough of both columns impurities of other proteins with the same molecular weight due to incomplete binding to the matrix could not be excluded. Second, minor impurities of proteins with molecular weights close to the NB-p260 as judged by Coomassie and silver staining were always present in the NB-p260 preparations. In particular impurities of human fatty acid synthase (FAS), previously termed NB-p220, were always present in small amounts as its molecular weight was too close to get a sufficient separation from the NB-p260 by preparative gelelectrophoresis alone.

To this end the original protocol for the purification of the NB-p260 was modified to meet these concerns (Figure 27: Lane 1-7).

To exclude impurities of the same molecular weight due to incomplete binding to the matrix the NB-p260 needed to be bound to the matrix in the first step. Therefore LAN-1 cell extracts (Lane 1) were applied to a HighQ anion exchange chromatography column instead of the formerly used EconoQ column as both the resolution of bound proteins and the binding capacity were much better on the HighQ matrix. The NB-p260 eluted between a step gradient of 175 and 225 mM sodium chloride (Lane 2). The buffer exchanged material was then applied to the cation exchange chromatography column EconoS according to the old protocol and the NB-p260 was recovered in the breakthrough (Lane 3).

To get a better separation from impurities with molecular weights close to that of the NB-p260 a third chromatography matrix was introduced. A CHTII hydroxyapatite chromatography column was chosen as this matrix gave the best results regarding purity and yield out of a variety of chromatography media evaluated, including different hydrophobic interaction and ion exchange matrices. FAS could be completely separated from the NB-p260 using a step gradient between 50 and 160 mM sodium phosphate (Lane 4). The NB-p260 was then eluted in a step gradient from 160 to 350 mM sodium phosphate (Lane 5). Preparative gelelectrophoresis as final purification step yielded the purified NB-p260 (Lane 6 and 7). No impurities were visible neither by Coomassie nor by silver staining.

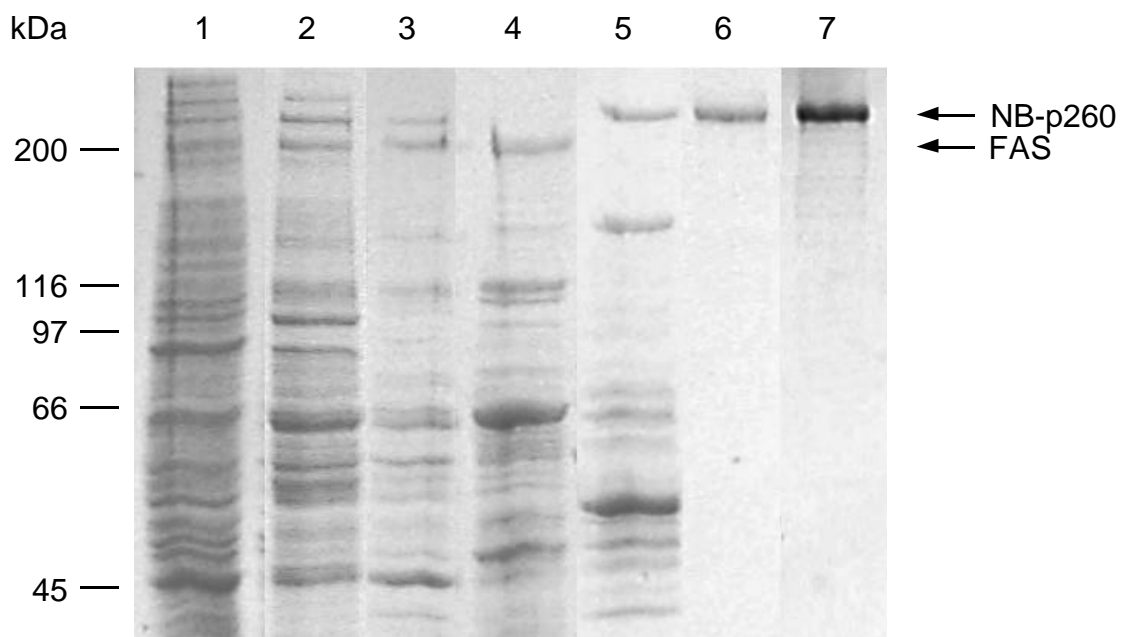


Figure 27: Purification of NB-p260 from LAN-1 NB cells

Evaluation of the purification process of the NB-p260 by SDS-PAGE (7.5%) under reducing conditions and Coomassie staining (Lane 1 to 6) and silver staining, respectively (Lane 7).

Lane 1: LAN-1 cell extracts

Lane 2: anion exchange column, 175-225 mM sodium chloride

Lane 3: cation exchange column, breakthrough in 50 mM sodium phosphate

Lane 4: hydroxyapatite column, 50-160 mM sodium phosphate

Lane 5: hydroxyapatite column, 160-350 mM sodium phosphate

Lane 6: preparative gelelectrophoresis (ultrafiltrate)

Lane 7: preparative gelelectrophoresis (ultrafiltrate)

The purification procedure yielded approximately 100 µg of NB-p260 out of 5×10^9 cells (corresponding to 100 cell culture flasks of 175 cm²). Purification of the NB-p260 was monitored using purified human anti-NB IgM from a positive donor (Figure 28: Lanes 1-5). As expected, reactivity against the anti-NB IgM was detected in all NB-p260 containing fractions.

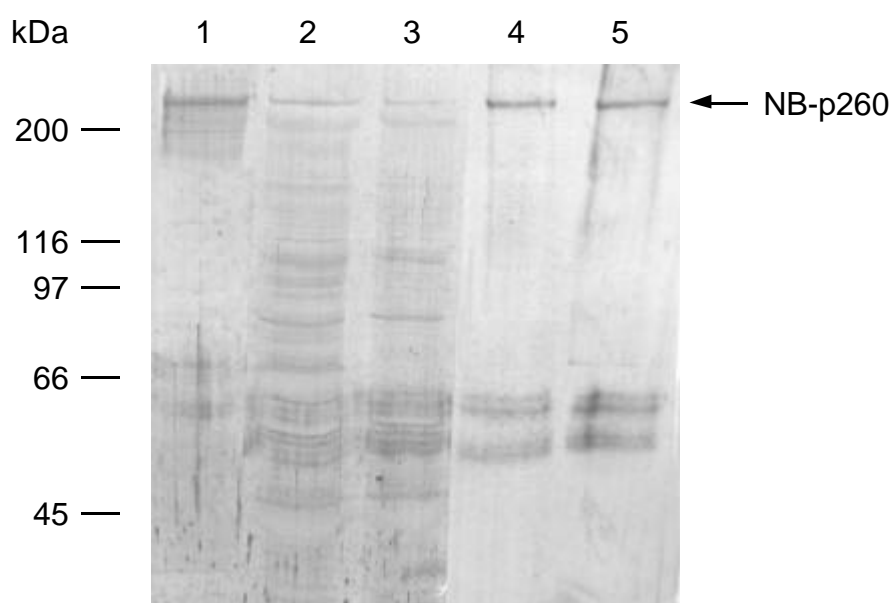


Figure 28: Immunoreactivity of the NB-p260 purification procedure against anti-NB IgM antibodies

Assessment of the purification procedure of the NB-p260 by immunoblot analysis against purified human anti-NB IgM from a positive donor after SDS-PAGE (7.5%) under reducing conditions. Immunodetection was done by color development using an AP-conjugated mouse anti-human IgM.

Lane 1: LAN-1 cell extracts

Lane 2: anion exchange column, 175-225 mM sodium chloride

Lane 3: cation exchange column, breakthrough in 50 mM sodium phosphate

Lane 4: hydroxyapatite column, 160-350 mM sodium phosphate

Lane 5: purified NB-p260 (preparative gelelectrophoresis)

4.2.1.2. Molecular characterization of the NB-p260

As previously mentioned N-terminal sequencing of the intact NB-p260 was impeded by its inherent instability. Therefore the generation of internal fragments by enzymatic digestion and their subsequent N-terminal sequencing was the next method of choice. Five different proteases were tested (trypsin, endoproteinases Lys-C, Glu-C, Asp-N and Arg-C) (not shown) of which endoproteinase Lys-C proved to be the most promising and hence was chosen for the generation of internal fragments of the purified NB-p260.

Two different approaches to generate either low or high molecular weight NB-p260 fragments were followed (Figure 29 and 30, respectively). The generation of low molecular fragments (10-40 kDa) was chosen for the advantage to yield fragments of presumably high stability, although the setback of this approach was that yields in general were low (Figure 29). The production of high molecular fragments (60-200 kDa) on the other hand gave seemingly high amounts of protein fragments, but their stability was questionable (Figure 30).

In both cases different endoproteinase Lys-C : NB-p260 ratios were examined (ranging from 1:20 to 1:200) at varying time points (2 h to 16 h) to find out the best parameters for the final digestion (data not shown).

For the generation of low molecular fragments an endoproteinase Lys-C : NB-p260 ratio from 1:50 and an incubation time of 15 h, adding new endoproteinase Lys-C every five hours, proved to be the most efficient conditions. 100 µg of purified NB-p260 were subsequently used and of the generated low molecular fragments five were chosen for N-terminal sequencing. N-terminal sequencing was done by Dr. Manfred Teppke at the in-house facility in the Department of Biochemistry and Molecular Biology at the University of Hamburg. Figure 29 shows a silver staining of an aliquot (2 %) of the total reaction.

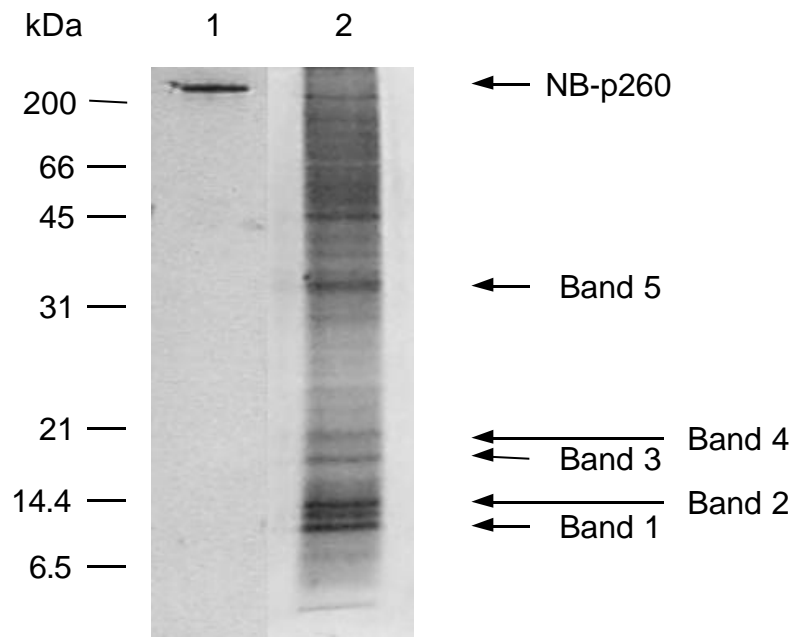


Figure 29: Generation of low molecular weight fragments of NB-p260 by endoproteinase Lys-C digestion

Evaluation of the resulting protein fragments after digestion of purified NB-p260 with endoproteinase Lys-C (50:1) for 15 h adding new enzyme every 5 h was done by SDS-PAGE (13,5%) under reducing conditions and silverstaining. Indicated bands were subjected to N-terminal sequence analysis.

Lane 1: purified NB-p260

Lane 2: NB-p260 fragments generated with endoproteinase Lys-C

For the generation of high molecular fragments an endoproteinase Lys-C : NB-p260 ratio of 1:100 and an incubation time of 4 h at 25°C proved to be best. Again, 100 µg of purified NB-p260 were used. Under this conditions all visible fragments ranged between molecular weights of 60 and 200 kDa, whereas no more intact NB-p260 was detectable at all (Figure 30). 10 different bands were subjected to N-terminal sequencing (by Dr. Teppke). Indicated in figure 5 are the five bands that yielded usable sequence information.

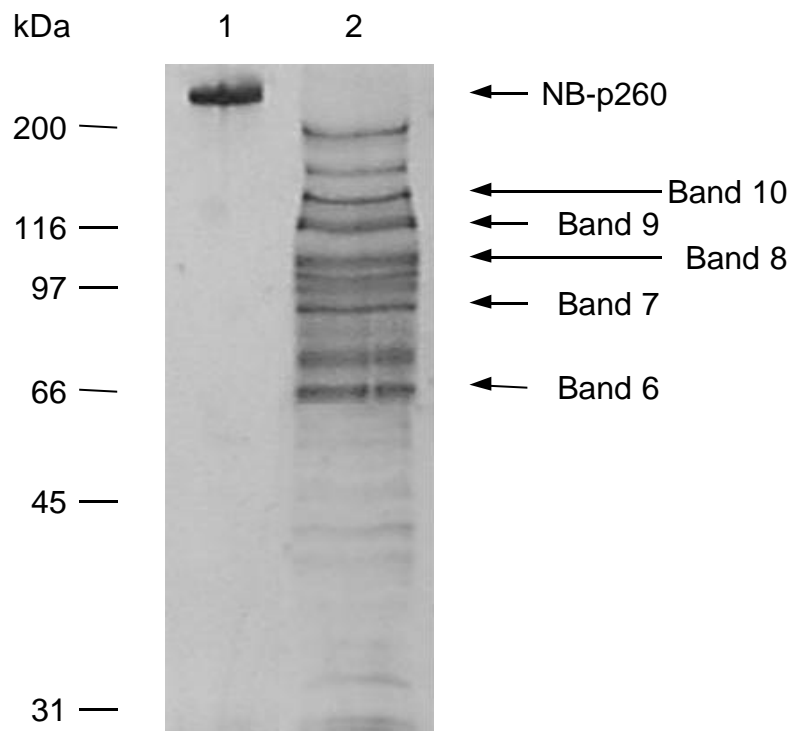


Figure 30: Generation of high molecular weight fragments of NB-p260 by endoproteinase Lys-C digestion

Assessment of the resulting protein fragments after digestion of purified NB-p260 with endoproteinase Lys-C (100:1) for 4 h was done by SDS-PAGE (10%) under reducing conditions and silverstaining. Indicated are the five bands that yielded usable sequence information after N-terminal sequence analysis.

Lane 1: purified NB-p260

Lane 2: NB-p260 fragments generated with endoproteinase Lys-C

The sequence information obtained from the indicated bands (see Figure 29 and 30) is shown in table 1. No significant similarities (greater 80 %) were found for six of the ten bands. ABP-280 was the only protein that matched to more than one sequenced band, although none of the other 6 bands showed greater similarity.

| Band | Molecular weight [kDa] | Amino acid sequence | Corresponding protein |
|------|------------------------|--------------------------|-----------------------|
| 1 | 10 | SAGXG VEEXP V P YG | - |
| 2 | 12 | AIVDG NLKLI LGLI | ABP-280 (14/14) |
| 3 | 18 | SGTYA VSYVP LGA D T G | ABP-280 (7/13) |
| 4 | 20 | STDEG VEAIG GAV P L | - |
| 5 | 35 | XNEEG XA | - |
| 6 | 65 | XXTEK DLAED | ABP-280 (8/8) |
| 7 | 95 | DAGRG GLXLAIE P | ABP-280 (11/12) |
| 8 | 100 | DLPVV EVTVD G | - |
| 9 | 110 | XXPKG ELXVT V A | - |
| 10 | 140 | XLXVX EVTXX V | - |

Table 1: N-terminal sequence information of fragments generated by endo-proteinase Lys-C digestion of purified NB-p260

In case two amino acids were possible at one position the amino acid with the higher probability is indicated in the upper line. In parenthesis the number of matching amino acids with ABP-280 is shown.

Since ABP-280 was the only protein that matched to more than one fragment, the purification procedure of the NB-p260 was screened against a monoclonal anti-ABP-280 antibody by immunoblotting. As demonstrated in Figure 31 all NB-p260 containing fractions showed strong reactivity against the anti-ABP-280 antibody. This results did not seem very reasonable at this point and therefore the possibility that the NB-p260 consist of two proteins with identical molecular weights and binding properties had to be considered.

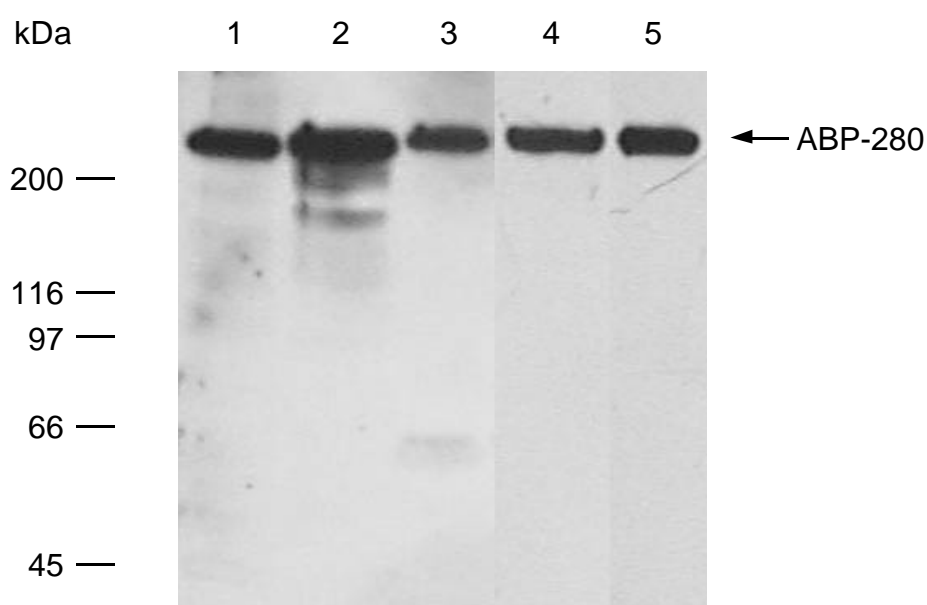


Figure 31: Immunoreactivity of the NB-p260 purification procedure against a monoclonal anti-ABP-280 antibody

Assessment of the NB-p260 purification procedure by immunoblotting against a monoclonal mouse anti-ABP-280 antibody after SDS-PAGE (7.5%) under reducing conditions. Immunodetection was done with the ECL system using a HRP-conjugated anti-mouse IgG.

Lane 1: LAN-1 cell extracts

Lane 2: anion exchange column, 175-225 mM sodium chloride

Lane 3: cation exchange column, breakthrough in 50 mM sodium phosphate

Lane 4: hydroxyapatite column, 160-350 mM sodium phosphate

Lane 5: purified NB-p260 (preparative gelelectrophoresis)

To investigate this possibility a linear gradient between 160 and 350 mM sodium phosphate on the hydroxyapatite chromatography column was introduced in addition to the original step gradient between 160 and 350 mM. Indeed reactivity against the anti-ABP-280 antibody started first in fractions corresponding to a sodium phosphate content of approximately 250 mM although Coomassie staining showed bands of similar molecular weight in all fractions (data not shown). Subsequently an additional gradient between 160 and 240 mM sodium phosphate was applied and separation by hydroxyapatite chromatography yielded two proteins with identical molecular weight of approximately 260 kDa as shown in Figure 32.

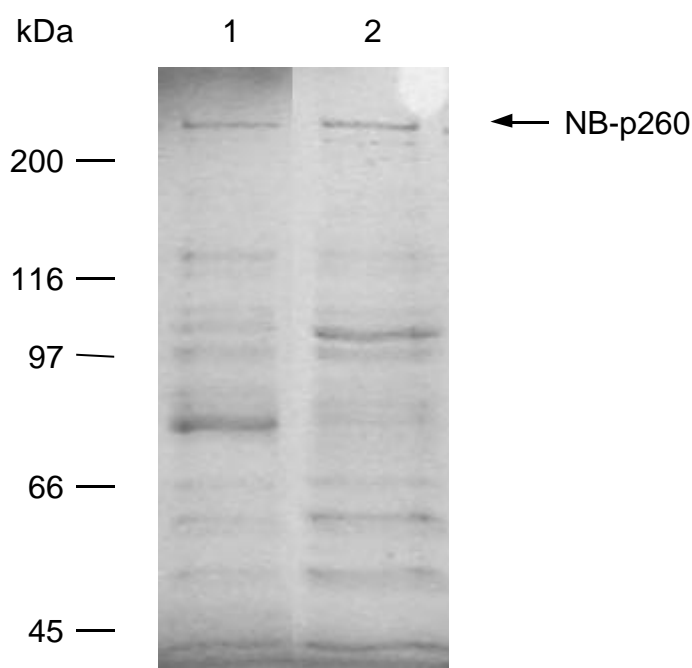


Figure 32: Separation of NB-p260 by hydroxyapatite chromatography

Evaluation of the separation of NB-p260 in two different NB-p260 containing fractions by hydroxyapatite chromatography and SDS-PAGE (7.5%) under reducing conditions and Coomassie staining.

Lane 1: hydroxyapatite column, 160-240 mM sodium phosphate

Lane 2: hydroxyapatite column, 240-350 mM sodium phosphate

Subsequently both fractions were screened against a monoclonal anti-ABP-280 antibody and purified human anti-NB IgM (Figure 33 A and B). Both fractions were positive against the anti-NB IgM antibodies whereas reactivity against the monoclonal anti-ABP-280 antibody was only observable in the latter fraction (240-350 mM sodium phosphate).

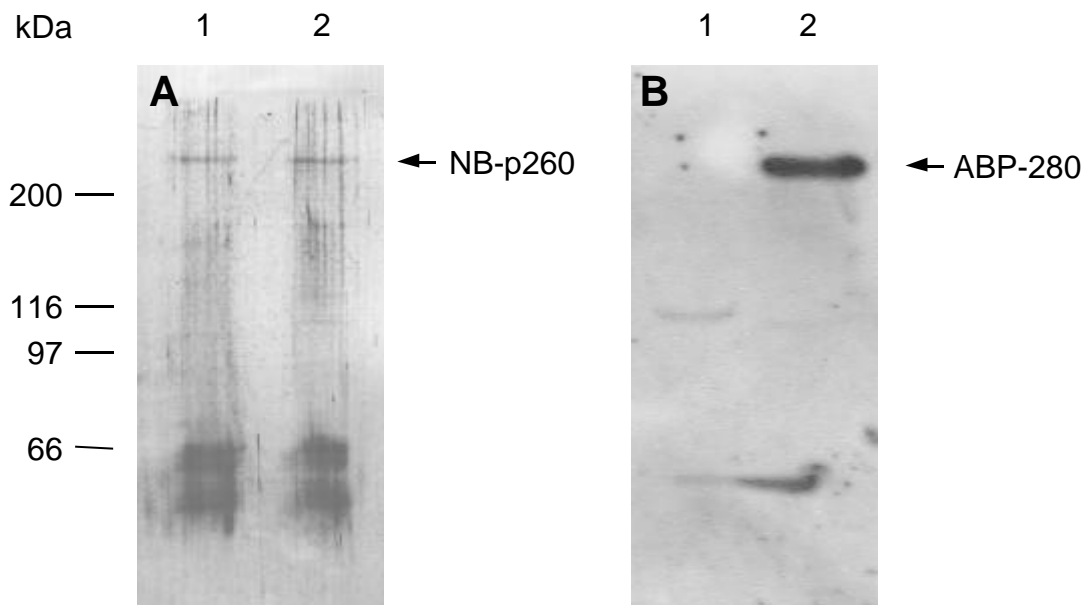


Figure 33: Immunoreactivity of NB-p260 separated by hydroxyapatite chromatography against an anti-ABP-280 antibody and purified human anti-NB IgM

Immunoblot analysis of NB-p260 in two different NB-p260 containing fractions after hydroxyapatite chromatography after SDS-PAGE (7.5%) under reducing conditions.

- A) Immunodetection by color development using human anti-NB IgM as primary antibody and an AP-conjugated anti-human IgM as secondary antibody.
- B) Immunodetection using the ECL system and a monoclonal mouse anti-ABP-280 antibody as first and a HRP-conjugated anti-mouse IgG as secondary antibody.

Lane 1 and 3: hydroxyapatite column, 160-240 mM sodium phosphate

Lane 2 and 4: hydroxyapatite column, 240-350 mM sodium phosphate

The same results were obtained with two other monoclonal anti-ABP-280 antibodies against different epitopes in the ABP-280 protein (data not shown), unambiguously proving that the NB-p260 consist of (at least) two different proteins which both show reactivity with human anti-NB IgM antibodies.

To characterize the non ABP-280 component of the NB-p260 this protein was purified to homogeneity as outlined before (see 4.2.1.) except that an additional step for the separation of the ABP-280 was introduced. Therefore the non ABP-280 containing fractions were eluted between 160 and 240 mM sodium phosphate on the hydroxyapatite chromatography column instead of the previously applied step gradient between 160 and 350 mM sodium phosphate. The amount of purified protein obtained by the modified purification procedure decreased significantly and was too low to allow the generation of internal fragments by enzymatic digestion of the purified protein and their subsequent N-terminal sequencing using the in-house sequencing facility under an economical and temporal point of view. Therefore the commercially available sequencing facility/service of the Toplab GmbH (Martinsried, Germany) was chosen. To this end the purified protein was again separated by SDS-PAGE (7.5 %), the bands of the purified protein were cut out and send for further manipulation to Toplab. At Toplab the bands were digested with endoproteinase Lys-C, the resulting peptides separated by HPLC and evaluated by MS-fingerprint analysis. Representative examples of the MS-fingerprint are shown in Table 2. One peptide was subjected to N-terminal sequencing and the obtained sequence is presented in Table 3. The obtained informations identified the protein unambiguously as ABP-278. Hence the NB-p260 termed protein consists of ABP-280 and ABP-278.

| Peak | Molecular weight [kDa] | Corresponding sequence | Position in ABP-278 |
|------|------------------------|-------------------------|---------------------|
| 1 | 654.7903 | (K)VTGLHK | 323-328 |
| 2 | 759.8372 | (K)DVVDPSK | 1417-1423 |
| 3 | 829.4783 | (K)AIVDGNLK | 101-108 |
| 4 | 845.9778 | (K)ISGEGRVK | 2089-2096 |
| 5 | 993.0646 | (K)YADEEIPR | 1497-1504 |
| 6 | 1044.2407 | (K)GLEELVKQK | 496-504 |
| 7 | 1150.3247 | (K)ERGDYVLAVK | 2577-2586 |
| 8 | 1342.5189 | (K)GEITGEVHMPGK | 1758-1770 |
| 9 | 1342.5398 | (K)NKTYEVEYLPK | 312-322 |
| 10 | 1372.5206 | (K)MDCQETPEGYK | 2429-2439 |
| 11 | 1501.9063 | (K)LKPGAPLKPKNPK | 242-255 |
| 12 | 1656.8862 | (K)GAGGQGKLDVTILSPSR | 970-986 |
| 13 | 1779.0289 | (K)SGCIVNNLAEFTVDPK | 658-673 |
| 14 | 2047.2776 | (K)LVSPGSANETSSILVESVTR | 2476-2495 |

Table 2: Identification of ABP-278 by MS-fingerprint

Shown are representative examples of the MS-fingerprint of the purified non-ABP-280 reactive NB-p260 component after endoproteinase Lys-C digestion and separation of the resulting peptides by HPLC.

| Amino acid sequence | Corresponding protein |
|---------------------|------------------------------------|
| SPFTV GVAAP LDLSK | ABP-278 (15/15) ABP-280 (12/15) |

Table 3: Identification of ABP-278 by N-terminal sequence analysis

Shown is the amino acid sequence obtained by N-terminal sequencing of one peptide generated by endoproteinase Lys-C digestion of the purified non-ABP-280 reactive component of NB-p260.

Indicated In parenthesis is the number of matching amino acids with ABP-278 and ABP-280, respectively.

4.2.1.3. Function of NB-p260 as apoptosis inducing receptor

To test whether (ABP-280 or) ABP-278 indeed function as apoptosis-inducing cell surface receptor the ability of purified NB-p260 to deplete the IgM pool of the apoptosis-inducing IgM antibodies was investigated. To this end purified NB-p260 was immobilized onto nitrocellulose membranes and used for preadsorption of purified anti-NB IgM pools from different positive donors. Controls consisted of membranes immobilized with non fat dry milk alone. The depleted (nonbound) IgM pool was subsequently evaluated for its ability to induce apoptosis by cytofluorometry after staining with Annexin V-FITC and propidium iodide. As shown in Figure 34 A the induction of apoptosis in three different NB cell lines (LAN-1, IMR-32 and NMB-7) could be completely abolished by preadsorption of the anti-NB IgM with purified NB-p260. On the other hand anti-NB IgM preadsorbed at non fat dry milk alone showed similar extents of apoptosis than non preadsorbed anti-NB IgM. Identical results were obtained with natural anti-NB IgM from three different donors (Figure 34 B).

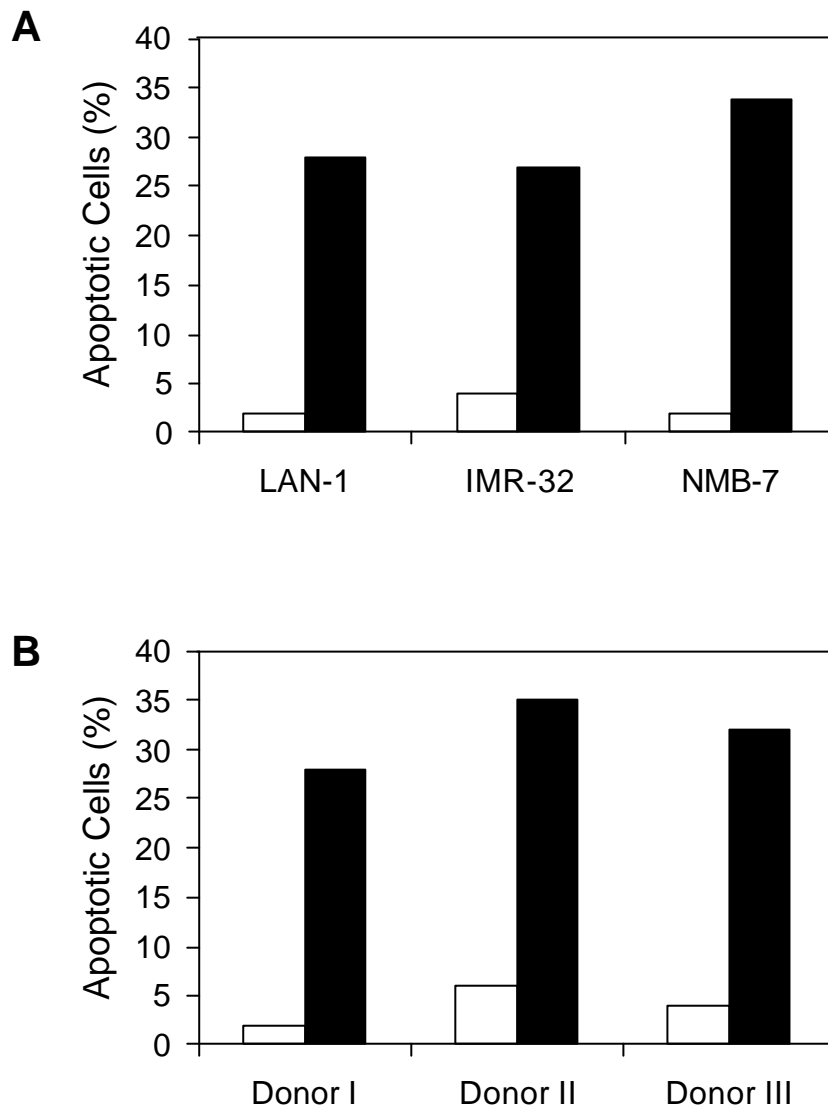


Figure 34: Inhibition of anti-NB IgM induced apoptosis by purified NB-p260

A) Extent of apoptosis of LAN-1, IMR-32 and NMB-7 cells after treatment for 4 h with anti-NB IgM after preincubation with purified NB-260 (white bars) or control protein (black bars).

B) Extent of apoptosis of LAN-1 cells treated for 4 h with anti-NB IgM from three different donors after preincubation with purified NB-p260 (white bars) or control proteins (black bars).

The extent of apoptosis was determined by FACScan analysis after staining with Annexin V-FITC and propidium iodide (by courtesy of Dr. David).

This experiments were accomplished before the NB-p260 was identified as a mixture of ABP-278 and ABP-280. Since ABP-278 and ABP-280 showed a very high degree of homology (> 70 %) and the polyclonal anti-NB IgM pools recognized both ABPs, no different results were to be expected by repeating the experiment with purified ABP-278.

4.2.1.4. Cell surface expression of ABP-278 and ABP-280

To evaluate the cell surface expression of ABP-278 and ABP-280 cell surface proteins were selectively biotinylated with the non-membrane-permeable sulfobiotin derivate Sulfo-NHS-LC-Biotin to avoid biotinylation of internal proteins. Intact LAN-1 cells were used and the viability of the cells was checked after the biotinylation procedure. Cells were only used for further experiments when cell viability was greater 95% to assure that no significant biotinylation of internal proteins occurred due to disintegrated plasma membranes. After biotinylation ABP-278 and ABP-280 were purified as outlined before by anion exchange, cation exchange and hydroxyapatite chromatography (Figure 35: Lane 1-5). The final purification step by preparative gelelectrophoresis was skipped as separation of ABP-278 and ABP-280 was obtained by hydroxyapatite chromatography and the yield of protein decreased significantly in the last purification step.

Biotinylation of the NB-p260 was obvious in LAN-1 cell extracts (Figure 35: lane 1) as well as in the HighQ (lane 2) and EconoS (lane 3) fractions containing the NB-p260. After separation by hydroxyapatite chromatography only ABP-278 (lane 4) showed biotinylation whereas ABP-280 (lane 5) did not. It is therefore likely that ABP-278 is partially expressed on the cell surface and may serve as an apoptosis-mediating receptor.

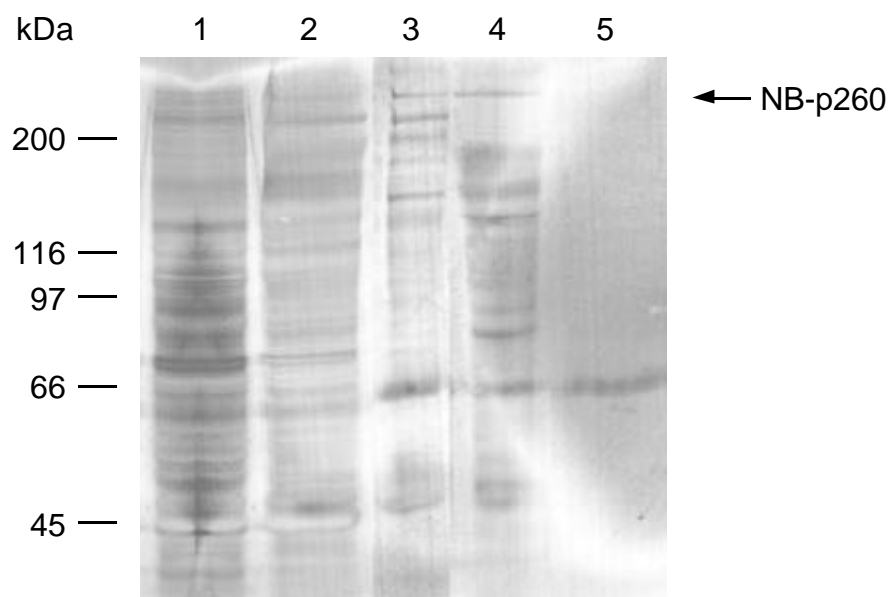


Figure 35: Investigation of cell surface expression of ABP-278 and ABP-280 in intact LAN-1 NB cells by biotinylation analysis

Intact LAN-1 NB cells were biotinylated using a non-membran-permeable sulfobiotin derivate. After purification of ABP-278 and ABP-280 their biotinylation status was investigated by immunoblot analysis after separating by SDS-PAGE (7.5%). Immunodetection was performed using AP-conjugated streptavidin and color development.

Lane 1: LAN-1 cell extracts

Lane 2: anion exchange column, 175-225 mM sodium chloride

Lane 3: cation exchange column, breakthrough in 50 mM sodium phosphate

Lane 4: hydroxyapatite column, 160-240 mM sodium phosphate

Lane 5: hydroxyapatite column, 240-350 mM sodium phosphate

4.2.2. Possible role of heat shock proteins

4.2.2.1. Cell surface expression of heat shock proteins on NB cells

The cell surface expression of the additional putative apoptosis-mediating receptor hsp 90 as well as the one of hsp 60 and hsp 70 on LAN-1 cells was investigated using two different approaches. First, the ability of monoclonal antibodies against the respective heat shock proteins to bind to the surface of intact LAN-1 cells was evaluated. As demonstrated in Figure 36 monoclonal antibodies against hsp 60 and hsp 90 showed significant binding on LAN-1 cells while no binding was observed against hsp 70. Controls using the employed secondary antibodies alone also showed no binding.

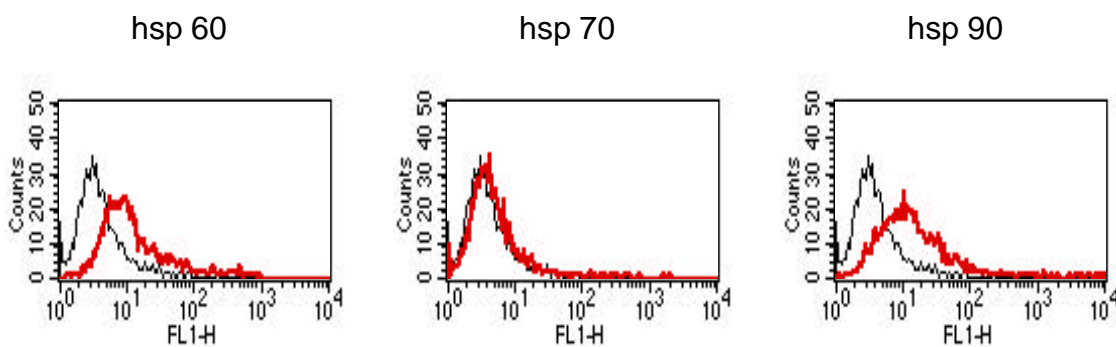


Figure 36: Cell surface expression of heat shock proteins hsp 60, hsp 70 and hsp 90 on LAN-1 cells

Cell surface expression of hsp 60, hsp 70 and hsp 90 was measured by binding of monoclonal anti-hsp antibodies against the indicated proteins on the surface of intact LAN-1 cells. Evaluation was done by FACScan analysis using FITC-conjugated anti-mouse/rat IgG antibodies as secondary antibodies (red lines). Negative controls were obtained by binding of the FITC-conjugated secondary antibodies only to the surface on LAN-1 cells (black lines). FACScan analysis by courtesy of Dr. David.

In a second approach cell surface proteins on LAN-1 cells were selectively labeled with a non-membrane-permeable sulfobiotin derivate, the biotinylated proteins isolated by a monomeric avidin matrix and subsequently the presence of HSPs was probed by immunoblot analysis using monoclonal anti-hsp antibodies (Figure 37). The heat shock proteins hsp 60 and hsp 90 showed significant signals in the biotinylated fractions, strongly indicating that these proteins are present on the surface of LAN-1 cells. On the other hand hsp 70 showed only a very weak signal in the biotinylated fraction, either and most likely due to biotinylation of internal proteins of damaged cells or due to only very low amounts of hsp 70 present on the surface. In summary both approaches to evaluate the cell surface expression of heat shock proteins on LAN-1 cells yielded similar results indicating that hsp 60 and hsp 90 are expressed on the cell surface whereas hsp 70 is apparently not. Identical results were obtained with the four other NB cell lines IMR-32, NMB-7, SK-N-SH and SH-SY5Y (data not shown).

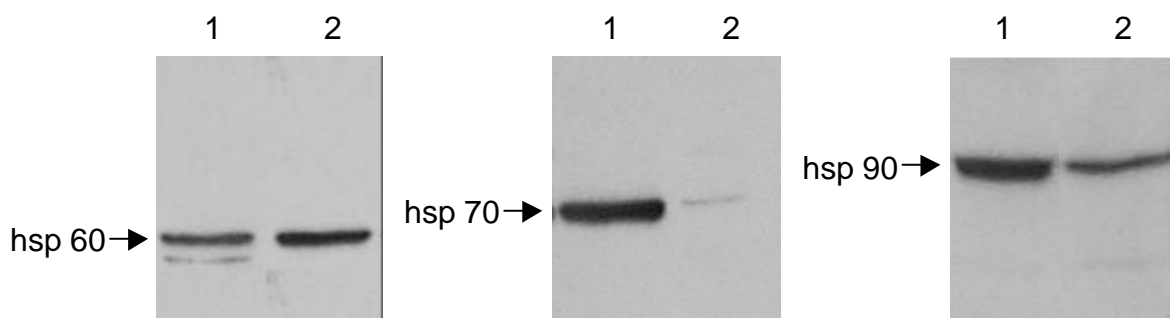


Figure 37: Biotinylation analysis of cell surface expression of the heat shock proteins hsp 60, hsp 70 and hsp 90 on LAN-1 cells

Cell surface expressed proteins were isolated after labeling with a sulfobiotin-derivate by monomeric avidin and expression of the investigated proteins was subsequently analyzed by immunoblotting against monoclonal mouse or rat anti-hsp antibodies. Immunodetection was done by chemiluminescence.

Lane 1: avidin column, breakthrough

Lane 2: avidin column, biotinylated eluate

4.2.2.2. Reactivity of patient sera against heat shock proteins

To test for immunoreactivity against the different HSPs, hsp 60, hsp 70 and hsp 90 needed to be purified to homogeneity first.

Hsp 60 from LAN-1 cell extracts (Figure 38 A: Lane 1) was purified by anion exchange chromatography applying a step gradient between 150 and 250 mM NaCl (Lane 2). The buffer exchanged material was then applied to the cation exchanger and hsp 60 was recovered in the breakthrough (Lane 3). Further purification was achieved by hydroxyapatite chromatography where hsp 60 eluted in a step gradient between 150 and 225 mM sodium phosphate (Lane 4). Purification of hsp 60 was completed by preparative gelelectrophoresis with an 8.8 % separating gel (Lane 5). The identity of the purified protein was confirmed by western blot analysis (Figure 38 B: Lane 1).

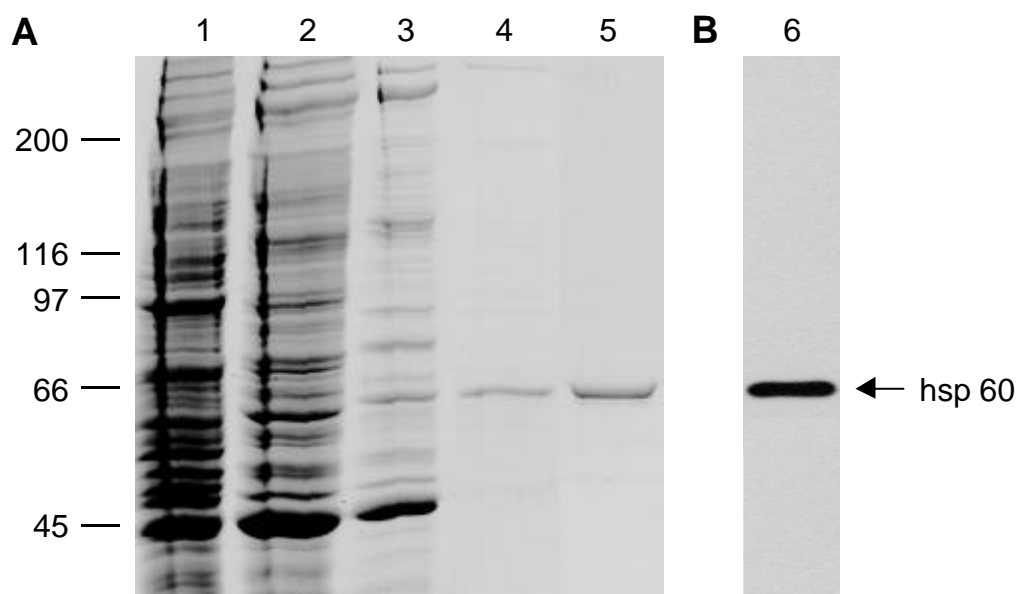


Figure 38: Purification of hsp 60 from LAN-1 cells

A) Assessment of the purification procedure of hsp 60 by SDS-PAGE (7.5%) under reducing conditions and Coomassie staining (Lane 1-5).

Lane 1: LAN-1 cell extracts

Lane 2: anion exchange chromatography, 150-250 mM NaCl in buffer A

Lane 3: cation exchange chromatography, breakthrough in buffer C

Lane 4: hydroxyapatite chromatography, 150-225 mM sodium phosphate in buffer B

Lane 5: preparative gelelectrophoresis, 8.8 % separating gel

B) Immunoblot analysis of the purified protein using a monoclonal mouse anti-hsp 60 antibody and the ECL system for detection (Lane 1).

Lane 1: immunoblot of purified hsp 60

Hsp 70 from LAN-1 cell extracts (Figure 39 A: Lane 1) was eluted from the anion exchanger in a step gradient between 75 and 150 mM NaCl (Lane 2). After buffer exchange hsp 70 was applied to the cation exchanger and eluted in a step gradient between 0 and 1 M NaCl in buffer B (Lane 3). Subsequently hsp 70 containing fractions were again buffer exchanged, applied to an ADP agarose affinity chromatography column and eluted with 3 mM ADP (Lane 4). Final purification was achieved by preparative gelelectrophoresis with a 7.5 % separating gel (Lane 5). Western blot analysis using a monoclonal antibody against hsp 70 confirmed the identity of the purified protein (Figure 39 B: Lane 1).

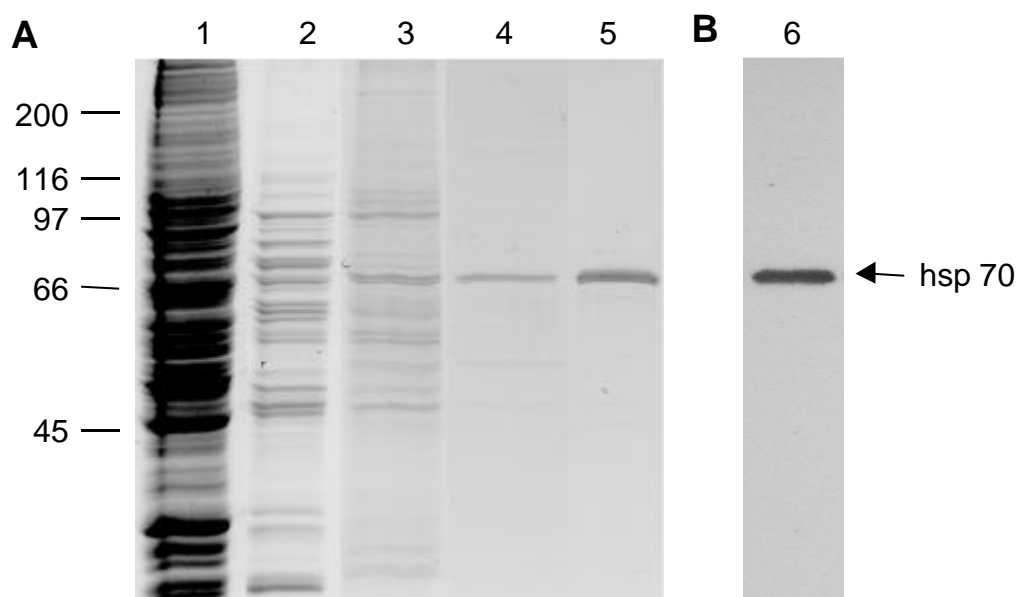


Figure 39: Purification of hsp 70 from LAN-1 cells

A) Evaluation of the purification procedure of hsp 70 by SDS-PAGE (10%) under reducing conditions and Coomassie staining (Lane 1-5).

Lane 1: LAN-1 cell extracts

Lane 2: anion exchange chromatography, 75-100 mM NaCl in buffer A

Lane 3: cation exchange chromatography, 0-1 M NaCl in buffer B

Lane 4: ADP agarose chromatography, 0-3 mM ATP in buffer D

Lane 5: preparative gelelectrophoresis, 7.5 % separating gel

B) Immunoblot analysis of the purified protein against a monoclonal mouse anti-hsp 70 antibody using the ECL system for immunodetection (Lane 1).

Lane 1: immunoblot of purified hsp 70

Hsp 90 from LAN-1 cell extracts (Figure 40 A: Lane 1) could be eluted in a narrow step gradient between 300 and 325 mM from the anion exchange column (Lane 2). Following buffer exchange to buffer C hsp 90 containing fractions were applied to a cation exchange column. Hsp 90 was recovered in the breakthrough (Lane 3) and directly applied to hydroxyapatite chromatography column and eluted between 200 and 250 mM sodium phosphate (Lane 4). Complete purification was accomplished by preparative gelelectrophoresis using a 6 % separating gel (Lane 5). The identity of the purified protein was confirmed by immunoblot analysis with a monoclonal anti hsp 90 antibody (Figure 40 B: Lane 1).

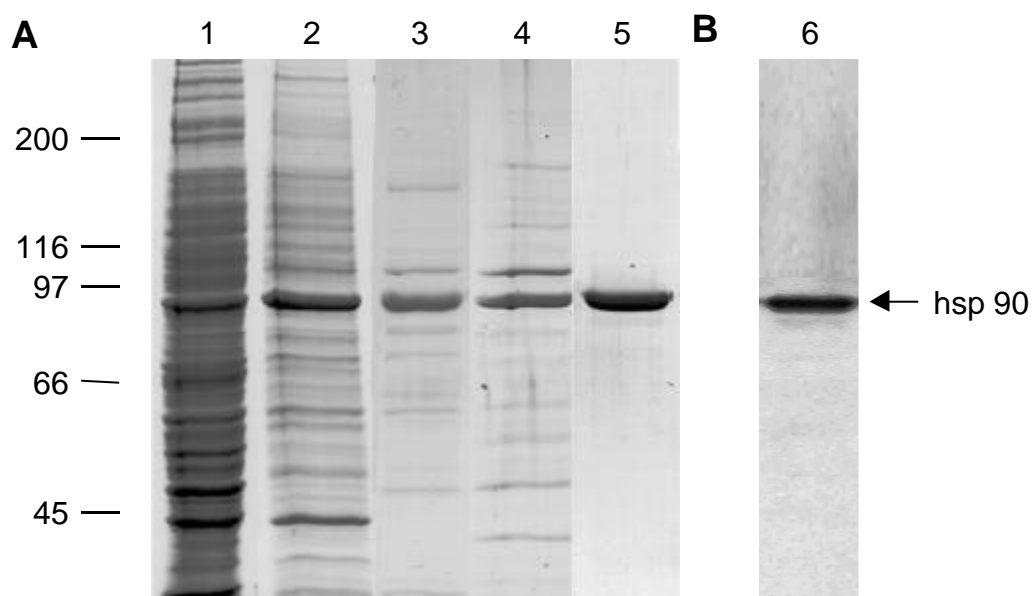


Figure 40: Purification of hsp 90 from LAN-1 cells

A) Evaluation of the purification procedure of hsp 90 by SDS-PAGE (7.5%) under reducing conditions and Coomassie staining (Lane 1-5).

Lane 1: LAN-1 cell extracts

Lane 2: anion exchange chromatography, 300-325 mM NaCl in buffer A

Lane 3: cation exchange chromatography, breakthrough in buffer C

Lane 4: hydroxyapatite chromatography, 200-250 mM sodium phosphate in buffer B

Lane 5: preparative gelelectrophoresis, 6 % separating gel

B) Analysis of the purified protein by immunoblotting against a monoclonal rat anti-hsp 90 antibody. The ECL system was used for detection (Lane 1).

Lane 1: immunoblot of purified hsp 90

The purified heat shock proteins hsp 60, hsp 70 and hsp 90 were subsequently screened against eight different sera from NB patients with unfavorable outcome (Table 4). None of the patient sera showed reactivity against hsp 90, whereas cytotoxic sera had shown reactivity (David 1996). In conjunction with the observed cell surface expression, it is thus possible that hsp 90 represents an additional putative apoptosis-mediating cell surface receptor. Considering the much higher ability of NB-p260 and antibodies raised against NB-p260 to inhibit the induction of apoptosis further investigations regarding the significance of hsp 90 are necessary.

In contrast all sera showed medium to strong reactivity against hsp 60 and weak to moderate detection of hsp 70. This indicates that hsp 60 and to a lesser extent hsp 70 serve as tumor antigens, but that it is unlikely that these proteins are involved in IgM mediated responses since hsp 60 and hsp 70 are already detected by sera of patients with no favorable outcome.

| donor \ hsp | hsp 60 | hsp 70 | hsp 90 |
|--------------|----------|----------|----------|
| L. M. K. | + | + | - |
| M. T. | + | - | - |
| F. T. | + | - | - |
| M. R. | o | o | o |
| D. T. | + | o | - |
| R. K. | + | + | - |
| K. A. | + | o | - |
| P. K. | + | + | - |
| Total | + | o | - |

Table 4: Reactivity of patient sera against heat shock proteins hsp 60, hsp 70 and hsp 90

+ = moderate to strong reactivity; o = weak to moderate reactivity; - = no reactivity

4.2.3. SEREX

The serological analysis of recombinant cDNA libraries (SEREX) with polyclonal IgG antibodies to identify potential tumor antigens has been successfully employed for a variety of tumors using polyclonal IgG antibodies but has never been evaluated with IgM antibodies (Sahin et al., 1995; Tuereci et al., 1997; Scanlan et al., 1998).

The aim of this project was therefore the evaluation whether polyclonal human anti-NB IgM are also suitable for the SEREX approach in order to identify further potential tumor antigens in NB cells. For this purpose a cDNA library from LAN-1 NB cells was constructed in the λ ZAP vector. To evaluate the quality of the constructed cDNA library and to establish the SEREX approach a screening against a polyclonal anti-grp 75 serum was done. Finally the suitability of polyclonal human anti-NB IgM antibodies for the serological analysis of the constructed cDNA library was investigated.

4.2.3.1. Construction of a cDNA library from LAN-1 NB cells

First poly(A)⁺-RNA from 2×10^7 LAN-1 cells were isolated and reverse transcribed using MMLV-RT and a linker primer containing an Xho I restriction site. The original mRNA strand was then translated into second-strand cDNA by RNase H and DNA polymerase I. After blunting the uneven cDNA termini by Pfu DNA polymerase, ligation of EcoR I adaptors by T4 DNA ligase, phosphorylation of the adaptors with T4 polynucleotid kinase the resulting cDNA was digested by Xho I to allow the sense orientation in the λ ZAP vector. The cDNA was then separated by gel filtration into the finished cDNA and the still present linker primer. The quantity of the cDNA in the different fractions was subsequently checked by an ethidium bromide plate assay (not shown), the size evaluated by

agarose gelelectrophoresis (Figure 41). The fractions 5 and 6 (lane 1 and 2, respectively) contained cDNA ranging from approximately 1 to 3.5 kBp, the fractions 7-9 contained small amounts of cDNA of approximately 1 kBp while fractions 10-12 showed strong signals at about 50 Bp apparently containing the linker primer. Hence separation between the cDNA and the linker primer was readily accomplished. Furthermore the quality of the cDNA with sizes up to approximately 3.5 kBp appeared very good. Approximately 100 ng cDNA of fraction 5 and 6 were then used for the ligation into the λ ZAP vector with the help of a packaging extract. The titer of the obtained primary library was 1.4×10^6 pfu. The efficiency of the packaging process was determined by blue white screening where only 4% of all plaques stained blue and accordingly contained no insert. Next the library was amplified to create a large, stable high-titer stock of the primary library. The titer of the amplified library yielded 10^{10} pfu. In summary the constructed cDNA library appeared very good as both the titer of the primary and the amplified library were above average, only 4% of the phages contained no insert and the size of the cDNA inserts reached up to at least 3.5 kBp.

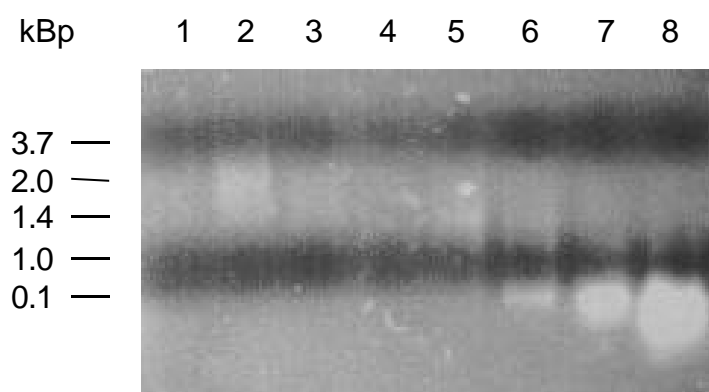


Figure 41: Evaluation of the cDNA size in the different fractions after separation by gelfiltration

Assessment of the cDNA size in the various fractions after separation of total cDNA by gelfiltration on Sepharose CL-2B media was done by agarose gelelectrophoresis (1%) and staining with ethidium bromide.

Lane 1-8: fractions 5-12 of the gelfiltration procedure

4.2.3.2 Assessment of the constructed cDNA library and establishment of the SEREX approach

A good cDNA library should consist of cDNA inserts with an average size of approximately 1 kBp. To assess the quality of the constructed cDNA library regarding the size of the inserted cDNA and to establish the SEREX approach, a screening with a polyclonal anti-grp 75 IgG serum was performed.

To that end approximately 5×10^4 plaques were screened. Five clones showed strong signals and were subjected to two more rounds of screening until all screened plaques turned positive, indicating that a monoclonal phage stock was obtained. The monoclonized phages were subsequently excised *in vivo* and mini plasmid preps were made of the resulting phagemids. The isolated phagemid DNA was subjected to a restriction digestion using the restriction enzymes Xho I and Pst I. The resulting cDNA inserts were analyzed by agarose gelelectrophoresis (Figure 42) and DNA sequence analysis (not shown). Of the analyzed five clones three showed insert sizes of approximately 2 kBp, one of 1.6 kBp and one of 1 kBp. DNA sequence analysis verified the grp 75 origin and the estimated sizes of the cDNA inserts in all five clones. Hence the quality of the library seemed good as the average size of the inserts were well above median (1 kBp). Furthermore the serological screening of the library was practicable, at least with a polyclonal IgG serum.

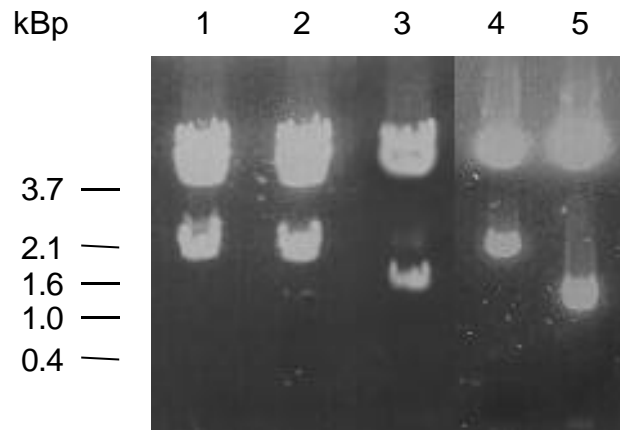


Figure 42: Evaluation of cDNA inserts of grp 75 positive plaques by restriction analysis

Assessment of the cDNA size in 5 different anti-grp 75 positive clones after restriction digestion with Pst I and Xho I by agarose gelectrophoresis (1%) and ethidium bromide staining.

Lane 1-5: clones 1-5

4.2.3.3 Screening of the cDNA expression library with human anti-NB IgM

Polyclonal sera usually contain antibodies that are cross-reactive with bacterial and phage proteins. It was therefore first probed whether the polyclonal human anti-NB IgM fractions showed reactivity against immobilized E.coli phage lysates. Strong signals against all plated plaques were obtained (data not shown). Thus preadsorption of the anti-NB IgM fractions was necessary to eliminate cross-reactional antibodies.

To preadsorb bacterial and phage proteins different E.coli phage lysates were immobilized on CNBr-activated sepharose and used to deplete the anti-NB IgM fractions from crossreactive proteins. Subsequently the fractions were tested for immunoreactivity in dot blots against LAN-1 cell extracts and E.coli phage lysate. A commercially available E.coli phage lysate and own prepared E. coli phage lysate using the λ ZAP phage and the E.coli strain XL1-Blue MRF^r were used for the preadsorption.

Although a significant reduction in reactivity against the phage lysates could be achieved after repeated preadsorption, a background was still observed that could not be decreased by further preadsorption. In accordance with this observations eluates from the used matrices showed decreasing reactivities against the E.coli phage lysates that finally diminished, indicating that no more cross-reactive antibodies in the preadsorbed fractions bound to the matrix at this point. The thereby preadsorbed anti-NB IgM fractions were then tested for the screening of the LAN-1 cDNA library and seemed to work well as only a few plaques turned positive in the first ($1-2 \times 10^4$ pfu) and usually the second round (about 100 pfu) of screening. Without any reasonable explanation in the third round of screening either all plaques turned positive or no positive plaques at all were observed. Even more disturbing was the observation that screening of the same phage stock in one attempt yielded only positive plaques and in the next attempt only negative clones.

The serological screening of cDNA expression libraries with polyclonal IgM therefore did not yield acceptable results, presumably due the nature of the IgM itself. Consultations with the group around Prof. Vollmert supported this point of view (AACR, April 2000). One focus of their work is the identification of antigens recognized by monoclonal IgM antibodies from patient sera and even with this monoclonal antibodies they experienced great difficulties to achieve consistent results in immunoblot analysis.

5. Diskussion

5.1. Cerulenin-mediated apoptosis

Human fatty acid synthase (FAS) has recently been identified as a tumor antigen in human NB cells (Heiligtag 1998). Human FAS is a homodimer of 260 kDa monomers that catalyzes seven distinct enzymatic reactions to synthesize fatty acids, mainly palmitic acid, from acetyl-CoA and malonyl-CoA in the presence of NADPH. It has been shown that tumor cells express elevated levels of FAS, presumably in order to use the endogeneously synthesized fatty acids for membrane biosynthesis (Pizer et al., 1996). In marked contrast normal cells preferentially utilize dietary lipids and show a low expression of FAS (Weiss et al., 1986). Previous studies have furthermore suggested that cerulenin which is known as a specific, noncompetitive inhibitor of FAS kills cell lines that overexpress FAS to a much greater extent than those cell lines that lack FAS overexpression (Kuhadjy et al., 1994; Pizer et al., 1996). It has therefore been hypothesized that the inhibition of FAS by cerulenin is responsible for its cytotoxic effects. Yet the mechanisms by which cerulenin mediates the cytotoxic effects are poorly understood.

Therefore the cytotoxic mechanism of cerulenin were first evaluated in a comprehensive approach. Ten different tumor cell lines as well as two primary cell lines were investigated for their response to treatment with cerulenin. After incubation with 15 µg/ml cerulenin for 24 hours all four NB cell lines (LAN-1, IMR-32, NMB-7 and SK-N-SH) as well as the transformed keratinocyte cell line HaCaT and the skin carcinoma cell line A431 showed dramatic effects with typical signs of apoptosis. The breast cancer cell lines MCF7 and SK-BR-3 and the melanoma cell line SK-MEL-93-2 showed only little signs of apoptosis whereas normal fibroblasts (NHLF) and keratinocytes (NHEK) as well as the colon

carcinoma cell line WiDr were totally refractory against cerulenin treatment. The biochemical evidence of the apoptotic process was then demonstrated by phosphatidylserine externalization to the cell surface as determined by Annexin V binding. Five tumor cell lines, which differed significantly in their morphological features in response to treatment with cerulenin, were investigated as well as the primary cell lines NHEK and NHLF. The normal cell lines as well as the tumor cell line WiDr showed only background levels of apoptosis whereas the tumor cell lines LAN-1, SK-N-SH and HaCaT revealed specific apoptosis of around 80 % and SK-BR-3 cells of approximately 50 %.

In the next set of experiments the dose-dependent effects of cerulenin were investigated by PARP cleavage. The cleavage of PARP increased in a dose-dependent manner from 5 µg/ml to 15 µg/ml in all susceptible tumor cell lines. The four NB cell lines, HaCaT and A431 cells showed the most dramatic effects in accordance with the observed morphological features. On the other hand no PARP cleavage at all was detectable in the tumor cell line WiDr and the primary cell line NHLF also confirming the previous results.

Next both the expression and the endogenous activity of FAS were determined in ten tumor cell lines and the two primary cell lines to evaluate whether a correlation between these parameters and the susceptibility to cerulenin exist. FAS expression levels were determined using purified human FAS as internal standard. FAS was therefore purified to homogeneity from LAN-1 NB cells by sequential ion exchange chromatography, hydroxyapatite chromatography and preparative gelelectrophoresis. Endogenous activity of FAS was determined by the incorporation of the ¹⁴C labeled precursor acetyl-CoA in fatty acids.

FAS expression and activity showed an extraordinary high correlation, proving that no inactivated FAS was present. SK-BR-3 cells expressed extraordinary high amounts of FAS in accordance with previous results

(Kuhajda et al., 1994; Pizer et al., 1996). However the obtained data did not confirm that tumor cells in general have a higher expression or activity of FAS than normal cells. Normal human keratinocytes, transformed keratinocytes (HaCaT) and the skin carcinoma cell line A431 showed virtually the same expression and activity of FAS, indicating that the switch to a more tumorigenic phenotype is not accompanied by higher FAS expression or activity. In addition, the melanoma cell line SK-MEL-93-2, the NB cell line SK-N-SH, as well as the colon carcinoma cell line WiDr showed lower expression and activity of FAS than the primary cell lines NHLF and NHEK. These data indicate that sensitivity to cerulenin is independent of FAS expression and activity and that overexpression of FAS does not promote the apoptosis-inducing effect of cerulenin.

In another subset of experiments the potency of cerulenin to inhibit endogenous FAS activity was evaluated in the same cell lines. Maximum FAS inhibition were already achieved after incubation with 5 µg/ml cerulenin resulting in 40 % to 70 % reduced activity. No further decreases were observed by increasing the concentrations to 10 µg/ml and 15 µg/ml. These results are in contrast to the dose dependent cytotoxic responses against cerulenin as shown by PARP cleavage, suggesting that inhibition of FAS is not responsible for triggering apoptosis.

The assumption that inhibition of FAS and the induction of apoptosis are independent events was further supported by the inability of palmitic acid, the main product of the FAS pathway, to rescue cells from undergoing apoptosis. This contradicts the hypothesis that starvation of cells due to lack of palmitic acid is the reason for cerulenin-mediated cytotoxicity as has been proposed (Kuhajda et al., 1994; Pizer et al., 1996). The only other possibility by which inhibition of FAS could induce cytotoxicity would be the accumulation of acetyl- or malonyl-CoA as

precursors of the FAS pathway. This is highly unlikely as this metabolic products are always present in high intracellular concentrations. This data strongly indicate that neither overexpression of FAS leads to higher sensitivity of tumor cells to cerulenin nor FAS inhibition is responsible for the induction of apoptosis by cerulenin. Accordingly other mechanisms need to be responsible for triggering apoptosis by cerulenin.

A variety of anticancer agents are known to induce apoptosis as a result of DNA damage (Dole et al., 1995; Kaufmann et al., 2000). In response to DNA damage the tumor suppressor protein p53 is overexpressed in p53 wild type cell lines and initiates the transcription of cell cycle regulatory and/or proapoptotic genes. The cells are then usually arrested in the G1 phase to either allow repair of the DNA damage or to induce apoptosis to eliminate the damaged cells.

Therefore in the next set of experiments the potential of cerulenin to induce DNA damage was evaluated by first investigating the expression of p53. Treatment with cerulenin led to an accumulation of p53 in all p53 wild-type cell lines (LAN-1, IMR-32, SK-N-SH, A-172 and MCF-7) whereas no increase was observed in the p53 mutated cell lines (NMB-7, HaCaT, A431, SK-BR-3, WiDr and SK-MEL-93-2). The overexpression of p53 strongly suggests that cerulenin induces genotoxic stress. This proposition was further confirmed by the detection of an increased expression of the growth arrest & DNA damage inducible protein GADD 153, which is a p53 independent cell cycle regulatory protein, in p53 wild type as well as in p53 mutant cell lines. These data indicate that the apoptotic pathway is induced as a response to DNA damage. Yet the induction of apoptosis apparently involves p53-dependent and independent mechanisms since sensitivity against cerulenin was equal in p53 mutant and p53 wild-type cell lines.

In addition to the increased expression of p53 the cell lines SK-N-SH, IMR-32 and MCF7 showed an additional band of approximately 42 kDa that increased in a time dependent manner. This band could represent a degradation product of the p53 protein, although this is not very likely as degradation of p53 is largely achieved through the ubiquitin-proteasome pathway and degradation is therefore not specific (Oren 1999). It is more likely that this 42 kDa protein band corresponds to a recently identified putative new member of the p53 family, namely p53CP (Bian et al., 1997). p53CP is approximately 40 kDa in size and has p53-like DNA binding activity. It is currently unclear which additional specialized functions p53CP might have, but it has been hypothesized that binding competition by p53CP might represent an additional mechanism to inactivate certain p53 functions.

Next the expression of the p53 responsible gene product p21/WAF was evaluated. p21/WAF is a cell cycle regulatory protein and usually responsible for p53 induced G1 phase arrest by inhibiting different cyclin dependent kinases (CDK's) that are necessary for the transition from G1 into S phase. Interestingly the overexpression of p53 did not induce an increased expression of p21/WAF. Even more puzzling was the observation of increased p21/WAF protein levels in all p53 mutated cell lines, an increase obviously not mediated by p53. Thus all investigated cell lines overexpressed GADD153 and either p53 or p21/WAF clearly showing the DNA damaging features of cerulenin. This results furthermore indicate that p53 mutated cell lines direct other mechanisms in response to cerulenin-induced DNA damage than do p53 wild-type cell lines. The influence of cerulenin on cell cycle progression in the p53 wild-type cell line LAN-1 and the p53 mutated cell line HaCaT revealed an S phase arrest (data not shown). This is a rare event in response to drug treatment (Agarwal et al., 1998), more common are G1 arrests which are mediated by p53. Why cells arrested in S phase rather than in G1 phase although they overexpressed either p53 or p21 is currently not clear.

The proapoptotic Bax protein is another important target gene of p53 and its expression was subsequently investigated. In both the p53 wild-type NB cell lines LAN-1, IMR-32 and SK-N-SH and the p53-mutated NB cell line NMB-7, the transformed keratinocyte cell line HaCaT and the skin carcinoma cell line A431 a significant overexpression of Bax after exposure to cerulenin was detected. This data strongly suggest that Bax is regulated in a p53-independent manner. Comparable results have been described for other systems, although the detailed mechanisms are still unknown (Liebermann et al., 1995; Strobel et al., 1996; Fulda et al., 1997). On the other hand no changes in Bax protein levels could be detected in the p53 wild-type cell lines MCF7 and A-172 as well as in the p53 mutated cell lines SK-BR-3, WiDr and SK-MEL-93-2, indicating that the increase in Bax is independent of the p53 status but rather dependent on the cell type. The overexpression of Bax paralleled the sensitivity of the respective cell lines against cerulenin, suggesting that Bax plays a pivotal role in the cerulenin-mediated apoptosis. Further on all NB cell lines showed a strong additional band of approximately 18 kDa after 24 h of cerulenin treatment. This band is presumably a recently described cleavage product of the Bax protein (p18 Bax) with even greater cytotoxicity than the full length Bax (Wood et al., 1998 and 1999).

Although this results in general are quite puzzling they clearly prove that cerulenin induces DNA damage, but that the induction of apoptosis is apparently independent of p53 induced pathways and that p53 function therefore might be impaired.

Such an impairment or even the abolishment of p53 function by a mutation-independent mechanism has previously been described in 95% of all undifferentiated NBs (Moll et al., 1996). In these cells wild-type p53 is abnormally sequestered in the cytoplasm. Consequently p53 is not able to translocate into the nucleus in order to fulfill its function as a

checkpoint after DNA damage. Surprisingly, the mechanism of p53 sequestration has also been described in the p53 wild-type cell line MCF7 (Takahashi et al., 1993). To investigate whether the sequestration of p53 might be responsible for its apparent non functionality, the p53 wild-type glioblastoma cell line A-172 was included in the investigations as p53 function in this cell line is not impaired due to sequestering in the cytoplasm (Fuse et al., 1996). Although a comparable increase in p53 expression in relation to the other p53 wild-type cell lines after cerulenin treatment was observed, p21/WAF levels (as well as Bax levels) did not increase. Hence the sequestration of p53 is evidently not the reason for the non functionality of p53. As the increases in p53 protein levels by cerulenin are not accompanied by the activation of p53 inducible genes the question arises whether this is indeed due to functional not activated p53 by a so far unknown mechanisms or due to insufficient amounts of accumulated p53 in order to induce the transcription of its target genes.

To evaluate the extent of DNA damage and the induction of apoptosis induced by known DNA damaging agents, doxorubicin and etoposide were investigated for their ability to induce cleavage of PARP and expression of p53, p21/WAF and Bax. The p53 wild-type cell lines SK-N-SH, which might have impaired p53 function due to sequestering, and A-172 with in any case functional p53 as well as the p53 mutant cell line HaCaT as a control were used. The commonly used NB cell line LAN-1 was not used due to resistance against both drugs. Treatment with both doxorubicin and etoposide led to comparable increases in p53 levels in the p53 wild-type cell lines as seen after treatment with cerulenin, indicating that the DNA damaging potential of all three drugs are equal. But in contrast to treatment with cerulenin both doxorubicin and etoposide induced a strong expression of p21/WAF (and Bax), proving that p53 is functional in response to DNA damage induced by these drugs. On the other hand no increases in p53, p21/WAF and Bax

expression were observed in the p53 mutated cell line HaCaT, proving that expression of p21/WAF (and Bax) is dependent on p53.

Since the DNA damaging potential measured by overexpression of p53 appears to be comparable for all three drugs, it is unlikely that the lack of induction of p53 inducible genes like p21/WAF can be explained by an insufficient accumulation of p53 after treatment with cerulenin. Yet only doxorubicin and etoposide induced the expression of p21/WAF. It thus seems likely that p53 - although overexpressed - is indeed not functional activated by cerulenin-induced DNA damage. Furthermore the results with doxorubicin and etoposide confirmed that sequestering of p53 can be excluded as p53 inactivating mechanism. Clearly other mechanism must be responsible for the impaired or non functionality of p53. Protein levels and activity of p53 are tightly regulated mostly by post-transcriptional mechanisms to ensure that high amounts of functional p53 can rapidly be accumulated in case of (severe) DNA damage (Agarwal et al., 1998; Oren 1999). Phosphorylation and acetylation are key events in the regulation of the biological activities of p53 (Lakin et al., 1999; Oda et al., 2000). It is therefore possible that post-transcriptional events necessary for p53 function (in order to activate genes like p21/WAF) are not triggered by cerulenin-induced DNA damage. However, more investigations are necessary to explain this results.

Interestingly, the induction of apoptosis by doxorubicin and etoposide was independent of the p53 status. Both drugs induced apoptosis to the same extent in all three cell lines as measured by PARP cleavage and observed by the typical morphological changes. Thus induction of apoptosis and p53 function caused by these drugs as much as caused by cerulenin appear to be independent events. This indicates that additional (apoptotic) mechanisms exist to respond to DNA damage beside induction of p53. The molecular requirements for the cerulenin-

induced apoptosis were then more thoroughly characterized in the p53 wild-type cell line LAN-1 and the p53 mutated cell line HaCaT. The induction of apoptosis by cerulenin measured by cleavage of PARP was a rapid process in both cell lines. The 89 kDa cleavage product of PARP was detectable after 9 h of treatment with cerulenin in LAN-1 cells and already after 6 h in HaCaT cells, respectively. Total degradation of intact PARP after 24 h emphasizes the high sensitivity against cerulenin. The broad-range caspase inhibitor zVAD-fmk completely blocked PARP cleavage in both cell lines. But although PARP cleavage was inhibited by zVAD-fmk, the induction of cell death was not. These data indicate that caspase activation occurs after commitment to cell death and that although activation of caspases is involved in the cerulenin-mediated apoptosis further mechanisms independent of caspases exist.

Interestingly caspase 8 appears not to be involved in the cerulenin-mediated apoptotic pathway. After ligation of transmembrane death receptors such as Fas caspase 8 is activated (Medema et al., 1997; Juin et al., 2000). In LAN-1 cells neither caspase-8 mRNA (Weigelt 2000) nor protein was detectable. These results are consistent with recently published data (Donaldsen et al., 2000; Eggert et al., 2000; Teitz et al., 2000) that showed a loss of caspase 8 in a variety of NB cell lines in correlation to the MYCN-amplification status. As apoptosis was induced in both caspase 8 deficient and in caspase 8 expressing NB cell lines to the same extent, cerulenin-mediated apoptosis does obviously not depend on caspase 8. In this respect, the pathway of cerulenin-induced apoptosis differs from previously identified mechanisms where treatment with some DNA damaging drugs like doxorubicin promotes cell death by inducing the surface expression of the Fas ligand and the subsequent activation of Fas and caspase 8 (Friesen et al., 1996; Fulda et al., 1997; Kaufmann et al., 2000; Teitz et al., 2000). NB cell lines deficient in caspase 8 show resistance to this drugs whereas treatment with

cerulenin could offer an extremely attractive opportunity especially in the treatment of NB.

In many types of drug-induced apoptotic processes mitochondria are key players (Kroemer et al., 1997 and 2000; Cai et al., 1998; Green 1998; Bossy-Wetzel et al., 1999). The permeabilization of the outer mitochondrial membrane and the subsequent release of cytochrome C from the mitochondrial intermembrane space into the cytosol is followed by caspase activation (Green 1998; Finucane et al., 1999; Slee et al., 1999). In the presence of cytochrome C, dATP, Apaf-1 and procaspase 9 formation of the so called apoptosom takes place and leads to the activation of procaspase 9. Subsequently, active caspase 9 can activate the effector caspase 3 (Li et al., 1997; Zou et al., 1997; Cain et al., 1999). Treatment with cerulenin led to the release of cytochrome C already after three and six hours in LAN-1 and HaCaT cells, respectively, indicating a rapid permeabilization of the outer membrane. The early release of cytochrome C was followed by the sequential activation of caspase 9 and caspase 3, proving that induction of apoptosis by cerulenin is consistent with the classical mitochondrial pathway.

Permeabilization of the outer (and the inner) mitochondrial membrane, mitochondrial cytochrome C release and sometimes loss of mitochondrial membrane potential is usually initiated/mediated by pro-apoptotic members of the Bcl-2 family such as Bax who have channel-forming properties. To explain the mitochondrial membrane permeabilization mainly three different models exist. First, interaction of Bax with the adenoside nucleotide transporter (ANT) located in the inner mitochondrial membrane leads to the permeabilization of the inner membran and the subsequent rupture of the outer membrane. As as consequence cytochrome C is released into the cytosol and the mitochondrial potential breaks down. In the second model, the voltage dependent anion channel (VDAC) located in the outer membrane is

opened by replacement of the antiapoptotic Bcl-2 by Bax leading to a selective permeabilization of the outer membrane which is accompanied by cytochrome C release but not by a breakdown of the mitochondrial potential. In the third model, Bax forms independent of interactions with other channel-forming proteins an autonomous protein-translocating channel resulting in mitochondrial cytochrome C release but again without influencing the mitochondrial potential. These changes are in all cases tightly regulated by anti-apoptotic members of the Bcl-2 family such as Bcl-2 itself, which can bind the proapoptotic Bcl-2 members thereby preventing the formation of channels/pores. Induction of apoptosis by Bax is usually accompanied by its overexpression, the replacement of Bcl-2 by Bax and translocation and/or insertion into the outer mitochondrial membrane.

However, the release of cytochrome C was neither accompanied by an overexpression of Bax nor a break down of the mitochondrial potential at that time, indicating that only permeabilization of the outer membrane has occurred. To explain the early release of cytochrome C that is evidently independent of overexpression of Bax three mechanisms appear conceivable. First, the early release of cytochrome C is completely independent of Bax and the result of another mechanism. Second, conformational changes of the Bax protein loosely associated to the outer mitochondrial membrane are responsible for the insertion of Bax in the outer mitochondrial membrane and the subsequent release of cytochrome C. Third, although Bax is not overexpressed, its translocation from the cytosol to the mitochondria and the consecutive insertion in the outer membrane induces the release of cytochrome C.

Interestingly, a loss of the mitochondrial potential was observed in LAN-1 cells as a late event that followed the release of mitochondrial proteins instead of preceding them. On the contrary, the mitochondrial potential in HaCaT cells remained intact although the overexpression of Bax in HaCaT cells was comparable to that in LAN-1 cells. This strongly

indicates that the mere overexpression of Bax is not sufficient to induce a breakdown of the mitochondrial potential. The time dependent change of the mitochondrial potential in LAN-1 cells paralleled the appearance of an 18 kDa Bax cleavage fragment which is probably responsible for the loss of the mitochondrial membrane potential in LAN-1 cells. A possible explanation is the integration of the p18 Bax in the inner mitochondrial membrane inducing the osmotic swelling of the intermembran space, the complete rupture of the outer membrane and loss of mitochondrial potential. These findings are consistent with recent reports demonstrating a higher cytotoxicity of p18 Bax than of full length Bax (Wood et al., 1999). In cerulenin treated NB cells, p18 Bax may function as an enhancer system causing cell death more efficiently by directly inducing mitochondrial dysfunction.

In summary, cerulenin was identified as a potent apoptosis-inducing drug. Apparently the induction of apoptosis is independent of its function as inhibitor of FAS but related to its DNA damaging properties. The induction of apoptosis as well as the regulation of p21 and Bax are independent of p53. As mutations in the p53 gene and the subsequent abrogation of the p53 tumor suppressor activities occur in about 50 % of all human tumors and are the main reason for unsatisfactory responses to cancer treatment, cerulenin is a promising new drug candidate. Cerulenin is an effective inducer of apoptosis especially in human NB cells but also in other cell lines with the mitochondria of pivotal importance. The release of cytochrome C is an early event which is independent of overexpression of Bax. As a consequence of cytochrome C release, caspase 9 and caspase 3 are activated. A later overexpression of Bax as well as the accumulation of the p18 cleavage product seems to enhance the effects of cerulenin in NB cells by leading to a breakdown of the mitochondrial potential. Since cerulenin functions not only independent of p53 but also independent of caspase 8 it is a very promising agent in particular for the treatment of NB.

5.2. Anti-NB IgM mediated apoptosis

Previous work in our group has demonstrated that naturally occurring anti-NB IgM antibodies which induce apoptosis in a host of NB cell lines predominantly recognize a 260 kDa antigen, termed NB-p260. Several experiments demonstrated that it is very likely that this protein serves as the apoptosis-mediating receptor. Preincubation of human NB cells with polyclonal murine IgG sera raised against the purified NB-p260 inhibited the binding of natural human anti-NB IgM and vice versa. While the murine anti-NB-p260 IgG antibodies did not induce apoptosis of human NB cells, they were able to abolish the induction of apoptosis by anti-NB IgM antibodies in a dose dependent manner (David et al., 1999). Interestingly chicken anti-NB-p260 IgY antibodies were even able to induce apoptosis in different NB cell lines but not in other tumor cell lines thereby exhibiting the same specificity as the anti-NB IgM (Weigelt 2000). These results strongly indicate that NB-p260 is the predominant antigen on human NB cells recognized by apoptosis-inducing natural anti-NB IgM. Unfortunately, the characterization of the NB-p260 proved to be extremely difficult due to rapid autodegradation, presumably due to an inherent proteolytic activity that could not be inhibited by a variety of protease inhibitors (Heiligtag 1998). This rapid autodegradation prevented the N-terminal sequence analysis of the purified protein. Hence the generation of stable internal fragments by digestion of the purified NB-p260 and their subsequent N-terminal sequencing was the next approach. Initial experiments demonstrated that the NB-p260 showed a highly heterogenous fragmentation pattern upon digestion with different proteases and therefore high amounts of the NB-p260 were needed to generate fragments of reasonable yields for subsequent sequence analysis. The established purification procedure of the NB-p260 needed to be modified to obtain the protein very pure for the

following enzymatic fragmentation, because in case the contaminating proteins would show a more restricted and homogenous digestion pattern they might yield fragments in considerable amounts thereby complicating the analysis.

The two major disadvantages of the established protocol were first, that purification of the NB-p260 by sequential ion exchange chromatography yielded the protein in the breakthrough on both applied columns. Therefore contaminating proteins of the same molecular weight could not be excluded. Second, other proteins with related molecular weights were always present in preparations of purified NB-p260 in small amounts, most prominently human FAS (Heiligtag 1998). Although these impurities in general were small the digestion patterns of these proteins were unknown. To overcome these setbacks the anion exchange chromatography column EconoQ which was applied in the first purification step was replaced by the anion exchanger HighQ. This matrix showed higher binding capacities and better resolutions of bound proteins. The NB-p260 was bound to the matrix and could be eluted in a sharp step gradient of only 50 mM sodium chloride. In addition a third chromatographic step was introduced in particular to allow the separation of impurities with related molecular weights, predominantly FAS. Of various chromatography media evaluated, including different hydrophobic interaction and ion exchange media, the hydroxyapatite media CHTII gave by far the best results regarding purity (and yield) and allowed the complete separation from FAS. The modified purification procedure yielded the NB-p260 without any visible contaminations as judged by Coomassie and silverstaining. However the yield decreased by approximately 50 % with regard to the former purification procedure mainly due to losses on the newly introduced hydroxyapatite chromatography column.

The purified protein was then digested with endoproteinase Lys-C which gave the best digestion patterns under various conditions of five different proteases tested (trypsin, endoproteinases Arg-C, Asp-N, Glu-C, and Lys-C). Two different approaches for the production of internal fragments were used to generate low and high molecular fragments. Low molecular fragments in the range between 10 and 40 kDa had the advantage of presumably higher stability, but the disadvantage of rather low yields. The stability of high molecular fragments on the other hand was dubious as previous results had shown (Heiligtag 1998), but yields proved to be better. Although apparently sufficient amounts between 10 and 20 pmol of protein fragments were subjected to N-terminal sequencing the obtained (sequence) information was poor. The reason for this unpleasant outcome remains unclear as fragments of other proteins that were subjected to N-terminal sequencing resulted in highly accurate information. For example, N-terminal sequence analysis of similar amounts of eight internal fragments of human FAS, likewise obtained after digestion with endoproteinase Lys-C, gave conformities between 95 and 100 % for all eight fragments (Heiligtag 1998). Furthermore a fragment of endoproteinase Lys-C that was used for the digestion of NB-p260 yielded 100 % conformity with a yield of only 1.2 pmol.

In any case the only usable sequence information pointed to ABP-280 (actin-binding protein 280 or filamin), a protein of 2,647 amino acids corresponding to a molecular weight of approximately 280 kDa. At least with respect to the molecular weight APB-280 seemed a possible candidate for the NB-p260. This assumption was verified by immunoblot analysis with monoclonal antibodies against ABP-280, although it could not explain the difficulties experienced during the sequence analysis as no reports describe any problems with stability or N-terminal sequencing of ABP-280.

ABP-280 is a dimeric protein that self-associates in nonmuscle cells and defines the three-dimensional organization of actin filaments in the submembraneous cortex (Gorlin et al., 1990). It is located in the cytoplasm where it usually links the cytoskeleton to membranes. ABP-280 is moreover expressed ubiquitously in all tissues which can neither explain its possible function as apoptosis-mediating receptor nor its immunogenicity. Thus the possibility that the NB-p260 consists of two proteins with similar molecular weights which additionally showed the same binding properties on three different columns had to be considered.

This hypothesis was confirmed after introducing a linear gradients on the hydroxyapatite column instead of the previously applied step gradient between 160 and 350 mM sodium phosphate. Indeed reactivity against ABP-280 was only observed in the latter fractions corresponding to approximately 250-350 mM sodium phosphate whereas the anti-NB IgM antibodies showed reactivity over the whole range. Hence the NB-p260 consists of two different proteins that are both reactive with anti-NB IgM antibodies and of which one is ABP-280. Accordingly, the non-ABP-280 containing fractions (160-240 mM sodium phosphate) were purified to homogeneity, subjected to commercial MALDI-MS and N-terminal sequence analysis due to much higher sensitivity and unambiguously identified as ABP-278 (actin-binding protein 278 or β -filamin). ABP-278 is a recently identified member of the actin binding protein family and consists of 2,602 amino acids corresponding to a molecular weight of 278 kDa (Xu et al., 1998; Takafuta et al., 1998). Structural comparison between ABP-278 and ABP-280 shows a high degree of homology of approximately 70 %. Both proteins consist of an actin-binding domain at the N-terminus, followed by 24 internally homologous repeats that are approximately 96 amino acids in length and consist of 8 β -sheets in an immunoglobulin like fold (Figure 43).

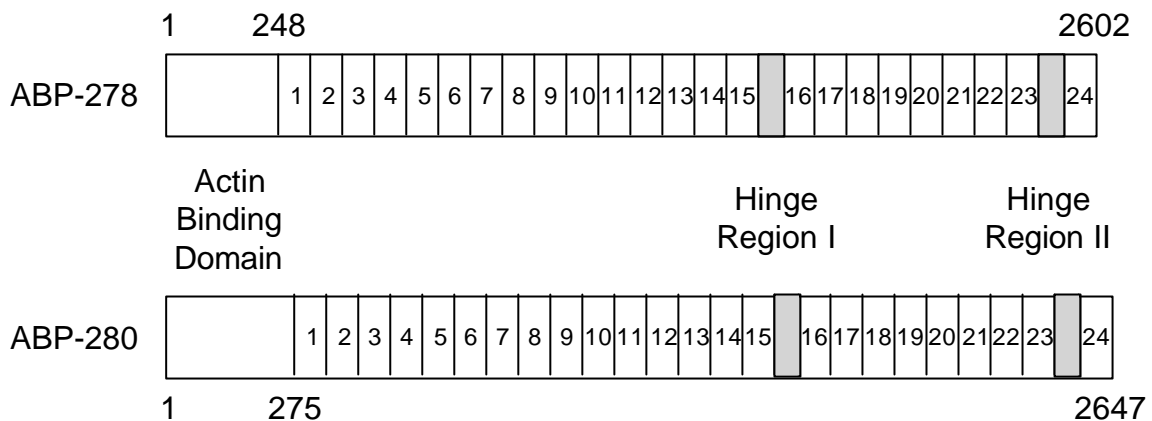


Figure 43: Structural comparison between ABP-278 and ABP-280

These repeats interact intramolecularly to form a rigid structure and are interrupted by two hinge regions (I and II) that are intercalated between repeats 15-16 and repeats 23-24, respectively. The hinge regions are believed to confer a certain degree of flexibility in the otherwise rigid structure and furthermore represent the main structural difference between ABP-278 and ABP-280. Hinge I region does not bore any sequence similarity at all, whereas hinge II region shows only moderate sequence conservation of about 40 %. The reason for these differences and its possible effects on function are currently not known.

APB-278/280 are dimeric proteins that self-associate through a self-association site in repeat 24. As mentioned, they function as promoters of actin polymerization and define the three-dimensional organization of the actin filaments. In addition several membrane receptors, including the immunoglobulin receptor FcγIR, the CD18 subunit of the β_2 integrin, or the thyroid stimulating hormone receptor (TSH-R) are associated with ABPs. In response to external ligand binding important functions such as clustering of receptors, focal adhesion, motility, and induction of signal transduction pathways are mediated or initiated. These functions are partly determined through the linkage between the actin cytoskeleton, the receptor and the respective ABP that led to changes in this

network upon ligand binding (Fox et al., 1988; Sharma et al., 1995). On the other hand the interaction between the receptor and the ABP can lead to the recruitment or activation of adaptor proteins that induce or mediate signal transduction pathways (Ohta et al., 1991; Marti et al., 1997). It has for example been shown that the ABP-280 deficient human melanoma cell line M2 fails to respond to TNF- α treatment and that transfection with ABP-280 restored responsiveness (Leonardi et al., 2000). It is therefore reasonable to assume that ABP-278/280 could induce signal transduction pathways on their own if expressed on the cell surface, although to date neither the cell surface expression and hence nor the direct binding of external ligands to ABP-278/280 have been demonstrated. But the cell surface expression of ABPs is not unlikely as it has been shown that ABP-280 contains two different lipid binding sites, namely residues 49-71 and 131-155, and is able to insert into membranes under in-vitro conditions (Goldmann et al., 1999). These two lipid binding sites are also found in ABP-278 with approximately 90 % homology.

The cell surface expression of ABP-278 but not of ABP-280 was then demonstrated by selective labeling of cell surface proteins with a non-membrane-permeable sulfobiotin derivate and their subsequent purification according to the procedure outlined above. Only ABP-278 proved to be biotinylated while in contrast no biotinylation of ABP-280 was observed. This indicates an exclusive intracellular expression of ABP-280 while ABP-278 apparently is also expressed on the cell surface and hence may function as receptor.

In the next step the function of ABP-278/280 as apoptosis-inducing receptor in different NB cell lines was demonstrated by preadsorption of various anti-NB IgM antibodies on immobilized NB-p260. The preadsorption virtually abolished their ability to induce apoptosis. This results corroborate the competitive binding assay data with murine

anti-NB-p260 IgG that were able to inhibit the binding and induction of apoptosis by anti-NB-IgM in a dose dependent manner (David et al., 2001). Chicken anti-NB-p260 IgY were even able to induce apoptosis exclusively in NB cell lines (Weigelt 2000). This results strongly indicate that the NB-p260 is the predominant apoptosis-mediating antigen on human NB cells.

The possible signal transduction pathway induced by binding of anti-NB IgM antibodies to APB-278 is currently under investigation. Recent results in our group have shown the rapid activation and cleavage of the downstream caspase 3 and the subsequent cleavage of PARP after induction of apoptosis with anti-NB IgM antibodies (Weigelt 2000). It is currently unknown which upstream effectors are responsible for the activation of caspase 3, but interestingly caspase 8 as the prototype transactivating caspase in receptor mediated apoptosis is most likely not involved. We and other groups have found that caspase 8 is silenced in different NB cell lines (Heiligtag et al., 2001; Teitz et al., 2000). As induction of apoptosis in caspase 8 deficient NB cell lines was similar to that induced in caspase 8 expressing NB cell lines it is highly unlikely that caspase 8 is the receptor associated transactivator/mediator. In addition no activation of caspase 10, a previously identified further caspase that can act as receptor associated caspase (Ng et al., 1999), was observed (Weigelt 2000). On the other hand we could prove that cleavage and/or activation of caspase 3 and PARP in response to treatment with anti-NB IgM antibodies could be abolished by preincubation with the tyrosine phosphate kinase inhibitor genistein, indicating that kinases are of pivotal importance in the signal transduction pathway (Heilmann 2000).

In accordance with this observations is an increasing number of reports that link the induction of apoptosis with the activation of the stress-activated protein kinases (SAPKs) c-Jun N-terminal kinase (JNK)

and p38 MAPK, both members of the mitogen-activated protein kinase (MAPK) family (Chen et al., 2000; Kanamoto et al., 1999; Ichijo et al., 1997). MAPKs are serine-threonine protein kinases that are activated in a highly conserved sequential phosphorylation cascade through phosphorylation of tyrosine residues in response to various extracellular signals. First, a MAPK kinase kinase (MAPKKK/MEKK) is activated by phosphorylation and in turn phosphorylates and activates a MAPK Kinase (MAPKK/MEK) who is then responsible for phosphorylation and activation of the respective MAPK. The activated MAPK subsequently regulates the activities of transcription factors or kinases further downstream by phosphorylation, and thereby controls gene expression and cellular functions (Leppä et al., 1999). The stress-activated members of the MAPK family JNK and p38 MAPK are key mediators of stress signals and inflammatory responses evoked by a variety of agents including oxidative stress, inflammatory cytokines, growth factor withdrawal or ligand binding to membrane receptors that eventually can lead to the induction of apoptosis (Chen et al., 1998; Ichijo 1999). Although many JNK/p38 MAPK activating stimuli are proapoptotic, the biological outcome is highly divergent and depends on cell type and cellular context. Particularly intriguing in this context is that cells of neuronal origin apparently differ from other cell types in their high susceptibility to apoptosis in response to SAPK activation (Watson et al., 1998; Le-Niculescu et al., 1999; Leppä et al., 1999; Kanamoto et al., 1999; Ham et al., 2000).

The involvement of SAPKs in apoptosis is probably most comprehensively investigated in the TNF pathway (Ichijo et al., 1997 and 1998; Kanamoto et al., 2000). TNF signals are mediated by two cell surface receptors (TNFR 1 and 2), which aggregate in response to binding of TNF- α , an inflammatory cytokine. This aggregation leads to the recruitment of different cytoplasmic adaptor proteins such as TNF

receptor associated factor 2 (TRAF2) who in turn can activate the so called apoptosis signal-regulated kinase (ASK1). ASK1 is a MAPKKK which in turn can phosphorylate and activate MAPKKs of both the JNK (MEK4/MEK7) and the p38 MAPK (MEK3/MEK4/MEK6) pathway. The subsequent activated JNKs and/or p38 MAPKs activate then further downstream targets leading eventually to the typical features of apoptosis, although the relationship between these kinases and the induction of apoptosis is unclear. However recent results have demonstrated that activation of these kinases can occur prior to and is necessary for caspase activation and cleavage. Various groups have shown that the inhibition of members of the JNK or p38 MAPK pathways prevented activation and cleavage of caspase 3 (and PARP) and induction of apoptosis (Chen et al., 1999; Harada et al., 1999; Shimizu et al., 1999; Stadheim et al., 2000).

Very intriguing in this context is the role of ABP-280 in the TNF- α pathway. Cells lacking expression of ABP-280 are not able to activate SAPKs in response to TNF- α stimulation whereas permanent transfection with ABP-280 restores responsiveness to TNF- α treatment. As a matter of fact, due to its interaction with at least two members of the TNF- α signaling pathway, namely TRAF2 and MEK4/SEK1, ABP-280 acts as an upstream regulator in the SAPK pathway. Binding to TRAF2 occurs between amino acids 1644 and 2118 whereas binding to SEK1 takes place in the C-terminal region between amino acids 2282 and 2454 (Marti et al., 1997; Leonardi et al., 2000). The binding sites for SEK1 and TRAF 2 are also conserved in ABP-278 which should thus be able to act in a similar way.

Considering this findings the following model is proposed by which binding of anti-NB IgM antibodies to cell surfaced expressed ABP-278 induces apoptosis in human NB cells (Figure 44). Upon binding of anti-NB IgM to ABP-278 an ABP associated factor (ABPAF) like TRAF2 is recruited if not already present. The pentameric character of the IgM could also lead to the aggregation of various ABP-278 molecules leading to close proximity between the different binding partners thereby facilitating their interactions. In the next step ASK1 is activated by ABPAF which in turn phosphorylates and activates SEK1, that is associated to the same or an adjacent ABP-278 molecule. Both JNK or p38 MAPK can then be recruited and activated by phosphorylation through the still associated activated SEK1. Supporting this data are preliminary results in our group that have demonstrated the activation of p38 MAPK (data not shown). The activated p38 MAPK initiates eventually the cleavage and activation of caspase 3 which is then responsible for the events resulting in cell death.

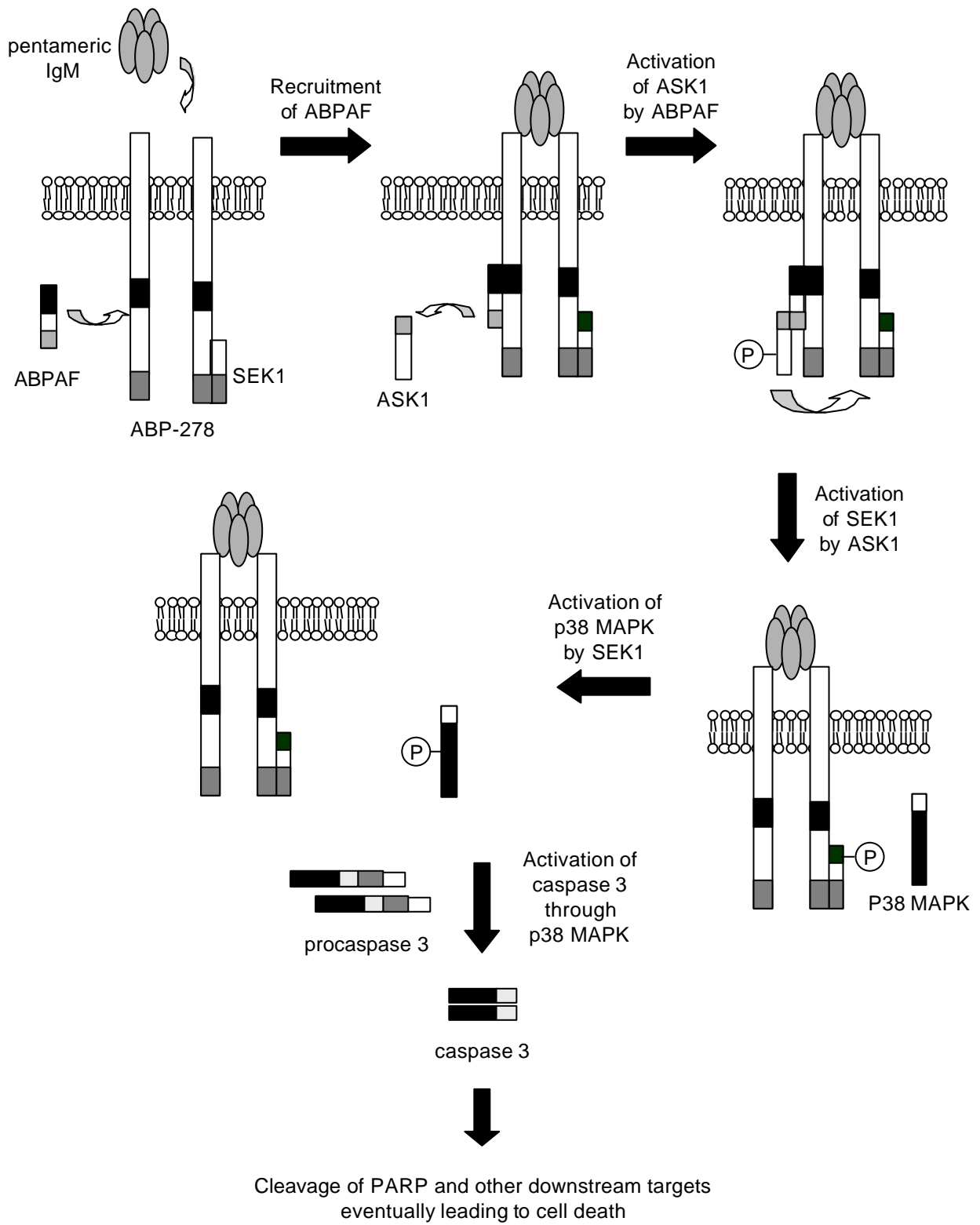


Figure 44: Model for the induction of apoptosis by human anti-NB IgM antibodies

In addition to ABP-278, which to date appears to be the dominant apoptosis-mediating antigen, it is not unlikely that heat shock protein hsp 90 may serve as a further apoptosis-mediating cell surface receptor. Previous results in our group had demonstrated that cytotoxic sera recognized hsp 90 in immunoblot analysis. Moreover, a monoclonal anti-hsp 90 IgM antibody was capable of inhibiting the binding of human anti-NB IgM antibodies to human NB cells in a dose-dependent manner, albeit the reduction in induction of apoptosis was rather low (David 1996). To further investigate the relevance of hsp 90 it was necessary to verify its cell surface expression and to demonstrate that sera of NB patients with unfavorable outcome do not recognize hsp 90. Both are necessary prerequisites for hsp 90 to serve as a putative apoptosis-mediating cell surface receptor. The cell surface expression of hsp 90 on the surface of LAN-1 NB cells was investigated by two different methods. First, the cell surface binding of monoclonal antibodies against hsp 90 was determined by FACScan analysis. Second, cell surface proteins were selectively labeled with a non-membrane-permeable sulfobiotin derivate, isolated by a monomeric avidin column and subsequently the presence of heat shock proteins was probed with monoclonal antibodies against hsp 90. Both methods provided identical results, identifying hsp 90 on the surface of LAN-1 NB cells. Interestingly hsp 60 (but not hsp 70) another major heat shock protein, could also be detected on the surface of LAN-1 NB cells by both methods, although hsp 60 has so far not been identified as a further protein recognized by anti-NB-IgM antibodies. The cell surface expression of hsp 60 and hsp 90 were confirmed in four other NB cell lines (IMR-32, NMB-7, SK-N-SH and SH-SY5Y), strongly indicating that hsp 60 and hsp 90 are indeed expressed on the surface of NB cells whereas hsp 70 is not. To evaluate the immunogenicity of hsp 60, hsp 70 and hsp 90, the purified proteins were probed against different patient sera of NB patients with fatal

outcome. To that end an economical purification method was developed that allowed the simultaneous purification of hsp 60, hsp 70 and hsp 90 from the same source (cell extracts). In the first step all three HSPs were separated from each other by anion exchange chromatography. Complete purification of hsp 60 and hsp 90 was then achieved by cation exchange-, hydroxyapatite chromatography and preparative gelelectrophoresis whereas hsp 70 was completely purified by cation exchange- and ADP affinity chromatography. The purified heat shock proteins were subsequently probed for immunoreactivity against sera of eight NB patients. Whereas cytotoxic sera had shown reactivity (David 1996), none of the patient sera showed reactivity against hsp 90, indicating that hsp 90 is exclusively detected by the cytotoxic sera. In combination with the observed cell surface expression, hsp 90 can thus represent an additional putative apoptosis-mediating cell surface receptor. The participation of HSPs in the immune response has been discussed for a long time since hsp 60, hsp 70 and hsp 90 are involved in important aspects of viral and bacterial infections, in autoimmune diseases and in cancer immunity. HSPs act as immunological target structures either by themselves because of an unusual expression pattern including their cell surface expression (mostly hsp 60 and hsp 90), or they are carrier proteins for immunogenic peptides which has predominantly been described for hsp 70 (Udono et al., 1994; Multhoff et al., 1998). The recognition of HSPs by both antibodies and T cells has been reported (Chen et al., 1999; Laad et al., 1999; Paul et al., 2000). In addition the presence of autoantibodies against hsp 60 or hsp 90 has been described in different autoimmune diseases such as atherosclerosis or schizophrenia (Conroy et al., 1995; Schett et al., 1995; Mazeh et al., 1998; Trieb et al., 2000). It seems therefore possible that autoantibodies against hsp 90 in addition to the apparently apoptosis-mediating anti-ABP-278 IgM antibodies exist. However,

considering the much higher ability of purified NB-p260 as well as of different antibodies raised against NB-p260 to inhibit the induction of apoptosis by anti-NB IgM antibodies, it is not likely that hsp 90 is such a predominant apoptosis-mediating receptor in NB such as ABP-278. Further investigations regarding the significance of hsp 90 as apoptosis-mediating receptor are therefore necessary, in particular the validation of hsp 90 as a target structure in a greater number of cytotoxic sera.

On the other hand all patients showed moderate to strong reactivities against hsp 60 and hsp 70, suggesting that these proteins act as tumor antigens. Yet it is unlikely that hsp 60 and hsp 70 are involved in potential immune responses in NB since the presence of antibodies against these tumorantigens evidently does not prevent fatal outcome in these patients or is related to a higher cytotoxicity of their sera. Nevertheless the cell surface expression of both hsp 60 and hsp 90 was quite surprising. However, the presence of heat shock proteins on the surface of human NB cells is not unlikely. Recently, several HSPs have been shown to be located on the surface of certain cells including tumor cells as well as virus- and bacteria-infected cells. Hsp 60 for example has been found on mycobacteria-infected cells ((Wand-Wuerttenberger et al., 1991), while members of the hsp 70 family have been identified on HIV- and HTLV-infected cell lines (Di-Cesare et al., 1992; Chouchane et al., 1994) Furthermore, cell surface expression on tumor cells has been described for the major hsp families hsp 60, hsp 70 and hsp 90 (Sapozhnikov et al., 1999; Ferrarini et al., 1992; Multhoff et al., 1995; Udono et al., 1994). In view of these studies, the presence of hsp 60 and hsp 90 on the surface of human NB cells appears to be just another example of cell surface-expressed HSPs. Their potential therapeutic value has to be determined in the future.

6. Appendix

I. Amino acid sequence of ABP-280

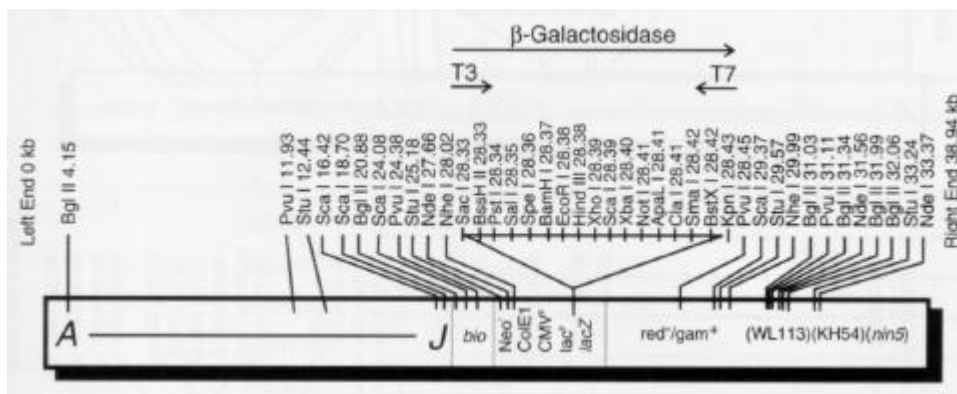
1 mssshsragq saagaapggg vdtrdaempa tekdlaedap wkkiqqntft rwcnehlkcv
 61 skrianlqtd lsdglrlial levlsqkkmh rkhnqrptfr qmqlenvsva lefldresik
 121 lvsidskaiv dgnlklilgl iwtlilhysi smpmwdeeed eeakkqtpkq rllgwiqnkl
 181 pqlpitnfsr dwqsgralga lvdscaapglc pdwdsdask pvtnareamq qaddwlgipq
 241 vitpeeivdp nvdehsvmty lsqfpkaklk pgaplrpkln pkkaraypgg ieptgnmvkk
 301 raftvetrs agqgevlvyy edpaghqeaa kvtanndknr tfsvwyvpev tgthkvtvlf
 361 agghiakspf evyvdksggd askvtaqpgg lepsgniank ttyfeiftag agtgevevvi
 421 qdpmgqkgtv epqleargds tyrcsyqptm egvhtvhvtf agvpiprspy tvvtvgqacnp
 481 sacravgrgl qpkgvrvtket adfkvytkga gsgelkvtvk gpkgeervkq kdlgdgvvygf
 541 eyypmvpoty ivtitwggqn igrspfevkv gtecgngkvr awgpgleggv vgsadfvve
 601 aigddvgtlg fsvegpsqak iecddkgdgs cdvrywpqea geyavhvlcn sedirlspfm
 661 adirdapqdf hpdvrkargp glektgvavn kpaftvdak hggkaplrvt vqdnegcpve
 721 alvkdngngt yscsyvprkp vkhtamvswg gvsipnspfr vnvagagshpn kvkvygpgva
 781 ktglkahept yftvdcaeaq qgdvsigikc apgvvypaea didfdiirnd ndtftvkytp
 841 rgagsytmv lfadqatpts pirvkvepsh daskvkaegp glsrtgvelg kpthftvna
 901 aagkgkldvq fsgltkgdav rdvdiidhhd ntytvkytpv qggpvgvntv yggdppksp
 961 fsvavspsls lskikvsglg ekvdvkgdqe ftvkskgagg qgkvaskivg psgaavpckv
 1021 epglgadnsv vrflpreegp yevevtydgv pvpgspfppl avaptkpskv kafgpglqgg
 1081 sagsparfti dtkgagtggg gltvegpcea qleclndngd tcsvsyvppe pgdyninilf
 1141 adthipgspf kahvvpcfda skvkcsppgl eratagevgg fqvdcssags aeltieicse
 1201 aglpaevyiq dhgdgttit yiplcpgayt vtikyggqv pnfpsklqve pavdtsgvqc
 1261 ygggieggv freattefsv daraltqtgg phvkarvanp sgnltetyvq drgdgmykve
 1321 ytpyeeglhs vdvtydgsppv psspfqvpvt egcdpsrvrv hgpqiagstt nkpnkftvet
 1381 rgagtggglg avegpseakm scmdnkdgsc sveyipyeag tyslnvtygg hqvpgspfkv
 1441 pvhdvtdask vkcsppglsp gmvrnlpqs fqvdtaskagv aplqvkvqgp kglvepvdv
 1501 dnadgtqtn yvpsregpys isvlygdeev prspfkvkvl pthdaskvka sggplnttg
 1561 paslpvefti dakdagegll avqitdpegk pkkthiqdnh dgtytvayvp dvtgrytili
 1621 kyggdeipfs pyravrptg daskctvtvs igghglgagi gptiqigeet vitvdtkaag
 1681 kgkvtctvct pdgsevdvdv venedgtfdi fytapqpgky vicvrfggeh vpsnspfvta
 1741 lagdqpsvqp plrsqqlapq ytyaqqgqqt waperplvgv nglvdtslrp fdlvipftik
 1801 kgeitgevmr psgkvaqpti tdnkdgtvtv ryapseaglh emdirydnmh ipgsplqfyv
 1861 dyvncghvta yggplthgvv nkpatftvnt kdageggsls aiegpskaei sctdnqdgtc
 1921 svsylpvlpg dysilvkyne qhvpgspfta rvtgddsmrm shlkvgsaad ipinisetdl
 1981 sltatvvpv sgreepcllk rlrnghvgis fvpketgehl vhwkngqhv asspipvvis
 2041 qseigdasrv rvsgqglheg htfepeafii dtrdagyggl slsiegpskv dintedledg
 2101 tcrvtycpte pgnyiinikf adqhvpgspf svkvtgegrv kesitrrrra psvanvgshc
 2161 dlslkipeis iqdmataqvt psgktheaei vegenhtyici rfvpaemgth tvsvkykgqh
 2221 vpgspfqftv gplgeggahk vragggler aeagvpaefs iwtreagagg laiavegpsk
 2281 aeisfedrkd gscgvayvvq epgyevsvk fneehipdsp fvvvvaspsg darrltvssl
 2341 qesglkvnqp asfavslnga kgaidakvhs psgaleecyv teidqdkyav rfiprengvy
 2401 lidvkfngth ipgspfkirv gepghggdpg lvsaygagle ggvtgnpaef vvntsnagag
 2461 alsvtidgps kvkmdcqcq egyrvtytpm apgsylisik yggpyhiggs pfkakvtgpr
 2521 lvsnhslhet ssvfvdsltk atcapqhgag gpgpadaskv vakglglska yvgqkssftv
 2581 dcskagnnml lvgvhgprtp ceelivkhvg srlsvsyll kdkgeytlvv kwghehipgs
 2641 pyrvvvp

II. Amino acid sequence of ABP-278

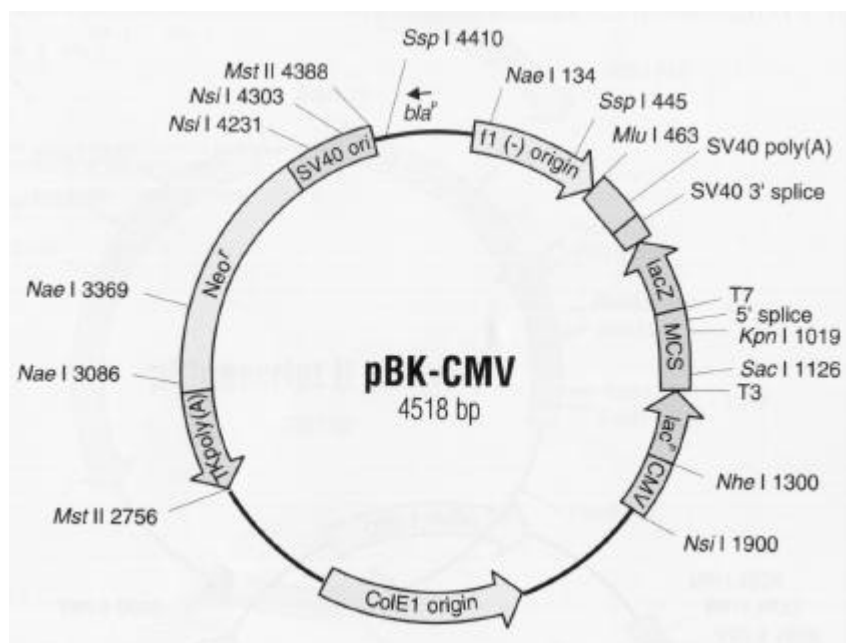
1 mpvtekdlae dapwkkiqqn tftrwcnehl kcvnkrignl qtldsdglrl iallevlsqk
 61 rmyrkyhgrp tfrmqqlenv svalefldre siklvsidsk aivdgnlkli lglvwtlilh
 121 ysismpvwed egdddakkqt pkqrllgwiq nkipylpitn fnqnwqdgka lgalvdscap
 181 glcpdweswd pqkpvdnare amqqaddwlg vpqvitpeei ihpdvdehsv mtylsqfpka
 241 klkpgaplkp klnpkkaray grgieptgnm vkqpakftvd tisagqgdvm vfvedpegnk
 301 eeaqvtpdsd knktysveyvl pkvtglhkvt vlfagqhisk spfevsvdka qgdaskvtak
 361 gpgleavgni ankptyfdiy tagagvgdig vevedpqqkn tvellvedkg nqvyrvcvykp
 421 mqpgphvcki fflagdtipks pfvqvgeac npnacrasgr glqpkgvrir ettdfkvdtk
 481 aagsgelgvt mkgpkgleel vkqkdfldgv yafeyypstp grysiaitwg ghhpkspfe
 541 vqvgpeagmq kvrawgpplh ggivgrsadf vvesigsevg slgfaiegps qakieyndqn
 601 dgscdvkywp kepgeyavhi mcddedikds pymafihpat ggynpdlvra ypggleksgc
 661 ivnlnaeflv dpkdagkapl kifaqdgegq ridiqmknrm dgtyacsytp vkaikhtiaiv
 721 vwggvniphs pyrvnigqgs hpqkvkvgfp gversglkan epthftvdct eagegdvsvg
 781 ikcdarvlse deedvdfdii hnandtftvk yvppaagryt ikvlfasqei paspfrvkvd
 841 pshdaskvka eggglskagv engkpthftv ytkgagkapl nvqfnsplpg davkdldiid
 901 nydyshtvky tptqqgnmqv lvtyggdpip kspftvgvaa pldlskikln glenrvevgk
 961 dqeftvdtrg agggqkldvt ilspsrkvvv clvtpvtgre nstakfipre eglyavdvty
 1021 dghpvpgspy tveaslppdp skvkahgppl egglvgkpaef tidtkgagt gglgltvegp
 1081 ceakiecsdn gdgtcsvsylv ptkpgeyfvn ilfeevhipg spfkadiemp fdpskvvasg
 1141 pglehgkvge agllsvncse agpgalglea vsdsgtkaev siqnnkdgty avtyvpltag
 1201 mytltmkygg elvphfparv kvepavdtsr ikvfgpgieg kdvfreattd ftvdsrpltq
 1261 vggdhikahi anpsgastec fvtndnadgty qveytpfekg lhvvevtydd vpipnspfkv
 1321 avtegcqpsr vqaqpgplke aftnkpnvft vvtrgagigg lgitvegpse skinrcrdnk
 1381 gscsaeyipf apgdydvnit yggahipgsp frvpvkdvvd pskvkiagpg lgsgvrarvl
 1441 qsftvdsska glaplevrvl gprglvepvn mvdngdgtht vtytspqegp ymvsvkyade
 1501 eiprspfkvk vlptydaskv tasgpglssy gvpaalpvdv aidardageg llavqitdqe
 1561 gkpkraivhd nkdgtyavty ipdktgrymi gvtyggddip lspyriratq tgaskclat
 1621 gpgiastvkt geevgfvvda ktagkqkvtc tvltpdgtea eadvienedg tydifytaak
 1681 pgtyviyvrff ggvdipnspf tvmatdgevt aveeapvnac ppgfrpwvte eayvpsdmn
 1741 glgfkpfdlv ipfavrkgei tgevhmppsgk tatpeivdnk dgtvtvryap tevglhemhi
 1801 kymgshipes plqfyvnypn sgsvsaypgp lvygvankta tftivtedag eggldlaieg
 1861 pskaeiscid nkdgtctvty lptlpgdysi lvkyndkhip gspftakitd dsrrcsqvk
 1921 gsaadflldi setdlsslta sikapsgrde pcellkrlpnn higisfipre vgehlvsikk
 1981 ngnhvanspv simvvqseig darrakvygr glsegtrfem sdfivdtrda gyggislave
 2041 gpskvdiqte dledgtckvs yfptvpgvyi vstkfadehv pgsfpfvkis gegrvkesit
 2101 rtsrapsvat vgsicdlnlk ipeinssdms ahvtspsgrv teaeivpmgk nshcvrfrvpq
 2161 emgvhtvsvk yrgqhvgtgsp fqftvgplge ggahkvragg pglgergeagv paefsiwtre
 2221 agagglsiav egpskaeitf ddhknsgcgv syiaqepgny evsikfndeh ipespylvpv
 2281 iapsddarrl tvmslqesgl kvnqpasfai rlngakgkid akvhspsgav eechvselep
 2341 dkyavrffiph engvhtidvk fngshvvgsp fkvrvgpepgg agnpalvsay gtgleggttg
 2401 iqseffintt ragpgtllsvt iegpskvkmd cqetpegykv mytpmapgny lisvkyggpn
 2461 hivgspfkak vtgqrlvspg sanetssilv esvtrsstet cysaipkass daskvtskga
 2521 glskafvgqk ssflvdcska gsnmlligvh gpttpceevs mkhvgnqqyn vtyvvkergd
 2581 yvlavkwgee hippgspfhvt vp

III. Lambda ZAP system

Map of the ZAP Express vector:



Map of the pBK-CMV phagemid vector:



7. Abstracts

1. Cerulenin Induces Apoptosis in Human Neuroblastoma Cells.
Kerstin David, Sven Heiligtag, Reinhard Bredehorst and
Carl-Wilhelm Vogel.
Proceedings of the AACR, Vol. 41, April 2000.
2. Mechanisms of Cerulenin-induced Apoptosis in Human
Neuroblastoma Cells.
Sven Heiligtag, Britta Weigelt, Carl-Wilhelm Vogel and
Kerstin David.
Biomedical Sciences Symposium, April 2000.
3. Cell Surface Expression of HSP90 and GRP75 Heat Shock
Proteins on Neuroblastoma Cells.
David K., Heiligtag S., Bredehorst R. and Vogel C.-W..
Advances in Neuroblastoma Research, May 2000.
4. Cerulenin is a Potent Inducer of Apoptosis in a p53-Dependent and
p53-Independent Manner.
Kerstin David, Sven Heiligtag, Reinhard Bredehorst and Carl-
Wilhelm Vogel.
Molecular Biology and New Therapeutic Strategies (Cancer
Research in the 21st Century), AACR, February 2001.
5. Cerulenin Induces Apoptosis Independent of Fatty Acid Synthesis
Inhibition.
Sven J. Heiligtag, Reinhard Bredehorst, Carl-Wilhelm Vogel and
Kerstin A. David.
Proceedings of the AACR, Vol. 42, March 2001.

8. Publications

1. Human natural immunoglobulin M antibodies induce apoptosis of human neuroblastoma cells by binding to a M_r 260,000 antigen.
Kerstin David, Markus W. Ollert, Caren Vollmert, Sven Heiligtag, Britta Eickhoff, Rudolf Erttmann, Reinhard Bredehorst and Carl-Wilhelm Vogel.
Cancer Res. 1999, 59: 3768-3775.
2. Initial characterization of the apoptosis-inducing receptor for natural human anti-neuroblastoma IgM.
Kerstin David, Sven Heiligtag, Markus W. Ollert, Manfred Teppke, Carl-Wilhelm Vogel and Reinhard Bredehorst.
Med. Pediatr. Oncol. 2001, 36:251-257.
3. Cerulenin induces apoptosis independent of fatty acid synthase inhibition.
Sven J. Heiligtag, Reinhard Bredehorst, Carl-Wilhelm Vogel and Kerstin A. David.
Submitted Cancer Research.
4. Cytochrome C release is an early event in the cerulenin-mediated apoptosis in human neuroblastoma cells
Sven J. Heiligtag, Britta Weigelt, Carl-Wilhelm Vogel and Kerstin A. David.
Submitted Cancer Research.
5. Cell surface expression of hsp60 and hsp90 correlates with its constitutively high expression in human neuroblastoma cells.
Kerstin A. David,¹ Sven J. Heiligtag, Reinhard Bredehorst, Carl-Wilhelm Vogel.
In preparation Journal of Neurochemistry.

9. References

Adam, A. & Hochholzer, L. (1981). Ganglioneuroblastoma of the posterior mediastinum: a clinicopathologic review of 80 cases. *Cancer* 47: 373-381.

Agarwal, M.L., Agarwal, A., Taylor, W.R., Chernova, O., Sharma, Y. & Stark, G.R. (1998). A p53-dependent S-phase checkpoint helps to protect from DNA damage in response to starvation for pyrimidine nucleotides. *Proc. Natl. Acad. Sci. USA* 95: 14775-14780.

Agarwal, M.L., Taylor, W.R., Chernov, M.V., Chernova, O.B. & Stark, G.R. (1998). The p53 network. *J. Biol. Chem.* 273: 1-4.

Ajiki, W., Tsukuma, H., Oshima, A. & Kawa, K. (1998). Effects of mass screening for neuroblastoma on incidence, mortality, and survival rates in Osaka, Japan. *Cancer Causes Control* 6: 631-636.

Alter, J.L., Gardner, K.L., Foxhall, L.E., Therell, B.L. Jr. & Bleyer W.A. (1998). Neuroblastoma screening in the United States: results of Texas Outreach Program for neuroblastoma screening. *Cancer* 15: 1593-1602.

Assefa, Z., Vantieghem, A., Declercq, W., Vandenabeele, P., Vandenheede, J.R., Merlevede, W., de Witte, P. & Agostinis, P. (1999). The activation of the c-Jun N-terminal and p38 mitogen-activated protein kinase signaling pathways protects HeLa cells from apoptosis following photodynamic therapy with hypericin. *J. Biol. Chem.* 274: 8788-8796.

Beckwith, J.B. & Perrin, E.V. (1963). In situ neuroblastomas: a contribution to the natural history of neural crest tumors. *Am. J. Path.* 43: 1089-1104.

Belka, C., Rudner, J., Wesselborg, S., Stepczynska, A., Marini, P., Lepple-Wienhaus, A., Faltin, H., Bamberg, M., Budach, W. & Schulze-Osthoff, K. (2000). Differential role of caspase-8 and BID activation during radiation- and CD95-induced apoptosis. *Oncogene* 19: 1181-1190.

Bian, J. & Sun, Y. (1997). p53CP, a putative p53 competing protein that specifically binds to the consensus p53 DNA binding sites: a third member of the p53 family?. *Proc. Natl. Acad. Sci. USA* 94: 14753-14758.

Berthold, F. (1990). *Overview: Biology of Neuroblastoma*. C. Pochedly (ed.) Boca Raton, Florida: CRC Press: 1-30.

Bolande, R.P. (1974). Congenital and infantile neoplasia of the kidney. *Lancet* 2: 1497-1499.

Bolande, R.P. (1990). The spontaneous regression of neuroblastoma. Experimental evidence for a natural host immunity. *Path.*: 187-199.

Bolande, R.P. & Mayer, D.C. (1990). The cytolysis of human neuroblastoma cells by a natural IgM "antibody"-complement system in pregnancy serum. *Cancer Invest.* 8: 601-643.

Bosslet, K., Mennel, H.D., Rodden, F., Bauer, B.L., Wagner, F., Altmannsberger, A., Sedlacek, H.H. & Wiegandt, H. (1989). Monoclonal antibodies against epitopes on ganglioside G_{D2} and its lactoses. *Cancer Immunol. Immunother.* 29: 171-178.

Bossy-Wetzel, E. & Green, D.R. (1999). Apoptosis: checkpoint at the mitochondrial frontier. *Mutat. Res.* 434: 243-251.

Boulares, A.H., Yakovlev, A.G., Ivanova, V., Stoica, B.A., Wang, G., Iyer, S. & Smulson, M. (1999). Role of Poly(ADP-ribose)Polymerase (PARP) cleavage in apoptosis. *J. Biol. Chem.* 274: 22932-22940.

Brodeur, G.M., Seeger, R.C., Sather, H., Dalton, A., Siegel, S.E. & Wong, K.Y. (1984). Amplification of N-myc in untreated human neuroblastomas correlates with advanced disease stage. *Science* 224: 1121-1124.

Bruchelt, G., Baader, S.L., Rieth, A.G., Lode, H.N., Gebhardt, S. & Niethammer, D. (1993). Rationale for the use of ascorbic acid in neuroblastoma therapy. In *Human neuroblastoma. Recent advances in clinical and genetic analysis.* (Ed. Schwab, M., Tonini, G.P. & Bénard, J.) 3-10 (Harwood Academic Publishers, Chur, Schweiz).

Budihardjo, I., Oliver, H., Lutter, M., Luo, X. & Wang, X. (1999). Biochemical pathways of caspase activation during apoptosis. *Annu. Rev. Cell. Dev. Biol.* 15: 269-90.

Cai, J., Yang, J. & Jones, D.P. (1998). Mitochondrial control of apoptosis: the role of cytochrome c. *Biochim. Biophys. Acta* 1366: 139-149.

Chalbos, D., Escot, C., Joyeux, C., Tissot-Carayon, M.J., Pages, A. & Rochefort, H. (1990). Expression of the progestin-induced fatty acid synthetase in benign mastopathies and breast cancer as measured by RNA in situ hybridization. *J. Natl. Cancer Inst.* 82: 602-606.

Chen, W., Syldath, U., Bellmann, K., Burkart, V. & Kolb, H. (1999). Human 60-kDa heat-shock protein: a danger signal to the innate immune system. *J. Immunol.* 162: 3212-3219.

Chen, Y.-R., Wang, W., Kong, A.-N. T. & Tan, T.-H. (1998). Molecular mechanisms of c-Jun N-terminal kinase-mediated apoptosis induced by anticarcinogenic isothiocyanates. *J. Biol. Chem.* 273: 1769-1775.

Chen, Y.-R. & Tan, T.H. (2000). The c-Jun N-terminal kinase pathway and apoptotic signaling. *Int. J. Oncol.* 16: 651-662.

- Chen, Y.-T., Scanlan, M.J., Sahin, U., Tuereci, U., Gure, A.O., Tsang, S., Williamson, B., Stockert, E., Pfreundschuh, M. & Old, L.J.** (1997). A testicular antigen aberrantly expressed in human cancers detected by autologous antibody screening. *Proc. Natl. Acad. Sci. USA* 94: 1914-1918.
- Chen, Z., Seimiya, H., Naito, M., Mashima, T., Kizaki, A., Dan, S., Imaizumi, M., Ichijo, H., Miyazono, K. & Tsuruo, T.** (1999). ASK1 mediates apoptotic cell death induced by genotoxic stress. *Oncogene* 18: 173-180.
- Chouchane, L., Bowers, F.S., Sawasdikosol, S., Simpson, R.M. & Kindt, T.J.** (1994). Heat shock proteins expressed on the surface of human T cell leukemia virus Type I-infected cell lines induce autoantibodies in rabbits. *J. Infect. Disease* 169: 253-259.
- Cheung, N.-K.V., Saarinen, U.M., Neely, J.E., Landmeier, B., Donovan, D. & Coccia, P.F.** (1985). Monoclonal antibodies to a glycolipid antigen on human neuroblastoma cells. *Cancer Res.* 45: 2642-2649.
- Cain, K., Brown, D.G., Langlais, C. & Cohen, G.M.** (1999). Caspase activation involves the formation of the apoptosome, a large (~700 kDa) caspase-activating complex. *J. Biol. Chem.* 274: 22686-22692.
- Cheung, N.K., Kushner, B.H., Yeh, S.D.J. & Larson, S.M.** (1998). 3F8 monoclonal antibody treatment of patients with stage 4 neuroblastoma: a phase II study. *Int. J. Oncol.* 12: 1299-1306.
- Cohen, G.M.** (1997). Caspases: the executioners of apoptosis. *Biochem. J.* 326: 1-16.
- Cohen, J.J.** (1993). Apoptosis. *Immunology Today* 14: 126-130.

Conford, P.A., Dodson, A.R., Parsons, K.F., Desmond, A.D., Woolfenden, A., Fordham, M., Neoptlemos, J.P., Ke, Y. & Foster, C.S. (2000). Heat shock protein expression independently predicts outcome in prostate cancer. *Cancer Res.* 60: 7099-7105.

Conroy, S.E., Gibson, S.L., Brunstrom, G., Isenberg, D., Lymani, Y. & Latchman, D.S. (1995). Autoantibodies to 90 kDa heat-shock protein in sera of breast cancer patients. *Lancet* 345: 126-130.

Cossarizza, A., Baccarani-Contri, M., Kalashnikova, G. & Franceschi, C. (1993). A new method for the cytofluorometric analysis of mitochondrial membrane potential using the J-aggregate forming lipophilic cation 5,5',6,6'-tetrachloro-1,1',3,3'-tetraethylbenzimidazolcarbocyanine iodide (JC-1). *Biochem. Biophys. Res. Commun.* 197: 40-45.

Cryns, V. & Yuan, J. (1998). Proteases to die for. *Genes & Develop.* 12: 1551-1570.

D'Agnolo, G., Rosenfeld, I.S., Awaya, J., Omura, S. & Vagelos, P.R. (1973). Inhibition of fatty acid synthesis by the antibiotic cerulenin. Specific inactivation of β -ketoacyl-acyl carrier protein synthetase. *Biochim. Biophys. Acta* 326: 155-166.

David, K. (1996). Natürliche zytotoxische Antikörper gegen humane Neuroblastom-Zellen. Ph. D. thesis, Department of Chemistry, University of Hamburg.

David, K., Ollert, M.W., Juhl, H., Vollmert, C., Erttmann, R., Vogel, C.-W. & Bredehorst, R. (1996). Growth arrest of large solid human neuroblastoma xenografts in nude rats by natural IgM from healthy humans. *Nature Med.* 2: 686-689.

David, K., Ehrhardt, A., Ollert, M.W., Erttmann, R., Bredehorst, R. & Vogel, C.-W. (1997). Expression of a 260 kDa neuroblastoma surface antigen, the target of cytotoxic natural human IgM: correlation to MYCN amplification and effects of retinoic acid. *Eur. J. Cancer* 33: 1937-1941.

David, K., Ollert, M.W., Vollmert, C., Heiligtag, S., Eickhoff, B., Erttmann, R., Bredehorst, R. & Vogel, C.-W. (1999). Human natural Immunoglobulin M antibodies induce apoptosis of human neuroblastoma cells by binding to a M_r 260,000 Antigen. *Cancer Res.* 59: 3768-3775.

Di-Cesare, S., Poccia, F., Mastino, A. & Colizzi, V. (1992). Surface expressed heat-shock proteins by stressed or human immunodeficiency virus (HIV)-infected lymphoid cells represent the target for antibody-dependent cellular cytotoxicity. *Immunology* 76: 341-343.

Dive, C. & Hickman, J.A. (1991). Drug-target interactions: only the first step in the commitment to a programmed cell death?. *Br. J. Cancer* 64: 192-196.

Di Vinci, A., Geido, E., Infusini, E. & Giaretti, W. (1994). Neuroblastoma cell apoptosis induced by the synthetic retinoid N-(4-hydroxyphenyl)retinamide. *Int. J. Cancer* 59: 422-426.

Dole, M.G., Jasty, R., Cooper, M.J., Thompson, C.B., Nunez, G., & Castle, V.P. (1995). Bcl-xL is expressed in neuroblastoma cells and modulates chemotherapy-induced apoptosis. *Cancer Res.* 55: 2576-2582.

Donaldson, S., Bodmer, J.-L., Bourlout, K.B., Tschopp, J. & Gross, N. (2000). Aggressive human neuroblastomas do not express caspase 8 and are resistant to trail mediated apoptosis. *Proceedings of the AACR 2000, Abstract #3546.*

- Eggert, A., Zuzak, T., Grotzer, M.A., Ikegaki, N. & Brodeur, G.M.** (2000). Expression and function of the Trail ligand/receptor system in neuroblastoma. Proceedings of the AACR 2000, Abstract #3547.
- Erttmann, R., Erb, N., Wonkler, K. & Lanbeck, G.** (1989). Massenscreening zur Früherkennung des Neuroblastoms im Säuglingsalter. *Hamburger Ärzteblatt* 44: 416-418.
- Erttmann, R., Erb, N., Wonkler, K. & Lanbeck, G.** (1990). Früherkennung des Neuroblastoms: Vorstellung eines Konzeptes für ein Massenscreening im Säuglingsalter. *Der Kinderarzt* 21: 377-380.
- Erttmann, R., Schmitt, C., Ollert, M.W., David, K., Bredehorst, R. & Vogel, C.-W.** (1996). Naturally occurring humoral cytotoxicity against neuroblastoma (NB) cells in healthy persons and NB patients. *Pediatric Hematol. Oncol.* 13: 545-548.
- Eskes, R., Antonsson, B., Osen-Sand, A., Montessuit, S., Richter, C., Sadoul, R., Mazzei, G., Nichols, A. & Martinou, J.-C.** (1998). Bax-induced cytochrome C release from mitochondria is independent of the permeability transition pore but highly dependent on Mg²⁺ ions. *J. Cell Biol.* 143: 217-224.
- Eskes, R., Desagher, S., Antonsson, B. & Martinou, J.-C.** (2000). Bid induces the oligomerization and insertion of bax into the outer mitochondrial membrane. *Mol. Cell Biol.* 20: 929-935.
- Evans, A.E., D'Angio, G.J. & Randolph, J.** (1971). A proposed staging for children with neuroblastoma. *Cancer* 27: 374-378.
- Fasok, V.A., Voelker, D.R., Campbell, P.A., Cohen, J.J., Bratton, D.L. & Henson, P.M.** (1992). Exposure of phosphatidylserine on the surface of apoptotic lymphocytes triggers specific recognition and removal by macrophages. *J. Immunol.* 148: 2207-2216.

Fenton, H.J.H. (1984). Oxidation of tartaric acid in the presence of iron. *J. Chem. Soc.* 65: 899-910.

Ferrarini, M., Heltai, S., Zocchi, R. & Rugarly, C. (1992). Unusual expression and localization of heat-shock proteins in human tumor cells. *Int. J. Cancer* 51: 613-619.

Finucane, D.M., Bossy-Wetzel, E., Waterhouse, N.J., Cotter, T.G. & Green, D.R. (1999). Bax-induced caspase activation and apoptosis via cytochrome c release from mitochondria is inhibitable by Bcl-xL. *J. Biol. Chem.* 274: 2225-2233.

Fox, J.E., Boyles, J.K., Berndt, M.C., Steffen, P.K. & Anderson, L.K. (1988). Identification of a membrane skeleton in platelets. *J. Cell Biol.* 106: 1525-1538.

Frey, T. (1995). Nucleic acid dyes for detection of apoptosis in live cells. *Cytometry* 21: 265-274.

Friesen, C., Fulda, S. & Debatin, K.M. (1999). Cytotoxic drugs and the CD95 pathway. *Leukemia* 13: 1854-1858.

Fulda, S., Lutz, W., Schwab, M. & Debatin, K.-M. (1998). MycN sensitizes neuroblastoma cells for drug-induced apoptosis. *Oncogene* 18: 1479-1486.

Fulda, S., Susin, S.A., Kroemer, G. & Debatin, K.M. (1998). Molecular ordering of apoptosis induced by anticancer drugs in neuroblastoma cells. *Cancer Res.* 58: 4453-60.

Fulda, S., Scaffidi, C., Pietsch, T., Krammer, P.H., Peter, M.E. & Debatin, K.M. (1998). Activation of the CD95 (APO-1/Fas) pathway in drug- and gamma-irradiation-induced apoptosis of brain tumor cells. *Cell Death Differ.* 5: 884-893.

Funabashi, H., Kawaguchi, A., Tomoda, H., Omura, S., Okuda, S. & Iwasaki, S. (1989). Binding site of cerulenin in fatty acid synthetase. *J. Biochem.* 105: 751-755.

Furuya, Y., Akimoto, S., Yasuda, K. & Ito, H. (1997). Apoptosis of androgen-independent prostate cell line induced by inhibition of fatty acid synthesis. *Anticancer Res.* 17: 4589-4593.

Fuse, T., Yamada, K., Asai, K., Kato, T. & Nakanishi, M. (1996). Heat shock-mediated cell cycle arrest is accompanied by induction of p21. *Biochem. Biophys. Res. Commun.* 225: 759-763.

Goldman, S.C., Chen, C.-Y., Lansing, T.J., Gilmer, T.M. & Kastan, M.B. (1996). The p53 signal transduction pathway is intact in human neuroblastoma despite cytoplasmatic localization. *Amer. J. Path.* 148: 1381-1385.

Goldmann, W.H., Teodoridis, J.M., Sharma, C.P., Hu, B. & Isenburg G. (1999). Fragments from actin binding protein (ABP-280; filamin) insert into reconstituted lipid layers. *Biochem. Biophys. Res. Comm.* 259: 108-112.

Goldstein, J.C., Waterhouse, N.J., Juin, P., Evan, G.I. & Green, D.R. (2000). The coordinate release of cytochrome c during apoptosis is rapid, complete and kinetically invariant. *Nat. Cell Biol.* 2: 156-162.

Goping, I.S., Gross, A., Lavoie, J.N., Nguyen, M., Jemmerson, R., Roth, K., Korsmeyer, S.J. & Shore, G.C. (1998). Regulated targeting of Bax to mitochondria. *J. Cell. Biol.* 143: 207-215.

Gorlin, J.B., Yamin, R., Egan, S., Stewart, M., Stossel, T.P., Kwiatowski, D.J. & Hartwig, J.H. (1990). Human endothelial actin-binding protein (ABP-280, nonmuscle filamin): a molecular leaf spring. *J. Cell Biol.* 111: 1089-1105.

-
- Green, D.R.** (1998). Apoptotic pathways: The road to ruin. *Cell* 94: 695-698.
- Green, D.R. & Kroemer, G.** (1998). The central executioners of apoptosis: caspases or mitochondria?. *Trends Cell Biol.* 8: 267-271.
- Gress, T.M., Müller-Pillasch, F., Weber, C., Lerch, M.M., Friess, H., Buchler, M., Beyer, H.G. & Adler, G.** (1994). Differential expression of heat shock proteins in pancreatic carcinoma. *Cancer Res.* 54: 547-551.
- Gross, A., Jockel, J., Wei, M.C. & Korsmeyer, S.J.** (1998). Enforced dimerization of Bax results in its translocation, mitochondrial dysfunction and apoptosis. *EMBO J.* 17: 3878-3885.
- Gross, A., McDonnell, J.M. & Korsmeyer, S.J.** (1999). Bcl-2 family members and the mitochondria in apoptosis. *Genes Dev.* 13: 1899-1911.
- Ham, J., Babij, C., Whitfield, J., Pfarr, C.M., Lallemand, D., Yaniv, M. & Rubin, L.L.** (1995). A c-Jun dominant negative mutant protects sympathetic neurons against programmed cell death. *Neuron.* 14: 927-939.
- Ham, J., Eilers, A., Whitfield, J., Neame, S.J. & Shah, B.** (2000). c-Jun and the transcriptional control of neuronal apoptosis. *Biochem. Pharmacol.* 60: 1015-1021.
- Harada, J. & Sugimoto, M.** (1999). An inhibitor of p38 and JNK MAP kinases prevents activation of caspase 3 and apoptosis of cultured cerebellar granule neurons. *Jpn. J. Pharmacol.* 79: 369-378.
- Harras, A.** (1996). *Cancer Rates and Risks.* National Cancer Institute. NIH Publications No. 96-691.

Hartl, F.U. (1996). Molecular chaperones in cellular folding. *Nature* 381: 571-579.

Heilmann, C. (2000). Abschlußbericht Postdoktoranden-Stipendium der Mildred-Scheel Stiftung.

Heiligtag, S. (1998). Strukturelle Charakterisierung der von humanen IgM-Antikörpern erkannten Neuroblastom-Antigene NB-p220 und NB-p260. Diploma thesis, Department of Biochemistry and Molecular Biology, University of Hamburg.

Hellstroem, I.E., Hellstroem, K.E., Pierce, G.E. & Bill, A.H. (1968). Demonstration of cell-bound and humoral immunity against neuroblastoma cells. *Proc. Natl. Acad. Sci. USA* 60: 1231-1238.

Hellstroem, K.E. & Hellstroem, I.E. (1976). Spontaneous tumor regression: possible relationships to in vitro parameters of tumor immunity. *Natl. Cancer Inst. Monogr.* 44: 131-133.

Hennigar, R.A., Pochet, M., Hunt, D.A., Lukacher, A.E., Venema, V.J., Seal, E. & Marrero, M.B. (1998). Characterization of fatty acid synthase in cell lines derived from experimental mammary tumors. *Biochim. Biophys. Acta* 1392: 85-100.

Hurst, H. (1997). Immunological Screening of λ -Phage cDNA expressions libraries. In *Methods of Molecular Biology: cDNA library protocols*, Vol. 69, Editors Cowell, I.G. & Austin C.A., 155-159.

Iancu, T.C., Shiloh, H. & Kedar, A. (1988). Neuroblastomas contain iron-rich ferritin. *Cancer* 61: 2497-2502.

Ichijo, H., Nishida, E., Irie, K., ten Dijke, P., Saitoh, M., Moriguchi, T., Takagi, M., Matsumoto, K., Miyazono, K. & Gotoh, Y. (1997). Induction of apoptosis by ASK1, a mammalian MAPKKK that activates SAPK/JNK and p38 signaling pathways. *Science* 275: 90-94.

Ichijo, H. (1999). From receptors to stress activated MAP kinases. *Oncogene* 18: 6087-6093.

Juhl, H., Petrella, E.C., Cheung, N.-K.V., Bredehorst, R. & Vogel, C.-W. (1990). Complement killing of human neuroblastoma cells: a cytotoxic monoclonal antibody and its F(ab)₂'-cobra venom factor conjugate are equally cytotoxic. *Mol. Immunol.* 27: 957-964.

Juin, P. & Evan, G. (2000). Caspase 8: The killer you can't live without. *Nature Med.* 6: 498-500.

Jurgensmeier, J.M., Xie, Z., Deveraux, Q., Ellerby, L., Bredesen, D. & Reed, J.C. (1998). Bax directly induces release of cytochrome c from isolated mitochondria. *Proc. Natl. Acad. Sci. USA* 95: 4997-5002.

Kaufmann, S.H. & Earnshaw, W.C. (2000). Induction of apoptosis by cancer chemotherapy. *Exp. Cell Res.* 256: 42-49.

Kanamoto, T., Mota, M., Takeda, K., Rubin, L.L., Miyazono, K., Ichijo, H., & Bazenet, C.E. (1999). Role of apoptosis signal-regulating kinase in regulation of the c-Jun N-terminal kinase pathway and apoptosis in sympathetic neurons. *Mol. Cell. Biol.* 20: 196-204.

Kroemer, G., Zamzami, N. & Susin, S.A. (1997). Mitochondrial control of apoptosis. *Immunol. Today* 18: 44-51.

Kromer, G. & Reed, J.C. (2000). Mitochondrial control of cell death. *Nature Med.* 6: 513-519.

Kuhajda, F.P., Pizer, E.S., Li, J.N., Mani, N.S., Frehywot, G.L. & Townsend, C.A. (2000). Synthesis and antitumor activity of an inhibitor of fatty acid synthase. *Proc. Natl. Acad. Sci. U S A* 97: 3450-3454.

Kuhajda, F.P., Jenner, K., Wood, F.D., Hennigar, R.A., Jacobs, L.B., Dick, J.D. & Pasternack, G.R. (1994). Fatty acid synthesis: a potential selective target for antineoplastic therapy. *Proc. Natl. Acad. Sci. U S A* 91: 6379-6383.

Laad, A.D., Thomas, M.L., Fakhri, A.R. & Chiplunkar, S.V. (1999). Human gamma delta T cells recognize heat shock protein-60 on oral tumor cells. *Int. J. Cancer* 80: 709-714.

Lämmli, U.K. (1970). Cleavage of structural proteins during the assembly of the head of bacteriophage T4. *Nature* 227: 680-685.

Lamarre, D., Talbot, B., de Murcia, G., Laplante, C., Leduc, Y., Mazon, A. & Poirier, G.G. (1988). Structural and functional analysis of poly(ADP-ribose) polymerase: an immunological study. *Biochim. Biophys. Acta* 950: 147-60.

Lakin, N.D. & Jackson, S.P. (1999). Regulation of p53 in response to DNA damage. *Oncogene* 18: 7644-7655.

Lazebnik, Y.A., Kaufmann, S.H., Desnoyers, S., Poirier, G.G. & Earnshaw, W.C. (1994). Cleavage of poly(ADP-ribose) polymerase by a proteinase with properties like ICE. *Nature* 371: 346-347.

Leedman, P.J., Faulkner-Jones, B., Cram, D.S., Harrison, P.J., West, J., O'Brien, E., Simpson, R., Coppel, R.L. & Harrison, L.C. (1993). Cloning from the thyroid of a protein related to actin binding protein that is recognized by Graves diseases immunoglobulins. *Proc. Natl. Acad. Sci. USA* 90: 5994-5998.

Le-Niculescu, H., Bonfoco, E., Kasuya, Y., Claret, F.X., Green, D.R. & Karin, M. (1999). Withdrawal of survival factors results in activation of the JNK pathway in neuronal cells leading to Fas ligand induction and cell death. *Mol. Cell. Biol.* 19: 751-763.

Leonardi, A., Ellinger-Ziegelbauer, H., Franzoso, G., Brown, K. & Siebenlist, U. (2000). Physical and functional interaction of filamin (actin-binding rotein-280) and tumor necrosis factor receptor-associated factor 2. *J. Biol. Chem.* 275: 271-278.

Leppä, S. & Bohmann, D. (1999). Diverse functions of JNK signaling and c-Jun in stress response and apoptosis. *Oncogene* 18: 6158-6162.

Li, P., Nijhawan, D., Budihardjo, I., Srinivasula, S.M., Ahmad, M., Alnemri, E.S. & Wang, X. (1997). Cytochrome c and dATP-dependent formation of APAF-1/caspase-9 complex initiates an apoptotic protease cascade. *Cell* 91: 479-489.

Li, H., Zhu, H., Xu, C.J. & Yuan, J. (1998). Cleavage of BID by caspase 8 mediates the mitochondrial damage in the Fas pathway of apoptosis. *Cell* 94: 491-501.

Liebermann, D.A., Hoffmann, B. & Steinman, R.A. (1995). Molecular controls of growth arrest and apoptosis: p53-dependent and independent pathways. *Oncogene* 11: 199-210.

Loftus, T.M., Jaworsky, D.E., Frehywot, G.L., Townsend, C.A., Ronnett, G.V., Lane, M.D. & Kuhajda, F.P. (2000). Reduced food intake and body weight in mice treated with fatty acid synthase inhibitors. *Science* 288: 2379-81.

Lowry, O.H., Rosebrough, A., Farr, L. & Randall, R.J. (1951). Protein measurement with the folin phenol reagent. *J. Biol. Chem.* 193: 265-275.

Luo, X., Budihardjo, I., Zou, H., Slaughter, C. & Wang, X. (1998). Bid, a Bcl-2 interacting protein, mediates cytochrome c release from mitochondria in response to activation of cell surface death receptors. *Cell* 94: 481-490.

Marti, A., Luo, Z., Cunningham, C., Ohta, Y., Hartwig, J., Stossel, T.P., Kyriakis, J.M. & Avruch, J. (1997). Actin-binding Protein-280 binds the stress-activated protein kinase (SAPK) activator SEK-1 and is required for tumor necrosis factor- α activation of SAPK in melanoma cells. *J. Biol.Chem.* 272: 2620-2628.

Mazeh, D., Sirota, P., Patya, M. & Novogrodsky, A. (1998). Antibodies to neuroblastoma cell line proteins in patients with schizophrenia. *J. Neuroimmunol.* 84: 218-222.

Medema, J.P., Scaffidi, C., Kischkel, F.C., Shevchenko, A., Mann, M., Krammer, P.H. & Peter, M.E. (1997). FLICE is activated by association with the CD95 death-inducing signaling complex (DISC). *EMBO J.* 16: 2794-2804.

Meyer, S.C., Sanan, D.A. & Fox, J.E.B. (1998). Role of actin-binding protein in insertion of adhesion receptors into the membrane. *J. Biol. Chem.* 273: 3013-3020.

Mignotte, B., Larcher, J.C., Zheng, D.Q., Esnault, C., Coulaud, D. & Feunteun, J. (1990). SV40 induced cellular immortalization: phenotypic changes associated with the loss of proliferative capacity in a conditionally immortalized cell line. *Oncogene* 5: 1529-1533.

Mignotte, B. & Vayssiere, J.L. (1998). Mitochondria and apoptosis. *Eur. J. Biochem.* 252: 1-15.

Miller, D.K. (1997). The role of caspase family of cysteine proteases in apoptosis. *Semin. Immunol.* 9: 35-49.

Moll, U.M., Ostermeyer, A.G., Haladay, R., Winkfield, B., Frazier, M. & Zambetti, G. (1996). Cytoplasmic sequestration of wild-type p53 proteins impairs the G₁ checkpoint after DNA damage. *Mol. Cell. Biol.* 16: 1126-1137.

- Multhoff, G., Botzler, C. & Issels, R.** (1998). The role of heat shock proteins in the stimulation of an immune response. *Biol. Chem.* 379: 295-300.
- Nagata, S.** (1997). Apoptosis by death factor. *Cell* 88: 355-365.
- Nagata, S.** (1999). Fas ligand-induced apoptosis. *Annu. Rev. Genet.* 33: 29-55.
- Ng, P.W.P., Porter, A.G. & Jänicke, R.U.** (1999). Molecular cloning and characterization of two novel pro-apoptotic isoforms of caspase 10. *J. Biol. Chem.* 274: 10301-10308.
- Nicoletti, I., Migliorati, G., Pagliacci, M.C., Grignani, F. & Riccardi, C.** (1991). A rapid and simple method for measuring thymocyte apoptosis by propidium iodide staining and flow cytometry. *J. Immunol. Methods* 139: 271-279.
- Noguchi, P., Wallace, R., Johnson, J., Farley, E.M., O'Brien, S., Ferrone, S., Pellegrino, M.A., Milstien, K., Needy, C., Browne, W. & Petriccioni, J.** (1979). Characterization of WiDr: a human colon carcinoma cell line. *In Vitro* 15: 401-408.
- Oberhammer, F., Wilson, J.W., Dive, C., Morris, I.D., Hickman, J.A., Wakeling, A.E., Walker, P.R. & Sikorska, M.** (1993). Apoptotic death in epithelial cells: cleavage of DNA to 300 and/or 50 kb fragments prior to or in the absence of internucleosomal fragmentation. *EMBO J.* 12: 3679-3684.
- Oda, K., Arakawa, H., Tanaka, T., Matsuda, K., Tanikawa, C., Mori, T., Nishimori, H., Tamai, K., Tokino, T., Nakamura, Y. & Taya, Y.** (2000). p53AIP1, a potential mediator of p53-dependent apoptosis and its regulation by ser-46-phosphorylated p53. *Cell* 102: 849-862.

Ollert, M.W., David, K., Schmitt, C., Hauenschild, A., Bredehorst, R. & Vogel, C.-W. (1996). Normal human serum contains natural IgM antibodies cytotoxic for human neuroblastoma cells. *Proc. Natl. Acad. Sci. USA* 93: 4498-4503.

Oren, P. (1999). Regulation of the p53 tumor suppressor protein. *J. Biol. Chem.* 274: 36031-36034.

Otha, Y., Stossel, T. & Hartwig, J. (1991). Ligand-sensitive binding of actin-binding protein to immunoglobulin G Fc receptor I (Fc γ RI). *Cell* 67: 275-282.

Pahlmann, S., Mamaeva, S., Meyerson, G., Mattsson, M.E.K., Bjelfram, C., Oertoft, E. & Hammerling, U. (1990). Human neuroblastoma cells in culture: a model for neuronal cell differentiation and function. *Acta Physiol. Scand. Suppl.* 592: 25-37.

Park, D.J. & Patek, P.Q. (1998). Detergent and enzyme treatment of apoptotic cells for the observation of DNA fragmentation. *Biotechniques* 24: 558-560.

Papac, R.J. (1996). Spontaneous regression of cancer. *Cancer Treatment Reviews* 22: 395-423.

Pastorino, J.G., Chen, S.T., Tafani, M., Snyder, J.W. & Farber, J.L. (1998). The overexpression of Bax produces cell death upon induction of the mitochondrial permeability transition. *J. Biol. Chem.* 273: 7770-7775.

Pastorino, J.G., Tafani, M., Rothman, R.J., Marcinkeviciute, A., Hoek, J.B. & Farber, J.L. (1999). Functional consequences of the sustained or transient activation by Bax of the mitochondrial permeability transition pore. *J. Biol. Chem.* 274: 31734-31739.

Paul, A.G.A., van Kooten, P.J.S., van Eden, W. & van der Zee, R. (2000). Highly autoproliiferative T cells specific for 60-kDa heat shock protein produce IL-4/IL-10 and IFN- γ and are protective in adjuvant arthritis. *J. Immunol.* 165: 7270-7277.

Pawlowski, J. & Kraft, A. (2000). Bax-induced apoptotic cell death. *Proc. Natl. Acad. Sci. USA* 97: 529-531.

Pinkerton, C.R. (1993). Neuroblastoma in the 1990s. A clinical perspective. In *Human neuroblastoma. Recent advances in clinical and genetic analysis.* (Ed. Schwab, M., Tonini, G.P. & Bénard, J.) 3-10 (Harwood Academic Publishers, Chur, Schweiz).

Pizer, E.S., Thupari, J., Han, W.F., Pinn, M.L., Chrest, F.J., Frehywot, G.L., Townsend, C.A. & Kuhajda, F.P. (2000). Malonyl-coenzyme-A is a potential mediator of cytotoxicity induced by fatty-acid synthase inhibition in human breast cancer cells and xenografts. *Cancer Res.* 60: 213-218.

Pizer, E.S., Chrest, F.J., DiGiuseppe, J.A. & Han, W.F. (1998). Pharmacological inhibitors of mammalian fatty acid synthase suppress DNA replication and induce apoptosis in tumor cell lines. *Cancer Res.* 58: 4611-4615.

Pizer, E.S., Jackisch, C., Wood, F.D., Pasternack, G.R., Davidson, N.E. & Kuhajda, F.P. (1996). Inhibition of fatty acid synthesis induces programmed cell death in human breast cancer cells. *Cancer Res.* 56: 2745-2747.

Pizer, E.S., Wood, F.D., Heine, H.S., Romantsev, F.E., Pasternack, G.R. & Kuhajda, F.P. (1996). Inhibition of fatty acid synthesis delays disease progression in a xenograft model of ovarian cancer. *Cancer Res.* 56: 1189-1193.

- Pizer, E.S., Wood, F.D., Pasternack, G.R. & Kuhajda, F.P.** (1996). Fatty acid synthase (FAS): a target for cytotoxic antimetabolites in HL60 promyelocytic leukemia cells. *Cancer Res.* 56: 745-751.
- Ponzoni, M., Bocca, P., Chiesa, V., Decensi, A., Raffaghello, L., Rozzo, C. & Montaldo, P.G.** (1995). Differential effects of N-(4-hydroxyphenyl)retinamide and retinoic acid on neuroblastoma cells: apoptosis versus differentiation. *Cancer Res.* 55: 853-861.
- Poccia, F., Piselli, P., Vendetti, S., Bach, S., Amendola, A., Placido, R. & Collizi, V.** (1996). Heat shock protein expression on the membrane of T-cells undergoing apoptosis. *Immunol.* 88: 6-12.
- Prasannan, L., Misek, D.E., Hinderer, R., Michon, J., Geiger, J.D. & Hanash, S.M.** (2000). Identification of beta-tubulin isoforms as tumor antigens in neuroblastoma. *Clin. Cancer Res.* 6: 3949-3956.
- Raff, M.** (1998). Cell suicide for beginners. *Nature* 396: 119-122.
- Rashid, A., Pizer, E.S., Moga, M., Milgram, L.Z., Zahurak, M., Pasternack, G.R., Kuhajda, F.P. & Hamilton, S.R.** (1997). Elevated expression of fatty acid synthase and fatty acid synthetic activity in colorectal neoplasia. *Am. J. Pathol.* 150: 201-8.
- Reynolds, J.V., Shou, J., Choi, H., Sgar, R., Ziegler, M.M. & Daly, J.M.** (1989). The influence of natural killer cells in neuroblastoma. *Arch. Surg.* 124: 235-239.
- Sahin, U., Tuereci, O., Schmitt, H., Cochlovius, B., Johannes, T., Schmits, R., Stenner, F., Luo, G., Schobert, I. & Pfreundschuh, M.** (1995). Human neoplasms elicit multiple specific immune responses in the autologous host. *Proc. Natl. Acad. Sci. USA* 92: 11810-11813.

Salvioli, S., Ardizzoni, A., Franceschi, C. & Cossarizza, A. (1997). JC-1, but not DiOC₆(3) or rhodamine 123, is a reliable fluorescent probe to assess $\Delta\psi$ changes in intact cells: implications for studies on mitochondrial functionality during apoptosis. *FEBS Letters* 411: 77-82.

Sapozhnikov, A.M., Ponomarev, E.D., Tarasenko, T.N. & Telford, W.G. (1999). Spontaneous apoptosis and expression of cell surface heat shock proteins in cultured EL-4 lymphoma cells. *Cell Prolif.* 32: 363-378.

Scaffidi, C., Medema, J.P., Krammer, P.H. & Peter, M.E. (1997). FLICE is predominantly expressed as two functionally active isoforms, caspase-8/a and caspase-8/b. *J. Biol. Chem.* 272: 26953-26958.

Scanlan, M.J., Chen, Y.-T., Williamson, B., Gure, A.O., Stockert, E., Gordan, J.D., Tuereci, O., Sahin, U., Pfreundschuh, M. & Old, L.J. (1998). Characterization of human colon cancer antigens recognized by autologous antibodies. *Int. J. Cancer* 76: 652-658.

Schett, G., Xu, Q., Amberger, A., van der Zee, R., Recheis, H., Willeit, J. & Wick, G. (1995). Autoantibodies against heat shock protein 60 mediate endothelial cytotoxicity. *J. Clin. Invest.* 96: 2569-2577.

Schlesinger, M.J. (1990). Heat shock proteins. *J. Biol. Chem.* 265: 12111-12117.

Schulze-Osthoff, K., Ferrari, D., Los, M., Wesselborg, S. & Peter M.E. (1998). Apoptosis signaling by death receptors. *Eur. J. Biochem.* 15: 439-459.

Schwab, M., Alitalo, K. & Klempnauer, K.-H. (1983). Amplified DNA with limited homology to MYC cellular oncogene is shared by human neuroblastoma cell lines and a neuroblastoma tumor. *Nature* 305: 245-249.

- Sharma, C.P., Ezzell, R.M. & Arnaout, M.A.** (1995). Direct interaction of filamin (ABP-280) with the β 2-integrin subunit CD18. *J. Immunol.* 154: 3461-3470.
- Shimizu, H., Banno, Y., Sumi, N., Naganawa, T., Kitajima, Y. & Nozawa, Y.** (1999). Activation of p38 mitogen-activated protein kinase and caspases in UVB-induced apoptosis in human keratinocyte HaCaT cells. *J. Invest. Dermatol.* 112: 769-774.
- Shimizu, S. & Tsujimoto, Y.** (2000). Proapoptotic BH3-only Bcl-2 family members induce cytochrome C release, but not mitochondrial membrane potential loss, and do not directly modulate voltage-dependent anion channel activity. *Proc. Natl. Acad. Sci. USA* 97: 577-582.
- Siegel, P.K. & Sato, J.K.** (1986). Neuroblastoma. In *Oncology* (Ed. Moossa, A.R., Robson, M.C., Schimpfl, S.C.), 1211-1231 (Williams and Wilkins, Baltimore).
- Slee, E.A., Harte, M.T., Kluck, R.M., Wolf, B.B., Casiano, C.A., Newmeyer, D.D., Wang, H.-G., Reed, J.C., Nicholson, D.W., Alnemri, E.S., Green, D.R. & Martin, S.J.** (1999). Ordering the cytochrome c-initiated caspase cascade: hierarchical activation of caspase-2, -3, -6, -7, -8 and -10 in a caspase-9 dependent manner. *J. Cell Biol.* 144: 281-292.
- Smets, L.A., Loesberg, C., Janssen, M., Metwally, E.A. & Huiskamp, R.** (1989). Active uptake and extravesicular storage of m-iodobenzyl-guanidine in human neuroblastoma SK-N-SH cells. *Cancer Res.* 49: 2941-2944.
- Smith, P.K., Krohn, R.I., Hermanson, G.T., Mallia, A.K., Gartner, F.H., Provenzano, M.D., Fujimoto, E.K., Goeke, N.M., Olson, B.J. & Klenk, D.C.** (1985). Measurement of protein using bicinchonic acid. *Anal. Biochem.* 150: 76-85.

- Srivastava, P.K., DeLeo, A.B. & Old, L.J.** (1986). Tumor rejection antigens of chemically induced sarcomas of inbred mice. *Proc. Natl. Acad. Sci USA* 83: 3407-3411.
- Stadheim, T.A., Saluta, G.R. & Kucera, G.L.** (2000). Role of c-Jun N-terminal kinase/p38 stress signaling in 1-beta-D-arabinofuranosyl-cytosine-induced apoptosis. *Biochem. Pharmacol.* 59: 407-418.
- Strobel, T., Swanson, L., Korsmeyer, S. & Cannistra, S.A.** (1996). Bax enhances paclitaxel-induced apoptosis through a p53-independent pathway. *Proc. Natl. Acad. Sci. USA* 93: 1404-1409.
- Sun, X.M., MacFarlane, M., Zhuang, J., Wolf, B.B., Green, D.R. & Cohen, G.M.** (1999). Distinct caspase cascades are initiated in receptor-mediated and chemical-induced apoptosis. *J. Biol. Chem.* 274: 5053-60.
- Susin, S.A., Zamzami, N., & Kroemer, G.** (1998). Mitochondria as regulators of apoptosis: doubt no more. *Biochim. Biophys. Acta* 1366: 151-165.
- Takahashi, K. & Suzuki, K.** (1993). Association of insulin-like growth-factor-I-induced DNA synthesis with phosphorylation and nuclear exclusion of p53 in human breast cancer MCF-7 cells. *Int. J. Cancer* 55: 453-458.
- Teitz, T., Wie, T., Valentine, M.B., Vanin, E.F., Grenet, J., Valentine, V.A., Behm, F.G., Look, A.T., Lathi, J.M. & Kidd, V.J.** (2000). Caspase 8 is deleted or silenced preferentially in childhood neuroblastomas with amplification of MYCN. *Nature Med.* 5: 529-535.
- Tonini, G.P., Mazzocco, K., di Vinci, A., Geido, E., de Bernardi, B. & Giaretti, W.** (1997). Evidence of apoptosis in neuroblastoma at onset and relapse. An analysis of large series of tumors. *J. Neurooncol.* 31: 209-215.

Towbin, H., Staehelin, T. & Gordon, J. (1979). Electrophoretic transfer of proteins from polyacrylamid gels to nitrocellulose sheets: procedure and some applications. *Proc. Natl. Acad. Sci. USA* 76: 4350-4354.

Török, Z., Horvath, I., Goloubinoff, P., Kovacs, E., Glatz, E., Balogh, G. & Vigh, L. (1997). Evidence for a lipochaperonin: association of active protein-folding GroEL oligomers with lipids can stabilize membranes under heat shock conditions. *Proc. Natl. Acad. Sci. USA* 84: 2192-2197.

Trieb, K., Gerth, R., Holzer, G., Grohs, J.G., Berger, P. & Kotz, R. (2000). Antibodies to heat shock protein 90 in osteosarcoma patients correlate with response to neoadjuvant chemotherapy. *Br. J. Cancer* 82: 85-87.

Uckun, F.M., Tuel-Ahlgren, L., Song, C.W., Waddick, K., Myers, D.E., Kirihaara, J., Ledbetter, J.A. & Schieven, G.L. (1992). Ionizing radiation stimulates unidentified tyrosine-specific protein kinases in human B-lymphocyte precursors, triggering apoptosis and clonogenic cell death. *Proc. Natl. Acad. Sci. U S A.* 89: 9005-9009.

Udono, H. & Srivastava, K. (1994). Comparison of tumor-specific immunogenicities of stress-induced proteins gp96, hsp 90 and hsp 70. *J. Immunol.* 152: 5398-5404.

Ungar, D.R., Hailat, N., Strahler, J.R., Kuick, R.D., Brodeur, G.M., Seeger, R.C., Reynolds, C.P. & Hanash, S.M. (1994). Hsp27 expression in neuroblastoma: correlation with disease stage. *J. Natl. Cancer Inst.* 86: 780-784.

Verhagen, A.M. & Vaux, D.L. (1999). Molecular mechanisms of apoptosis: An Overview. In *Apoptosis: Biology and Mechanisms.* (Ed. Kumar, S.), 11-24 (Springer Verlag Berlin Heidelberg, Germany).

- Vermes, I., Haanen, C., Steffens-Nakken, H. & Reutlingsperger, C.** (1995). A novel assay for apoptosis. Flow cytometric detection of phosphatidylserine expression on early apoptotic cells using fluorescein labelled Annexin V. *J. Immunol. Meth.* 184: 39-51.
- Walker, J.M.** (1994). The bicinchoninic acid (BCA) assay for protein quantitation. *Methods Mol. Biol.* 32: 5-8.
- Watson, A., Eilers, A., Lallemand, D., Kyriakis, J., Rubin, L.L. & Ham, J.** (1998). Phosphorylation of c-Jun is necessary for apoptosis induced by survival signal withdrawal in cerebellar granule neurons. *J. Neurosci.* 18: 751-762.
- Weigelt, B.** (2000). Untersuchungen zur Signaltransduktion von Antikörper- und Cerulenin-vermittelter Apoptose bei humanen Tumorzellen. Diploma thesis, Department of Biochemistry and Molecular Biology, University of Hamburg.
- Wolf, B.B. & Green, D.R.** (1999). Suicidal tendencies: Apoptotic cell death by caspase family proteinases. *J. Biol. Chem.* 274: 20049-20052.
- Weiss, L., Hoffmann, G.E., Schreiber, R., Andres, H., Fuchs, E., Körber, E. & Kolb, H.J.** (1986). Fatty acid biosynthesis in man, a pathway of minor importance. Purification, optimal assay conditions and organ distribution of fatty acid synthase. *Biol. Chem.* 367: 905-912.
- Wolter, K.G., Hsu, Y.T., Smith, C.L., Nechushtan, A., Xi, X.G. & Youle, R.J.** (1997). Movement of Bax from the cytosol to mitochondria during apoptosis. *J. Cell Biol.* 139: 1281-1292.
- Wood, D.E. & Newcomb, E.W.** (1999). Caspase-dependent activation of calpain during drug-induced apoptosis. *J. Biol. Chem.* 274: 8309-15.

-
- Wood, D.E., Thomas, A., Devi, L.A., Berman, Y., Beavis, R.C., Reed, J.C. & Newcomb, E.W.** (1998). Bax cleavage is mediated by calpain during drug-induced apoptosis. *Oncogene* 17: 1069-78.
- Wray, W., Boulikas, T., Wray, V.P. & Hancock, R.** (1981). Silver staining of proteins in polyacrylamide gels. *Anal. Biochem.* 118: 197-203.
- Wyllie, A.H.** (1980). Glucocorticoid-induced thymocyte apoptosis is associated with endogenous endonuclease activation. *Nature* 284: 555-556.
- Wyllie, A.H.** (1997). Apoptosis and carcinogenesis. *Eur. J. Cancer* 73: 189-197.
- Xu, W.-F., Xie, Z.-W., Chung, D.W. & Davie, E.W.** (1998). A novel human actin-binding protein homologue that binds to platelet glycoprotein IB α . *Blood* 92: 1268-1276.
- Zou, H., Henzel, W.J., Liu, X., Lutschg, A. & Wang, X.** (1997). Apaf-1, a human protein homologous to *C. elegans* CED-4, participates in cytochrome c-dependent activation of Caspase 3. *Cell* 90: 405-413.

Curriculum Vitae

Personal Data

Name: Sven Jörg Heiligtag
 Date of Birth: 12. October 1971
 Birthplace: Hamburg
 Nationality: German

Education

08/78-06/91 Elementary School and Gymnasium, Hamburg, Germany
 12/91-03/93 Alternative service (Zivildienst), Hamburg, Germany
 04/93-03/98 **Studies of Chemistry**, University of Hamburg, Germany
 03/95 Vordiplom (sehr gut: 1.2)
 08/97 Diplom (sehr gut: 1.1)
 03/98 dissertation (sehr gut: 1.0)
 10/93-02/98 **Studies of Business Administration**
 facultative, University of Hamburg, Germany
 10/94 Vordiplom (gut: 1.8)
 02/98 Exams (sehr gut: 1.0)
 04/95-current **Studies of Economics**
 facultative, University of Hamburg, Germany
 08/96 Vordiplom (gut: 1.9)
 06/98-12/00 **Doctoral thesis**
 06/98-03/99 Department of Biochemistry and Molecular Biology,
 University of Hamburg, Germany
 06/99-12/00 Cancer Reseach Center of Hawaii, Honolulu, USA
 10/98-12/00 Scholarship from the Fond of the Chemical Industry and
 the Federal Ministry for Research and Education
 06/98-09/98
 01/01-current Scientific Assistent, University of Hamburg, Germany

Work Experience

05/96-05/97 **GlaxoWellcome**, Hamburg, Germany
 03/99-05/99 **Roland Berger & Partner**, Munich, Germany

Acknowledgements

First and foremost I would like to thank Prof. Dr. C.-W. Vogel for his supervision, the freedom and generous support he granted me in my research activities, the opportunity to accompany him to the CRCH and experience a different culture and way of living. Prof. Vogel's support and generosity gave the time in Hawaii a special note.

No less I would like to thank Dr. K. David for the excellent cooperation, interaction and friendship. The presented data would not have been accomplished without the innumerable discussions we had about our research activities both in the lab and in our leisure time.

I'm very grateful to Prof. Dr. R. Bredehorst for his support throughout my whole thesis. His advice as well as our discussions were always of great help for me.

Prof. Dr. J. Heck for his assistance and advice throughout my studies.

The "Fond der Chemischen Industrie" for their generous funding of my research activities.

The Hawaiian Community Foundation for their financial support (Grant 20000633, Principal Investigator K. David, Mechanism of Cerulenin-Induced Apoptosis in Human Neuroblastoma Cells).

Dr. M. Teppke for the countless N-terminal sequencings.

Dr. P. Ziegel Müller for his assistance in various molecular biology methods.

The members of the Molecular Carcinogenesis Department of the CRCH and of the Department for Biochemistry and Molecular Biology in Hamburg for the pleasant working environment, their good humor and help in various topics.

Kerstin Bartscherer, Britta Weigelt und Derrick Tracy for their assistance and good humor as well as their friendship.

My parents and my brother Jan for their support throughout my whole carrier.

Special thanks belong to my girlfriend Heike. The knowledge of her being there was of great encouragement and importance for me.

Affidavit

I hereby declare, that I have done the present work by myself, not used other than the stated sources and aids and that any uses statement from literature are notes as so.

I further confirm, that this dissertation is not submitted to any other institution to open the dissertation procedure.

Hamburg, 21st March 2001